Karady, George G. “Transmission System”
The Electric Power Engineering Handbook
Ed. L.L. Grigsby
Boca Raton: CRC Press LLC, 2001

4

Transmission System

George G. Karady
Arizona State University

4

Transmission System

George G. Karady
Arizona State University

Joe C. Pohlman
Consultant

R.G. Farmer
Arizona State University

Wilford Caulkins
Sherman & Reilly

Kristine Buchholz
Pacific Gas & Electric Company

Carlos V. Núñez-Noriega
Glendale Community College

Felimón Hernandez
Arizona Public Service Company

Manuel Reta-Hernández
Arizona State University

D.A. Douglass
Power Delivery Consultants, Inc.

Ridley Thrash
Southwire Company

Giao N. Trinh
Log-In

John G. Kappenman
Metatech Corporation

William A. Chisholm
Ontario Hydro Technologies

Rao S. Thallam
Salt River Project

4.1 Concept of Energy Transmission and Distribution

George G. Karady

The purpose of the electric transmission system is the interconnection of the electric energy producing power plants or generating stations with the loads. A three-phase AC system is used for most transmission lines. The operating frequency is 60 Hz in the U.S. and 50 Hz in Europe, Australia, and part of Asia. The three-phase system has three phase conductors. The system voltage is defined as the rms voltage between the conductors, also called line-to-line voltage. The voltage between the phase conductor and ground, called line-to-ground voltage, is equal to the line-to-line voltage divided by the square root of three. Figure 4.1 shows a typical system.

The figure shows the Phoenix area 230-kV system, which interconnects the local power plants and the substations supplying different areas of the city. The circles are the substations and the squares are the generating stations. The system contains loops that assure that each load substation is supplied by at least two lines. This assures that the outage of a single line does not cause loss of power to any customer. For example, the Aqua Fria generating station (marked: Power plant) has three outgoing lines. Three high-voltage cables supply the Country Club Substation (marked: Substation with cables). The Pinnacle Peak Substation (marked: Substation with transmission lines) is a terminal for six transmission lines. This example shows that the substations are the node points of the electric system. The system is

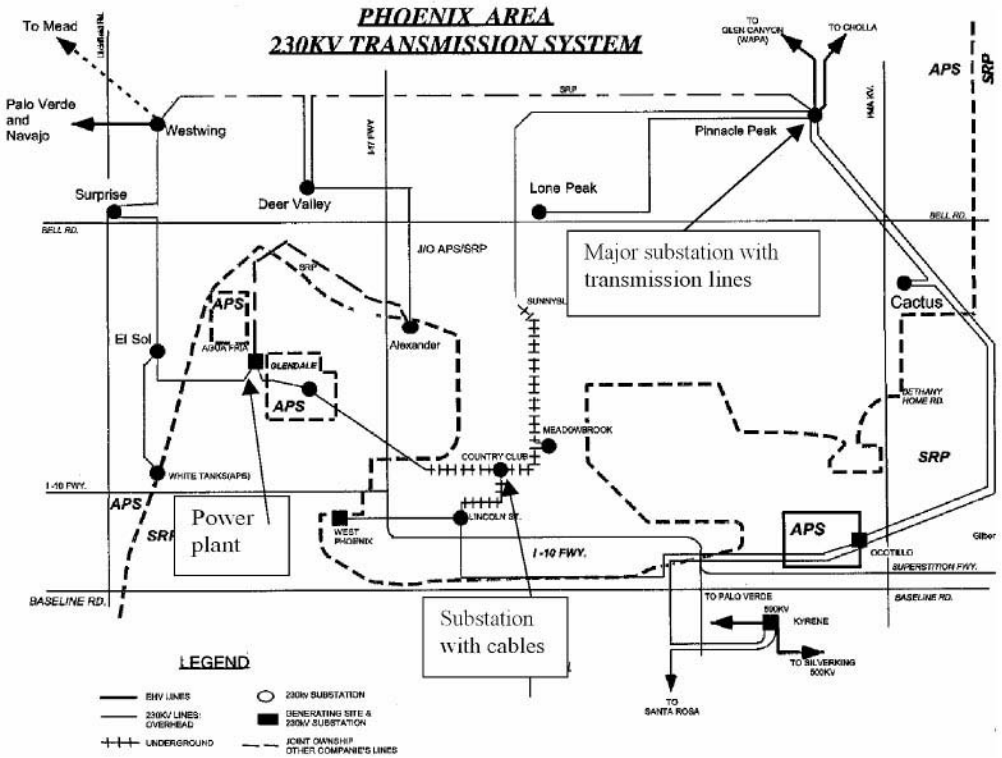

FIGURE 4.1 Typical electrical system.

interconnected with the neighboring systems. As an example, one line goes to Glen Canyon and the other to Cholla from the Pinnacle Peak substation.

In the middle of the system, which is in a congested urban area, high-voltage cables are used. In open areas, overhead transmission lines are used. The cost per mile of overhead transmission lines is 6 to 10% less than underground cables.

The major components of the electric system, the transmission lines, and cables are described briefly below.

Generation Stations

The generating station converts the stored energy of gas, oil, coal, nuclear fuel, or water position to electric energy. The most frequently used power plants are:

Thermal Power Plant. The fuel is pulverized coal or natural gas. Older plants may use oil. The fuel is mixed with air and burned in a boiler that generates steam. The high-pressure and high-temperature steam drives the turbine, which turns the generator that converts the mechanical energy to electric energy.

Nuclear Power Plant. Enriched uranium produces atomic fission that heats water and produces steam. The steam drives the turbine and generator.

Hydro Power Plants. A dam increases the water level on a river, which produces fast water flow to drive a hydro-turbine. The hydro-turbine drives a generator that produces electric energy.

Gas Turbine. Natural gas is mixed with air and burned. This generates a high-speed gas flow that drives the turbine, which turns the generator.

Combined Cycle Power Plant. This plant contains a gas turbine that generates electricity. The exhaust from the gas turbine is high-temperature gas. The gas supplies a heat exchanger to preheat the combustion air to the boiler of a thermal power plant. This process increases the efficiency of the combined cycle power plant. The steam drives a second turbine, which drives the second generator. This two-stage operation increases the efficiency of the plant.

Switchgear

The safe operation of the system requires switches to open lines automatically in case of a fault, or manually when the operation requires it. Figure 4.2 shows the simplified connection diagram of a generating station.

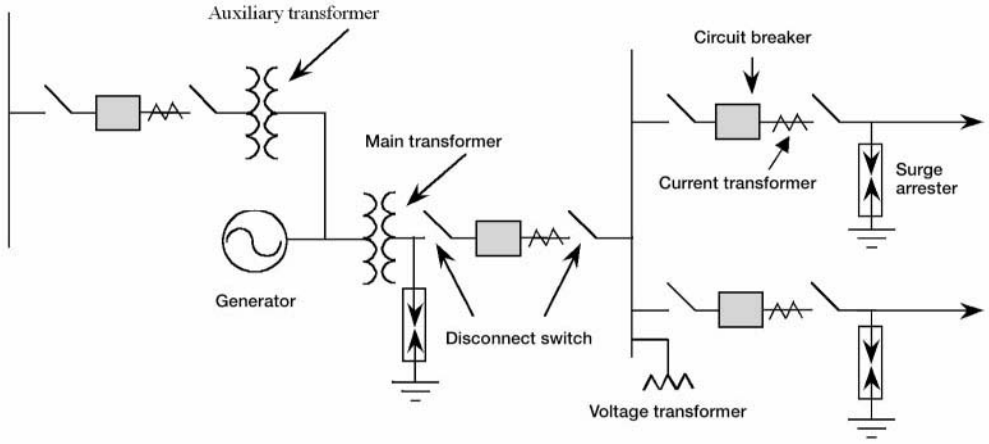

FIGURE 4.2 Simplified connection diagram of a generating station.

The generator is connected directly to the low-voltage winding of the main transformer. The transformer high-voltage winding is connected to the bus through a circuit breaker, disconnect switch, and current transformer. The generating station auxiliary power is supplied through an auxiliary transformer through a circuit breaker, disconnect switch, and current transformer. Generator circuit breakers, connected between the generator and transformer, are frequently used in Europe. These breakers have to interrupt the very large short-circuit current of the generators, which results in high cost.

The high-voltage bus supplies two outgoing lines. The station is protected from lightning and switching surges by a surge arrester.

Circuit breaker (CB) is a large switch that interrupts the load and fault current. Fault detection systems automatically open the CB, but it can be operated manually.

Disconnect switch provides visible circuit separation and permits CB maintenance. It can be operated only when the CB is open, in no-load condition.

Potential transformers (PT) and current transformers (CT) reduce the voltage to 120 V, the current to 5 A, and insulates the low-voltage circuit from the high-voltage. These quantities are used for metering and protective relays. The relays operate the appropriate CB in case of a fault.

Surge arresters are used for protection against lightning and switching overvoltages. They are voltage dependent, nonlinear resistors.

Control Devices

In an electric system the voltage and current can be controlled. The voltage control uses parallel connected devices, while the flow or current control requires devices connected in series with the lines.

Tap-changing transformers are frequently used to control the voltage. In this system, the turns-ratio of the transformer is regulated, which controls the voltage on the secondary side. The ordinary tap changer uses a mechanical switch. A thyristor-controlled tap changer has recently been introduced.

A shunt capacitor connected in parallel with the system through a switch is the most frequently used voltage control method. The capacitor reduces lagging-power-factor reactive power and improves the power factor. This increases voltage and reduces current and losses. Mechanical and thyristor switches are used to insert or remove the capacitor banks.

The frequently used Static Var Compensator (SVC) consists of a switched capacitor bank and a thyristor-controlled inductance. This permits continuous regulation of reactive power.

The current of a line can be controlled by a capacitor connected in series with the line. The capacitor reduces the inductance between the sending and receiving points of the line. The lower inductance increases the line current if a parallel path is available.

In recent years, electronically controlled series compensators have been installed in a few transmission lines. This compensator is connected in series with the line, and consists of several thyristor-controlled capacitors in series or parallel, and may include thyristor-controlled inductors.

Medium- and low-voltage systems use several other electronic control devices. The last part in this section gives an outline of the electronic control of the system.

Concept of Energy Transmission and Distribution

Figure 4.3 shows the concept of typical energy transmission and distribution systems. The generating station produces the electric energy. The generator voltage is around 15 to 25 kV. This relatively low voltage is not appropriate for the transmission of energy over long distances. At the generating station a transformer is used to increase the voltage and reduce the current. In Fig. 4.3 the voltage is increased to 500 kV and an extra-high-voltage (EHV) line transmits the generator-produced energy to a distant substation. Such substations are located on the outskirts of large cities or in the center of several large loads. As an example, in Arizona, a 500-kV transmission line connects the Palo Verde Nuclear Station to the Kyrene and Westwing substations, which supply a large part of the city of Phoenix.

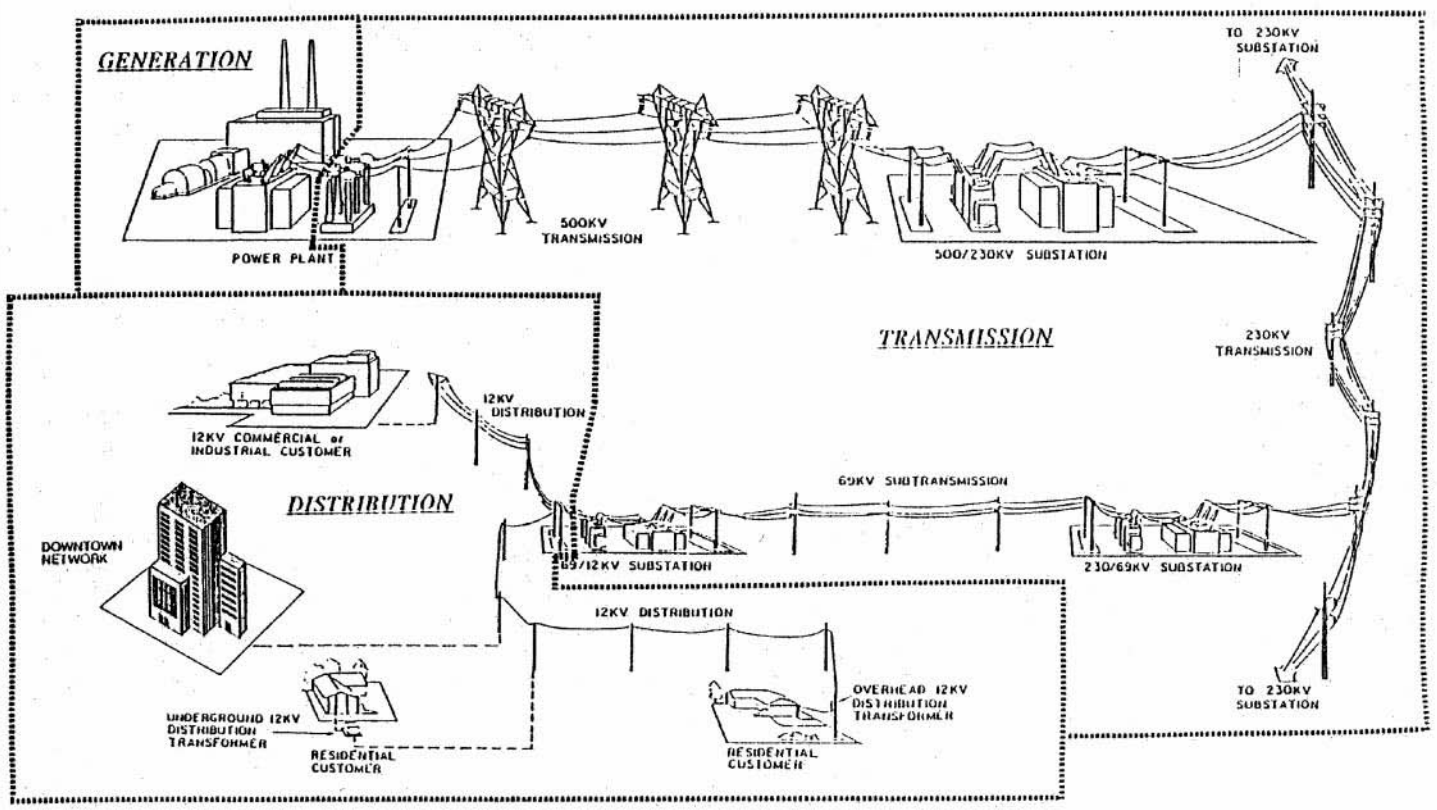

FIGURE 4.3 Concept of electric energy transmission.

The voltage is reduced at the 500 kV/220 kV EHV substation to the high-voltage level and high-voltage lines transmit the energy to high-voltage substations located within cities.

At the high-voltage substation the voltage is reduced to 69 kV. Sub-transmission lines connect the high-voltage substation to many local distribution stations located within cities. Sub-transmission lines are frequently located along major streets.

The voltage is reduced to 12 kV at the distribution substation. Several distribution lines emanate from each distribution substation as overhead or underground lines. Distribution lines distribute the energy along streets and alleys. Each line supplies several step-down transformers distributed along the line. The distribution transformer reduces the voltage to 230/115 V, which supplies houses, shopping centers, and other local loads. The large industrial plants and factories are supplied directly by a subtransmission line or a dedicated distribution line as shown in Fig. 4.3.

The overhead transmission lines are used in open areas such as interconnections between cities or along wide roads within the city. In congested areas within cities, underground cables are used for electric energy transmission. The underground transmission system is environmentally preferable but has a significantly higher cost. In Fig. 4.3 the 12-kV line is connected to a 12-kV cable which supplies commercial or industrial customers. The figure also shows 12-kV cable networks supplying downtown areas in a large city. Most newly developed residential areas are supplied by 12-kV cables through pad-mounted step-down transformers as shown in Fig. 4.3.

High-Voltage Transmission Lines

High-voltage and extra-high-voltage (EHV) transmission lines interconnect power plants and loads, and form an electric network. Figure 4.4 shows a typical high-voltage and EHV system.

This system contains 500-kV, 345-kV, 230-kV, and 115-kV lines. The figure also shows that the Arizona (AZ) system is interconnected with transmission systems in California, Utah, and New Mexico. These

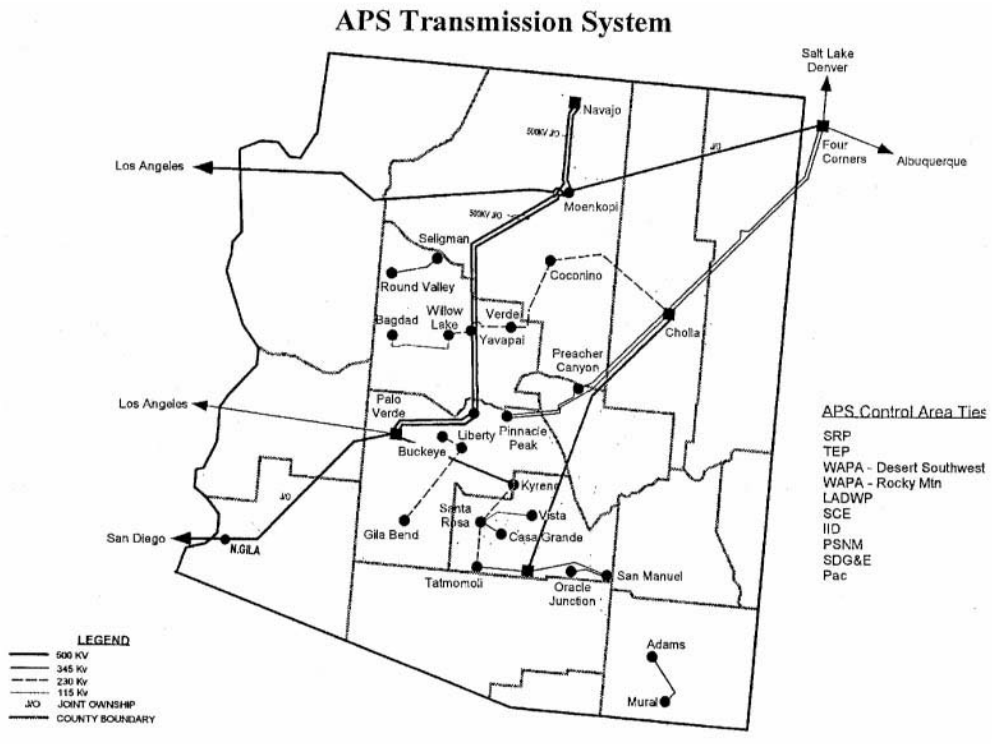

FIGURE 4.4 Typical high-voltage and EHV transmission system (Arizona Public Service, Phoenix area system).

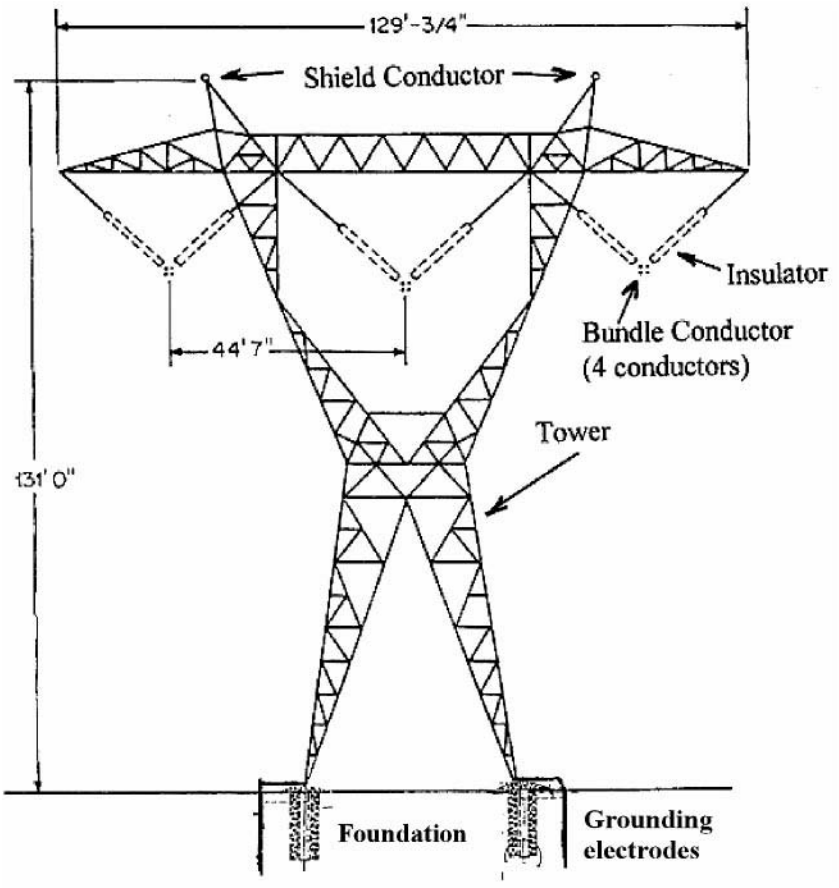

FIGURE 4.5 Typical high-voltage transmission line.

interconnections provide instantaneous help in case of lost generation in the AZ system. This also permits the export or import of energy, depending on the needs of the areas.

Presently, synchronous ties (AC lines) interconnect all networks in the eastern U.S. and Canada. Synchronous ties also (AC lines) interconnect all networks in the western U.S. and Canada. Several non-synchronous ties (DC lines) connect the East and the West. These interconnections increase the reliability of the electric supply systems.

In the U.S., the nominal voltage of the high-voltage lines is between 100 kV and 230 kV. The voltage of the extra-high-voltage lines is above 230 kV and below 800 kV. The voltage of an ultra-high-voltage line is above 800 kV. The maximum length of high-voltage lines is around 200 miles. Extra-high-voltage transmission lines generally supply energy up to 400–500 miles without intermediate switching and var support. Transmission lines are terminated at the bus of a substation.

The physical arrangement of most extra-high-voltage (EHV) lines is similar. Figure 4.5 shows the major components of an EHV, which are:

1. Tower: The figure shows a lattice, steel tower.
2. Insulator: V strings hold four bundled conductors in each phase.
3. Conductor: Each conductor is stranded, steel reinforced aluminum cable.
4. Foundation and grounding: Steel-reinforced concrete foundation and grounding electrodes placed in the ground.
5. Shield conductors: Two grounded shield conductors protect the phase conductors from lightning.

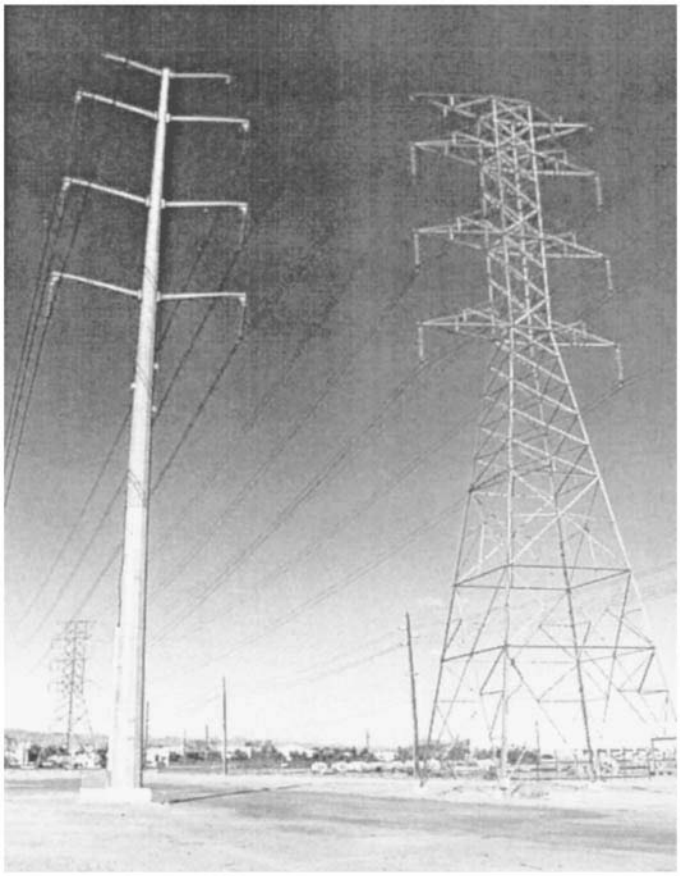

FIGURE 4.6 Typical 230-kV constructions.

At lower voltages the appearance of lines can be improved by using more aesthetically pleasing steel tubular towers. Steel tubular towers are made out of a tapered steel tube equipped with banded arms. The arms hold the insulators and the conductors. Figure 4.6 shows typical 230-kV steel tubular and lattice double-circuit towers. Both lines carry two three-phase circuits and are built with two conductor bundles to reduce corona and radio and TV noise. Grounded shield conductors protect the phase conductors from lightning.

High-Voltage DC Lines

High-voltage DC lines are used to transmit large amounts of energy over long distances or through waterways. One of the best known is the Pacific HVDC Intertie, which interconnects southern California with Oregon. Another DC system is the ±400 kV Coal Creek-Dickenson lines. Another famous HVDC system is the interconnection between England and France, which uses underwater cables. In Canada, Vancouver Island is supplied through a DC cable.

In an HVDC system the AC voltage is rectified and a DC line transmits the energy. At the end of the line an inverter converts the DC voltage to AC. A typical example is the Pacific HVDC Intertie that operates with ±500 kV voltage and interconnects Southern California with the hydro stations in Oregon.

Figure 4.7 shows a guyed tower arrangement used on the Pacific HVDC Intertie. Four guy wires balance the lattice tower. The tower carries a pair of two-conductor bundles supported by suspension insulators.

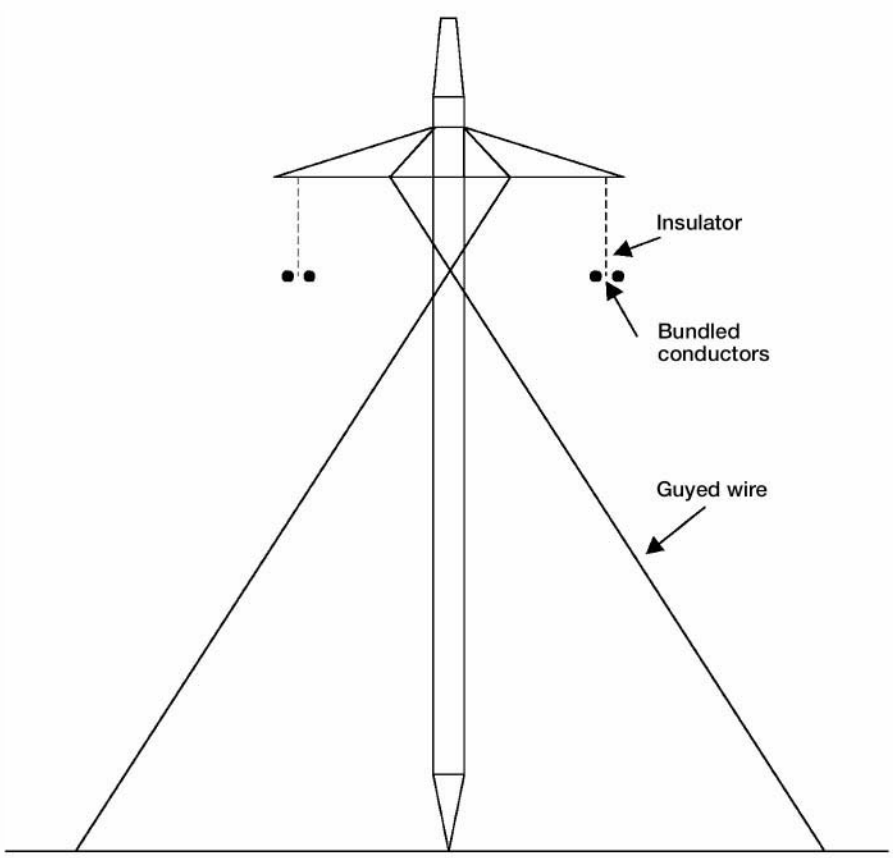

FIGURE 4.7 HVDC tower arrangement.

Sub-Transmission Lines

Typical sub-transmission lines interconnect the high-voltage substations with distribution stations within a city. The voltage of the subtransmission system is between 46 kV, 69 kV, and 115 kV. The maximum length of sub-transmission lines is in the range of 50–60 miles. Most subtransmission lines are located along streets and alleys. Figure 4.8 shows a typical sub-transmission system.

This system operates in a looped mode to enhance continuity of service. This arrangement assures that the failure of a line will not interrupt the customer's power.

Figure 4.9 shows a typical double-circuit sub-transmission line, with a wooden pole and post-type insulators. Steel tube or concrete towers are also used. The line has a single conductor in each phase. Post insulators hold the conductors without metal cross arms. One grounded shield conductor on the top of the tower shields the phase conductors from lightning. The shield conductor is grounded at each tower. Plate or vertical tube electrodes (ground rod) are used for grounding.

Distribution Lines

The distribution system is a radial system. Figure 4.10 shows the concept of a typical urban distribution system. In this system a main three-phase feeder goes through the main street. Single-phase subfeeders supply the crossroads. Secondary mains are supplied through transformers. The consumer's service drops supply the individual loads. The voltage of the distribution system is between 4.6 and 25 kV. Distribution feeders can supply loads up to 20–30 miles.

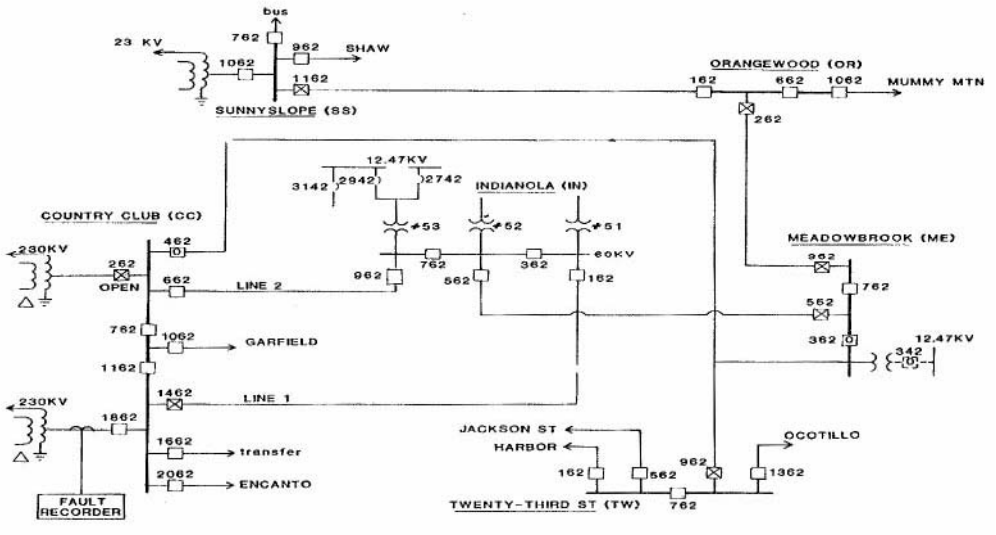

FIGURE 4.8 Subtransmission system.

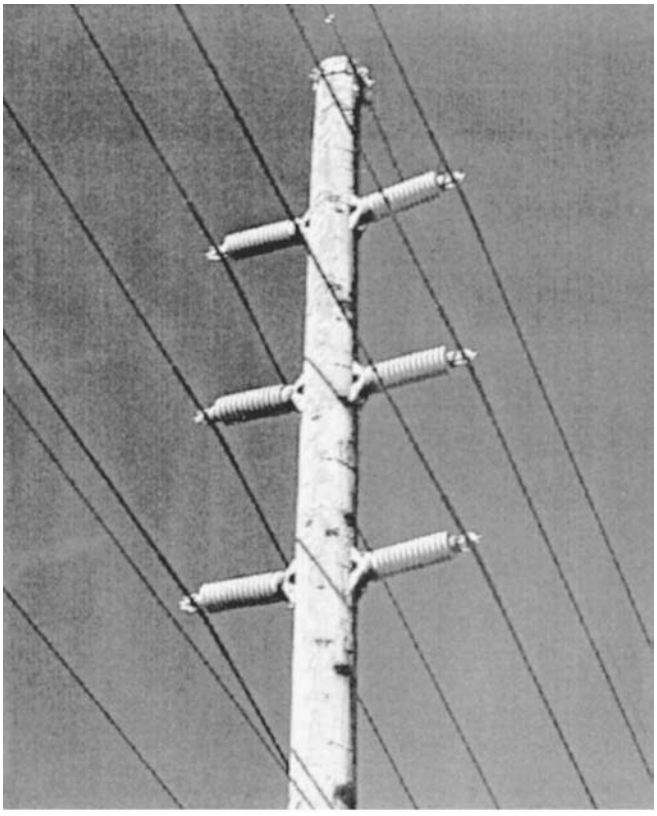

FIGURE 4.9 Typical subtransmission line.

Many distribution lines in the U.S. have been built with a wood pole and cross arm. The wood is treated with an injection of creosote or other wood preservative that protects the wood from rotting and termites. Most poles are buried in a hole without foundation. Lines built recently may use a simple

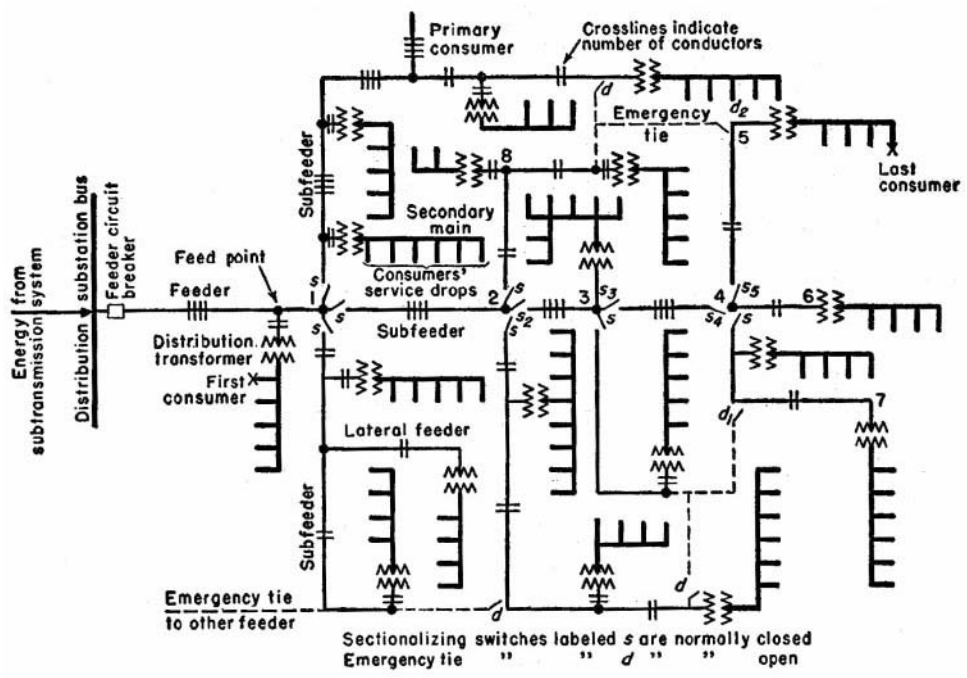

FIGURE 4.10 Concept of radial distribution system.

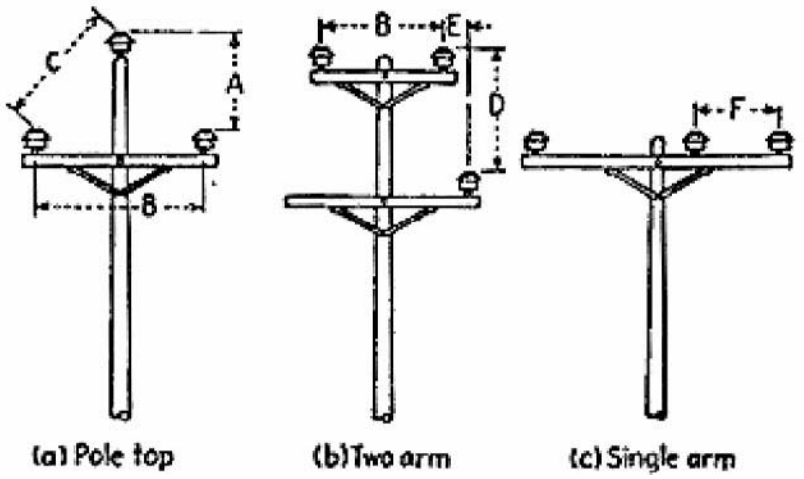

FIGURE 4.11 Distribution line arrangements.

concrete block foundation. Small porcelain or non-ceramic, pin-type insulators support the conductors. The insulator pin is grounded to eliminate leakage current, which can cause burning of the wood tower. A simple vertical copper rod is used for grounding. Shield conductors are seldom used. Figure 4.11 shows typical distribution line arrangements.

Because of the lack of space in urban areas, distribution lines are often installed on the subtransmission line towers. This is referred to as underbuild. A typical arrangement is shown in Figure 4.12.

The figure shows that small porcelain insulators support the conductors. The insulators are installed on metal brackets that are bolted onto the wood tower. This arrangement reduces the right-of-way requirement and saves space.

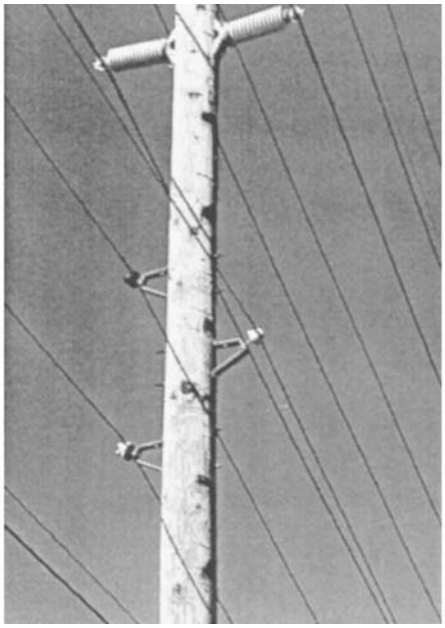

FIGURE 4.12 Distribution line installed under the subtransmission line.

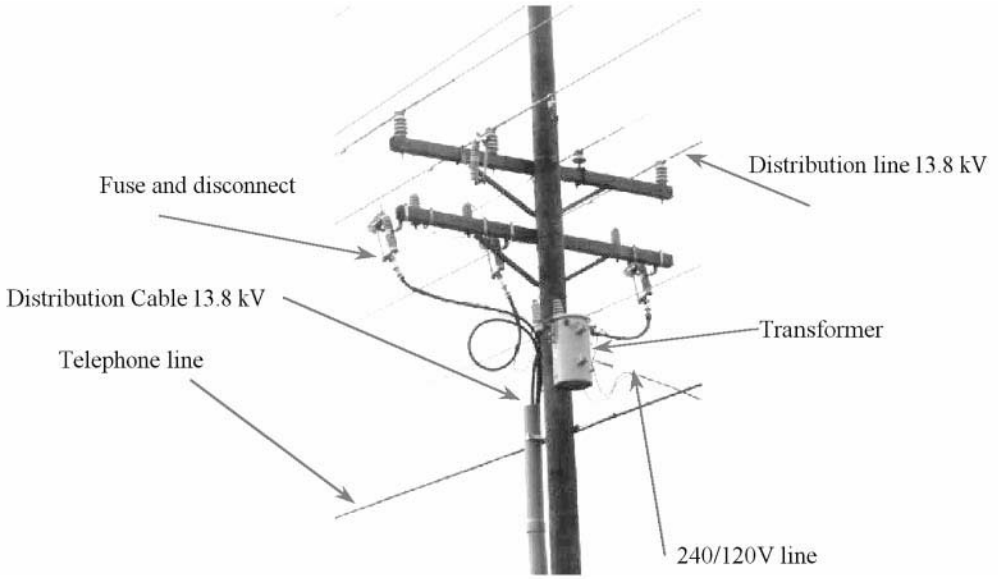

FIGURE 4.13 Service drop.

Transformers mounted on distribution poles frequently supply individual houses or groups of houses. Figure 4.13 shows a typical transformer pole, consisting of a transformer that supplies a 240/120-V service drop, and a 13.8-kV distribution cable. The latter supplies a nearby shopping center, located on the other side of the road. The 13.8-kV cable is protected by a cut-off switch that contains a fuse mounted on a pivoted insulator. The lineman can disconnect the cable by pulling the cut-off open with a long insulated rod (hot stick).

References

Electric Power Research Institute, *Transmission Line Reference Book, 345 kV and Above,* Electric Power Research Institute, Palo Alto, CA, 1987.

Fink, D.G. and Beaty, H.W., *Standard Hand Book for Electrical Engineering,* 11th ed., McGraw-Hill, New York, Sec. 18, 1978.

Gonen, T., *Electric Power Distribution System Engineering,* Wiley, New York, 1986.

Gonen, T., *Electric Power Transmission System Engineering,* Wiley, New York, 1986.

Zaborsky J.W. and Rittenhouse, *Electrical Power Transmission,* 3rd ed. The Rensselaer Bookstore, Troy, NY, 1969.

4.2 Transmission Line Structures

Joe C. Pohlman

An overhead transmission line (OHTL) is a very complex, continuous, electrical/mechanical system. Its function is to transport power safely from the circuit breaker on one end to the circuit breaker on the other. It is physically composed of many individual components made up of different materials having a wide variety of mechanical properties, such as:

- flexible vs. rigid
- ductile vs. brittle
- variant dispersions of strength
- wear and deterioration occurring at different rates when applied in different applications within one micro-environment or in the same application within different micro-environments

This discussion will address the nature of the structures which are required to provide the clearances between the current-carrying conductors, as well as their safe support above the earth. During this discussion, reference will be made to the following definitions:

Capability:	Capacity (×) availability
Reliability level:	Ability of a line (or component) to perform its expected capability
Security level:	Ability of a line to restrict progressive damage after the failure of the first component
Safety level:	Ability of a line to perform its function safely

Traditonal Line Design Practice

Present line design practice views the support structure as an isolated element supporting half span of conductors and overhead ground wires (OHGWs) on either side of the structure. Based on the voltage level of the line, the conductors and OHGWs are configured to provide, at least, the minimum clearances mandated by the National Electrical Safety Code (NESC) (IEEE, 1990), as well as other applicable codes. This configuration is designed to control the separation of:

- energized parts from other energized parts
- energized parts from the support structure of other objects located along the r-o-w
- energized parts above ground

The NESC divides the U.S. into three large global loading zones: heavy, medium, and light and specifies radial ice thickness/wind pressure/temperature relationships to define the minimum load levels that must be used within each loading zone. In addition, the Code introduces the concept of an Overload Capacity Factor (OCF) to cover uncertainties stemming from the:

- likelihood of occurrence of the specified load
- dispersion of structure strength

- grade of construction
- deterioration of strength during service life
- structure function (suspension, dead-end, angle)
- other line support components (guys, foundations, etc.)

Present line design practice normally consists of the following steps:

1. The owning utility prepares an agenda of loading events consisting of:
   - mandatory regulations from the NESC and other codes
   - climatic events believed to be representative of the line's specific location
   - contingency loading events of interest; i.e., broken conductor
   - special requirements and expectations

Each of these loading events is multiplied by its own OCF to cover uncertainties associated with it to produce an agenda of final ultimate design loads (see Fig. 4.14).

2. A ruling span is identified based on the sag/tension requirements for the preselected conductor.
3. A structure type is selected based on past experience or on recommendations of potential structure suppliers.
4. Ultimate design loads resulting from the ruling span are applied statically as components in the longitudinal, transverse, and vertical directions, and the structure deterministically designed.
5. Using the loads and structure configuration, ground line reactions are calculated and used to accomplish the foundation design.
6. The ruling span line configuration is adjusted to fit the actual r-o-w profile.
7. Structure/foundation designs are modified to account for variation in actual span lengths, changes in elevation, and running angles.
8. Since most utilities expect the tangent structure to be the weakest link in the line system, hardware, insulators, and other accessory components are selected to be stronger than the structure.

Inasmuch as structure types are available in a wide variety of concepts, materials, and costs, several iterations would normally be attempted in search of the most cost effective line design based on total installed costs (see Fig. 4.15).

While deterministic design using static loads applied in quadrature is a convenient mathematical approach, it is obviously not representative of the real-world exposure of the structural support system. OHTLs are tens of yards wide and miles long and usually extend over many widely variant microtopographical and microclimatic zones, each capable of delivering unique events consisting of magnitude of

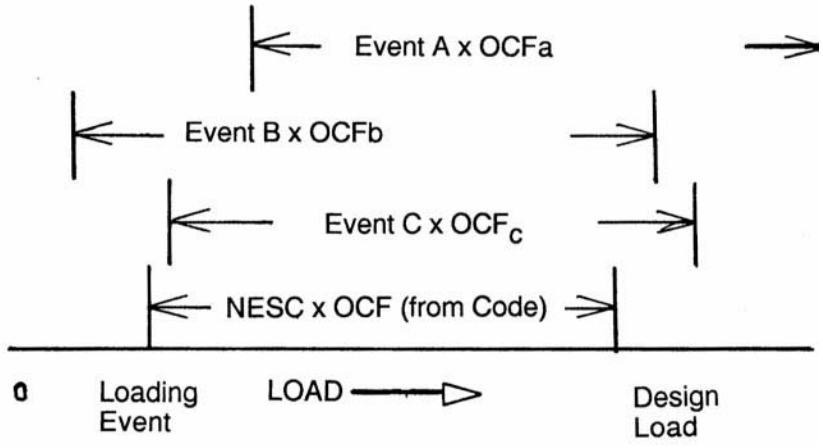

FIGURE 4.14 Development of a loading agenda.

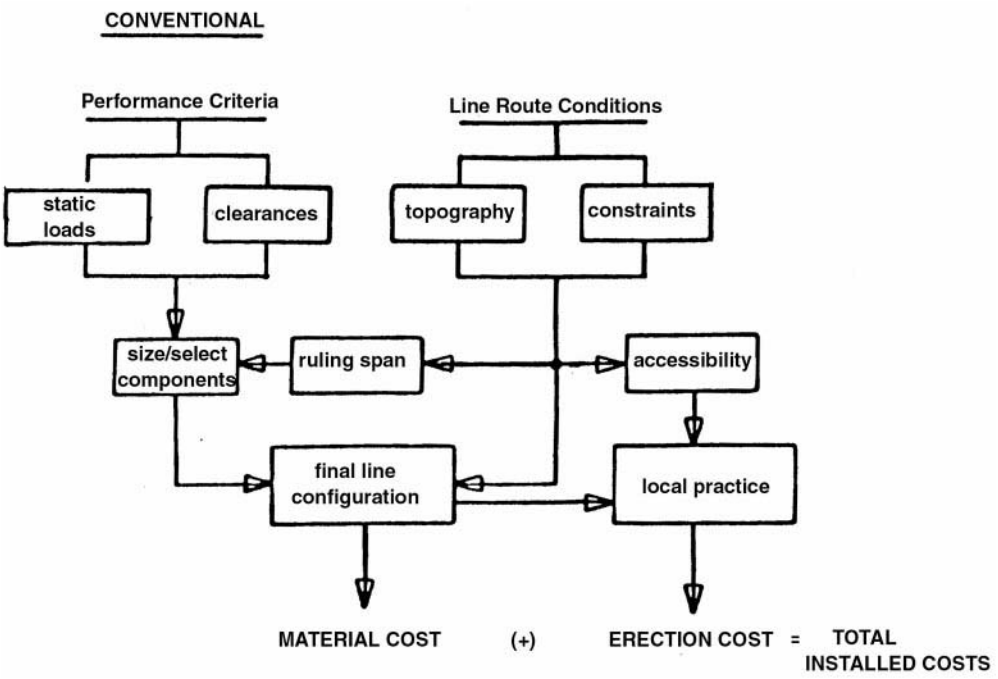

FIGURE 4.15 Search for cost effectiveness.

load at a probability-of-occurrence. That component along the r-o-w that has the highest probability of occurrence of failure from a loading event becomes the weak link in the structure design and establishes the reliability level for the total line section. Since different components are made from different materials that have different response characteristics and that wear, age, and deteriorate at different rates, it is to be expected that the weak link:

- will likely be different in different line designs
- will likely be different in different site locations within the same line
- can change from one component to another over time

Structure Types in Use

Structures come in a wide variety of styles:

- lattice towers
- cantilevered or guyed poles and masts
- framed structures
- combinations of the above

They are available in a wide variety of materials:

- Metal
  - galvanized steel and aluminum rods, bars and rolled shapes
  - fabricated plate
  - tubes
- Concrete
  - spun with pretensioned or post-tensioned reinforcing cable
  - statically cast nontensioned reinforcing steel
  - single or multiple piece

- Wood
  - as grown
  - glued laminar
- Plastics
- Composites
- Crossarms and braces
- Variations of all of the above

Depending on their style and material contents, structures vary considerably in how they respond to load. Some are rigid. Some are flexible. Those structures that can safely deflect under load and absorb energy while doing so, provide an ameliorating influence on progressive damage after the failure of the first element (Pohlman and Lummis, 1969).

Factors Affecting Structure Type Selection

There are usually many factors that impact on the selection of the structure type for use in an OHTL. Some of the more significant are briefly identified below.

Erection Technique: It is obvious that different structure types require different erection techniques. As an example, steel lattice towers consist of hundreds of individual members that must be bolted together, assembled, and erected onto the four previously installed foundations. A tapered steel pole, on the other hand, is likely to be produced in a single piece and erected directly on its previously installed foundation in one hoist. The lattice tower requires a large amount of labor to accomplish the considerable number of bolted joints, whereas the pole requires the installation of a few nuts applied to the foundation anchor bolts plus a few to install the crossarms. The steel pole requires a large-capacity crane with a high reach which would probably not be needed for the tower. Therefore, labor needs to be balanced against the need for large, special equipment and the site's accessibility for such equipment.

Public Concerns: Probably the most difficult factors to deal with arise as a result of the concerns of the general public living, working, or coming in proximity to the line. It is common practice to hold public hearings as part of the approval process for a new line. Such public hearings offer a platform for neighbors to express individual concerns that generally must be satisfactorily addressed before the required permit will be issued. A few comments demonstrate this problem.

The general public usually perceives transmission structures as "eyesores" and distractions in the local landscape. To combat this, an industry study was made in the late 1960s (Dreyfuss, 1968) sponsored by the Edison Electric Institute and accomplished by Henry Dreyfuss, the internationally recognized industrial designer. While the guidelines did not overcome all the objections, they did provide a means of satisfying certain very highly controversial installations (Pohlman and Harris, 1971).

Parents of small children and safety engineers often raise the issue of lattice masts, towers, and guys, constituting an "attractive challenge" to determined climbers, particularly youngsters.

Inspection, Assessment, and Maintenance: Depending on the owning utility, it is likely their in-house practices will influence the selection of the structure type for use in a specific line location. Inspections and assessment are usually made by human inspectors who use diagnostic technologies to augment their personal senses of sight and touch. The nature and location of the symptoms of critical interest are such that they can be most effectively examined from specific perspectives. Inspectors must work from the most advantageous location when making inspections. Methods can include observations from ground or fly-by patrol, climbing, bucket trucks, or helicopters. Likewise, there are certain maintenance activities that are known or believed to be required for particular structure types. The equipment necessary to maintain the structure should be taken into consideration during the structure type selection process to assure there will be no unexpected conflict between maintenance needs and r-o-w restrictions.

Future Upgrading or Uprating: Because of the difficulty of procuring r-o-w's and obtaining the necessary permits to build new lines, many utilities improve their future options by selecting structure types for current line projects that will permit future upgrading and/or uprating initiatives.

TANGENT AND LIGHT ANGLE SUSPENSION TOWER – 345 DOUBLE CIRCUIT
OHGW: Two 7/16" diameter galvanized steel strand
Conductors: Six twin conductor bundles of 1431 KCM 45/7 ACSR
Weight span: 1,650 feet
Wind span: 1,100 feet
Line angle: 0° to 2°

Load Case	Load Event	Radial Ice (")	Wind Pressure Wire (psf)	Wind Pressure Structure (psf)	Load Direction	OCF
1	NESC Heavy	1/2	4	5.1	T L V	2.54 1.65 1.27
2	One broken OHGW combined with wind and ice	1/2	8	13.0	T L V	1.0 1.0 1.0
3	One broken conductor bundle combined with wind and ice	1/2	8	13.0	T L V	1.0 1.0 1.0
4	Heavy wind	0	16	42.0	T L V	1.0 1.0 1.0
5	Wind on bare tower (no conductors or OHGW)	0	0	46.2	T L V	1.0 1.0 1.0
6	Vertical load at any OHGW support of 3780 lbs. (not simultaneously)	0	0	0	V	1.0
7	Vertical load at any conductor support of 17,790 lbs. (not simultaneously)	0	0	0	V	1.0

FIGURE 4.16 Example of loading agenda.

Current Deterministic Design Practice

Figure 4.16 shows a loading agenda for a double-circuit, 345-kV line built in the upper Midwest region of the U.S. on steel lattice towers. Over and above the requirements of the NESC, the utility had specified these loading events:

- a heavy wind condition (Pohlman and Harris, 1971)
- a wind on bare tower (Carton and Peyrot, 1992)
- two maximum vertical loads on the OHGW and conductor supports (Osterdorp, 1998; CIGRE, 1995)
- two broken wire contingencies (Pohlman and Lummis, 1969; Dreyfuss, 1968)

It was expected that this combination of loading events would result in a structural support design with the capability of sustaining 50-year recurrence loads likely to occur in the general area where the line was built. Figure 4.17 shows that different members of the structure, as designed, were under the control of different loading cases from this loading agenda. While interesting, this does not:

- provide a way to identify weak links in the support structure
- provide a means for predicting performance of the line system
- provide a framework for decision-making

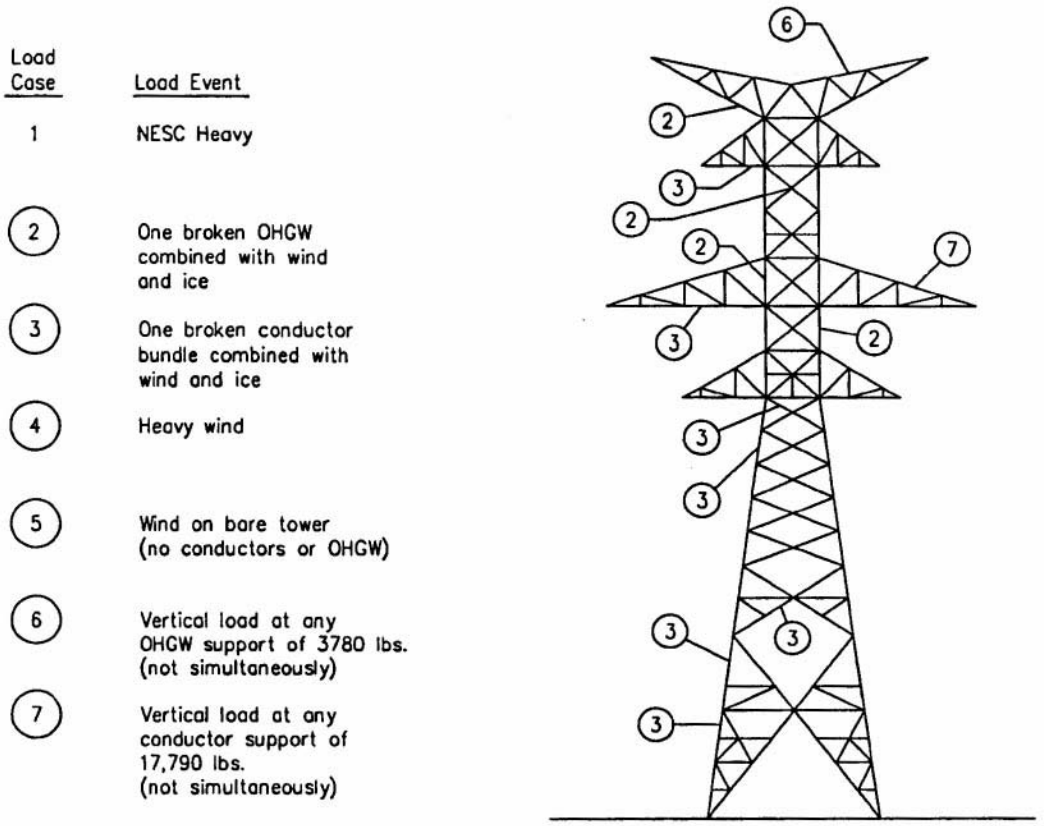

FIGURE 4.17 Results of deterministic design.

Reliability Level

The shortcomings of deterministic design can be demonstrated by using 3D modeling/simulation technology which is in current use (Carton and Peyrot, 1992) in forensic investigation of line failures. The approach is outlined in Fig. 4.18. After the structure (as designed) is properly modeled, loading events of increasing magnitude are analytically applied from different directions until the actual critical capacity for each key member of interest is reached. The probability of occurrence for those specific loading events can then be predicted for the specific location of that structure within that line section by professionals skilled in the art of micrometerology.

Figure 4.19 shows a few of the key members in the example for Fig. 4.17:

- The legs had a probability of failure in that location of once in 115 years.
- Tension chords in the conductor arm and OHGW arm had probabilities of failure of 110 and 35 years, respectively.
- A certain wind condition at an angle was found to be critical for the foundation design with a probability of occurrence at that location of once in 25 years.

Some interesting observations can be drawn:

- The legs were conservatively designed.
- The loss of an OHGW is a more likely event than the loss of a conductor.
- The foundation was found to be the weak link.

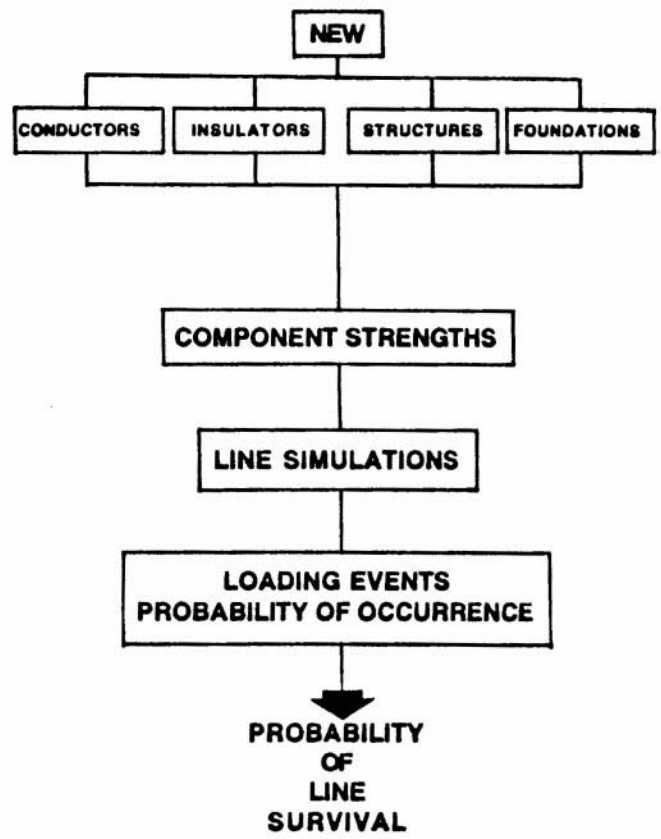

FIGURE 4.18 Line simulation study.

Member	Controlling Climatic Load Condition	Controlling Load Return Period (years)
Legs	Wind, no ice	115
Tension chord of conductor arm	Ice, no wind	110
Tension chord of OHGW arm	Ice, no wind	35
Foundation	Wind, no ice	25

Controlling Climatic Loads

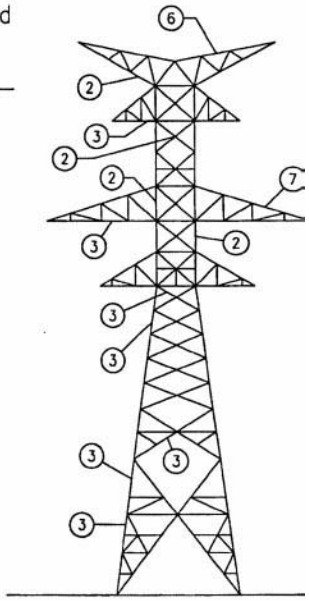

FIGURE 4.19 Simulation study output.

In addition to the interesting observations on relative reliability levels of different components within the structural support system, the output of the simulation study also provides the basis for a decision-making process which can be used to determine the cost effectiveness of management initiatives. Under the simple laws of statistics, when there are two independent outcomes to an event, the probability of the first outcome is equal to one minus the probability of the second. When these outcomes are survival and failure:

$$\begin{gathered}\text{Annual probability of survival} = 1 - \text{Annual probability of failure} \\ \text{Ps} = 1 - \text{Pf}\end{gathered} \tag{4.1}$$

If it is desired to know what the probability of survival is over an extended length of time, i.e., n years of service life:

$$\left[\text{Ps1} \times \text{Ps2} \times \text{Ps3} \times \ldots \text{Psn}\right] = \left(\text{ps}\right)\text{n} \tag{4.2}$$

Applying this principle to the components in the deterministic structure design and considering a 50-year service life as expected by the designers:

- the legs had a Ps of 65%
- the tension chord in the conductor arm had a Ps of 63%
- the tension chord of the OHGW arm had a Ps of 23%
- the foundation had a Ps of 13%

Security Level

It should be remembered, however, that the failure of every component does not necessarily progress into extensive damage. A comparison of the total risk that would result from the initial failure of components of interest can be accomplished by making a security-level check of the line design (Osterdorp, 1998).

Since the OHTL is a contiguous mechanical system, the forces from the conductors and OHGWs on one side of each tangent structure are balanced and restrained by those on the other side. When a critical component in the conductor/OHGW system fails, energy stored within the conductor system is released suddenly and sets up unbalanced transients that can cause failure of critical components at the next structure. This can set off a cascading effect that will continue to travel downline until it encounters a point in the line strong enough to withstand the unbalance. Unfortunately, a security check of the total line cannot be accomplished from the information describing the one structure in Fig. 4.17; but perhaps some generalized observations can be drawn for demonstration purposes.

Since the structure was designed for broken conductor bundle and broken OHGW contingencies, it appears the line would not be subjected to a cascade from a broken bare conductor, but what if the conductor was coated with ice at the time? Since ice increases the energy trapped within the conductor prior to release, it might be of interest to determine how much ice would be "enough." Three-dimensional modeling would be employed to simulate ice coating of increasing thicknesses until the critical amount is defined. A proper micrometerological study could then identify the probability of occurrence of a storm system capable of delivering that amount of ice at that specific location.

In the example, a wind condition with no ice was identified that would be capable of causing foundation failure once every 25 years. A security-level check would predict the amount of resulting losses and damages that would be expected from this initiating event compared to the broken-conductor-under-ice-load contingencies.

Improved Design Approaches

The above discussion indicates that technologies are available today for assessing the true capability of an OHTL that was created using the conventional practice of specifying ultimate static loads and designing a structure that would properly support them. Because there are many different structure types made

from different materials, this was not always straightforward. Accordingly, many technical societies prepared guidelines on how to design the specific structure needed. These are listed in the accompanying references. The interested reader should realize that these documents are subject to periodic review and revision and should, therefore, seek the most current version.

While the technical fraternity recognizes that the mentioned technologies are useful for analyzing existing lines and determining management initiatives, something more direct for designing new lines is needed. There are many efforts under way. The most promising of these is *Improved Design Criteria of OHTLs Based on Reliability Concepts* (Ostendorp, 1998), currently under development by CIGRE Study Committee 22: Recommendations for Overhead Lines. Appendix A outlines the methodology involved in words and in a diagram. The technique is based on the premise that loads and strengths are stochastic variables and the combined reliability is computable if the statistical functions of loads and strength are known. The referenced report has been circulated internationally for trial use and comment. It is expected that the returned comments will be carefully considered, integrated into the report, and the final version submitted to the International Electrotechnical Commission (IEC) for consideration as an International Standard.

References

1. Carton, T. and Peyrot, A., Computer Aided Structural and Geometric Design of Power Lines, *IEEE Trans. on Power Line Syst.*, 7(1), 1992.
2. Dreyfuss, H., *Electric Transmission Structures,* Edison Electric Institute Publication No. 67-61, 1968.
3. Guide for the Design and Use of Concrete Poles, ASCE 596-6, 1987.
4. Guide for the Design of Prestressed Concrete Poles, ASCE/PCI Joint Commission on Concrete Poles, February, 1992. Draft.
5. Guide for the Design of Transmission Towers, *ASCE Manual on Engineering Practice,* 52, 1988.
6. Guide for the Design Steel Transmission Poles, *ASCE Manual on Engineering Practice,* 72, 1990.
7. IEEE Trial-Use Design Guide for Wood Transmission Structures, IEEE Std. 751, February, 1991.
8. *Improved Design Criteria of Overhead Transmission Lines Based on Reliability Concepts, CIGRE SC-22 Report,* October 1995.
9. *National Electrical Safety Code ANSI C-2,* IEEE, 1990.
10. Ostendorp, M., Longitudinal Loading and Cascading Failure Assessment for Transmission Line Upgrades, *ESMO Conference '98,* Orlando, Florida, April 26-30, 1998.
11. Pohlman, J. and Harris, W., Tapered Steel H-Frames Gain Acceptance Through Scenic Valley, *Electric Light and Power Magazine,* 48(vii), 55-58, 1971.
12. Pohlman, J. and Lummis, J., Flexible Structures Offer Broken Wire Integrity at Low Cost, *Electric Light and Power,* 46(V, 144-148.4), 1969.

Appendix A — General Design Criteria — Methodology

The recommended methodology for designing transmission line components is summarized in Fig. 4.20 and can be described as follows:

a) Gather preliminary line design data and available climatic data.[1]
b1) Select the reliability level in terms of return period of design loads. (Note: Some national regulations and/or codes of practice sometimes impose design requirements, directly or indirectly, that may restrict the choice offered to designers).
b2) Select the security requirements (failure containment).
b3) List safety requirements imposed by mandatory regulations and construction and maintenance loads.
c) Calculate climatic variables corresponding to selected return period of design loads.

[1]In some countries, design wind speed, such as the 50-year return period, is given in National Standards.

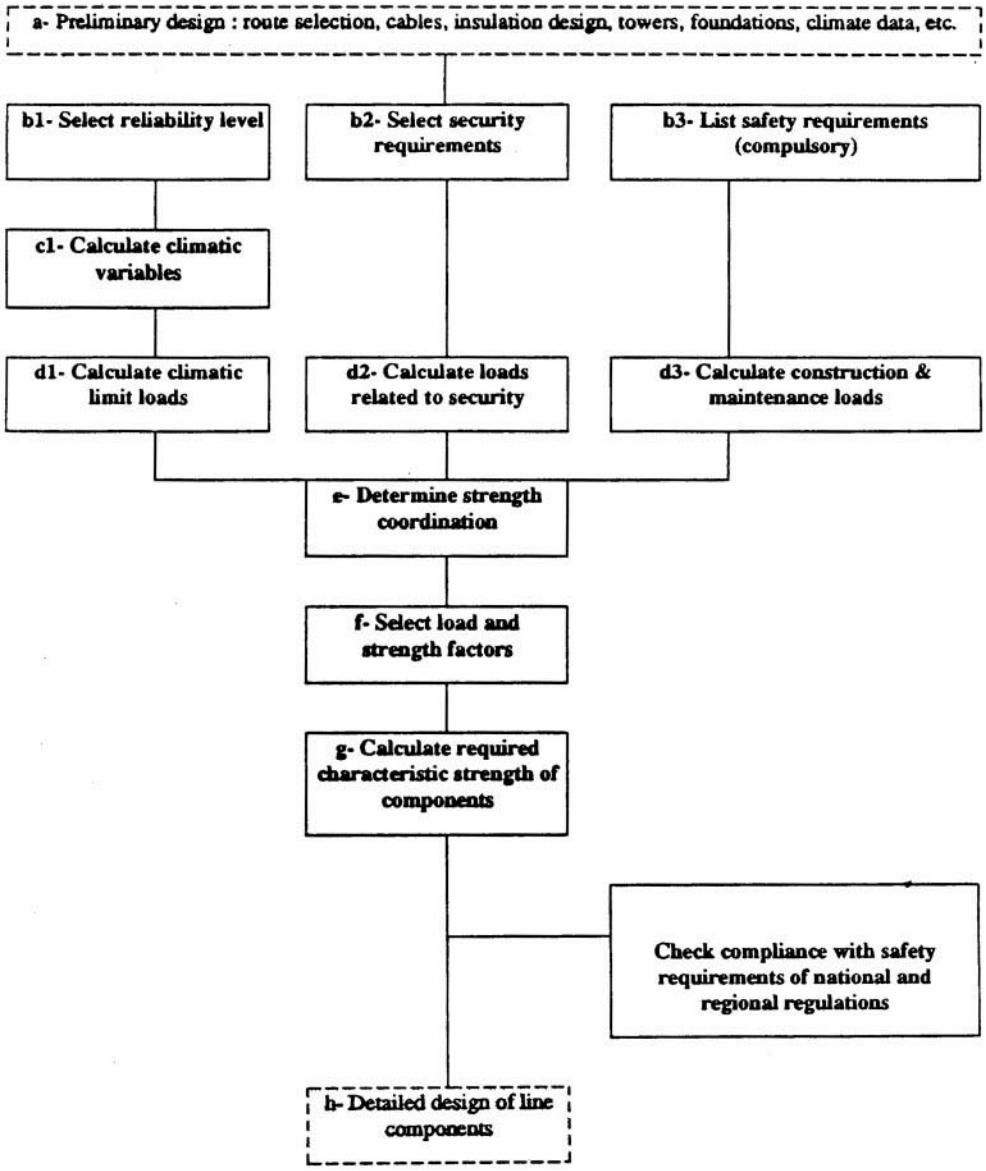

FIGURE 4.20 Methodology.

d1) Calculate climatic limit loadings on components.
d2) Calculate loads corresponding to security requirements.
d3) Calculate loads related to safety requirements during construction and maintenance.
e) Determine the suitable strength coordination between line components.
f) Select appropriate load and strength factors applicable to load and strength equations.
g) Calculate the characteristic strengths required for components.
h) Design line components for the above strength requirements.

This document deals with items b) to g). Items a) and h) are not part of the scope of this document. They are identified by a dotted frame in Fig. 4.20.

Source: Improved design criteria of overhead transmission lines based on reliability concepts, *CIGRE SC22 Report,* October, 1995.

4.3 Insulators and Accessories

George G. Karady and R.G. Farmer

Electric insulation is a vital part of an electrical power system. Although the cost of insulation is only a small fraction of the apparatus or line cost, line performance is highly dependent on insulation integrity. Insulation failure may cause permanent equipment damage and long-term outages. As an example, a short circuit in a 500-kV system may result in a loss of power to a large area for several hours. The potential financial losses emphasize the importance of a reliable design of the insulation.

The insulation of an electric system is divided into two broad categories:

1. Internal insulation
2. External insulation

Apparatus or equipment has mostly internal insulation. The insulation is enclosed in a grounded housing which protects it from the environment. External insulation is exposed to the environment. A typical example of internal insulation is the insulation for a large transformer where insulation between turns and between coils consists of solid (paper) and liquid (oil) insulation protected by a steel tank. An overvoltage can produce internal insulation breakdown and a permanent fault.

External insulation is exposed to the environment. Typical external insulation is the porcelain insulators supporting transmission line conductors. An overvoltage caused by flashover produces only a temporary fault. The insulation is self-restoring.

This section discusses external insulation used for transmission lines and substations.

Electrical Stresses on External Insulation

The external insulation (transmission line or substation) is exposed to electrical, mechanical, and environmental stresses. The applied voltage of an operating power system produces electrical stresses. The weather and the surroundings (industry, rural dust, oceans, etc.) produce additional environmental stresses. The conductor weight, wind, and ice can generate mechanical stresses. The insulators must withstand these stresses for long periods of time. It is anticipated that a line or substation will operate for more than 20–30 years without changing the insulators. However, regular maintenance is needed to minimize the number of faults per year. A typical number of insulation failure-caused faults is 0.5–10 per year, per 100 mi of line.

Transmission Lines and Substations

Transmission line and substation insulation integrity is one of the most dominant factors in power system reliability. We will describe typical transmission lines and substations to demonstrate the basic concept of external insulation application.

Figures 4.21 shows a high-voltage transmission line. The major components of the line are:

1. Conductors
2. Insulators
3. Support structure tower

The insulators are attached to the tower and support the conductors. In a suspension tower, the insulators are in a vertical position or in a V-arrangement. In a dead-end tower, the insulators are in a horizontal position. The typical transmission line is divided into sections and two dead-end towers terminate each section. Between 6 and 15 suspension towers are installed between the two dead-end towers. This sectionalizing prevents the propagation of a catastrophic mechanical fault beyond each section. As an example, a tornado caused collapse of one or two towers could create a domino effect, resulting in the collapse of many miles of towers, if there are no dead ends.

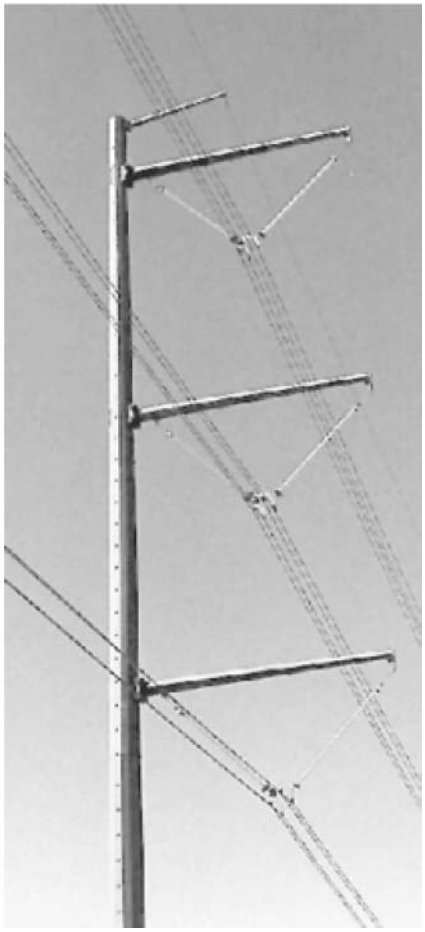

FIGURE 4.21 A 500-kV suspension tower with V string insulators.

Figure 4.22 shows a lower voltage line with post-type insulators. The rigid, slanted insulator supports the conductor. A high-voltage substation may use both suspension and post-type insulators.

Electrical Stresses

The electrical stresses on insulation are created by:

1. Continuous power frequency voltages
2. Temporary overvoltages
3. Switching overvoltages
4. Lightning overvoltages

Continuous Power Frequency Voltages

The insulation has to withstand normal operating voltages. The operating voltage fluctuates from changing load. The normal range of fluctuation is around ±10%. The line-to-ground voltage causes the voltage stress on the insulators. As an example, the insulation requirement of a 220-kV line is at least:

$$1.1 \times \frac{220\ \text{kV}}{\sqrt{3}} \cong 140\ \text{kV} \tag{4.3}$$

FIGURE 4.22 69-kV transmission line with post insulators.

This voltage is used for the selection of the number of insulators when the line is designed. The insulation can be laboratory tested by measuring the dry flashover voltage of the insulators. Because the line insulators are self-restoring, flashover tests do not cause any damage. The flashover voltage must be larger than the operating voltage to avoid outages. For a porcelain insulator, the required dry flashover voltage is about 2.5–3 times the rated voltage. A significant number of the apparatus standards recommend dry withstand testing of every kind of insulation to be two (2) times the rated voltage plus 1 kV for 1 min of time. This severe test eliminates most of the deficient units.

Temporary Overvoltages

These include ground faults, switching, load rejection, line energization and resonance, cause power frequency, or close-to-power frequency, and relatively long duration overvoltages. The duration is from 5 sec to several minutes. The expected peak amplitudes and duration are listed in Table 4.1.

The base is the crest value of the rated voltage. The dry withstand test, with two times the maximum operating voltage plus 1 kV for 1 minute, is well-suited to test the performance of insulation under temporary overvoltages.

TABLE 4.1 Expected Amplitude of Temporary Overvoltages

Type of Overvoltage	Expected Amplitude	Duration
Fault overvoltages		
Effectively grounded	1.3 per unit	1 sec
Resonant grounded	1.73 per unit or greater	10 sec
Load rejection		
System substation	1.2 per unit	1–5 sec
Generator station	1.5 per unit	3 sec
Resonance	3 per unit	2–5 min
Transformer energization	1.5–2.0 per unit	1–20 sec

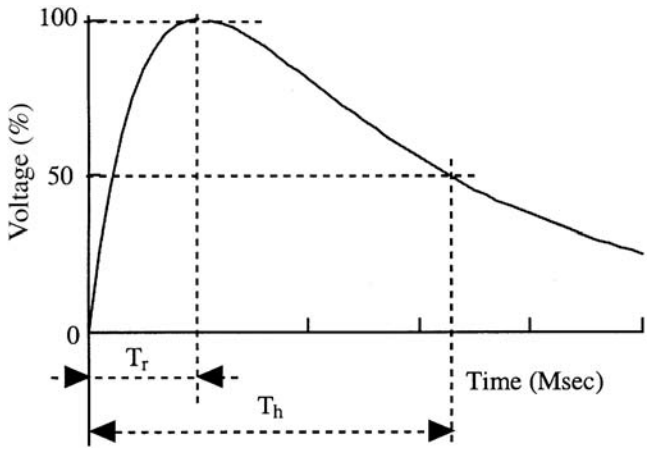

FIGURE 4.23 Switching overvoltages. T_r = 20–5000 μsec, T_h < 20,000 μsec, where T_r is the time-to-crest value and T_h is the time-to-half value.

Switching Overvoltages

The opening and closing of circuit breakers causes switching overvoltages. The most frequent causes of switching overvoltages are fault or ground fault clearing, line energization, load interruption, interruption of inductive current, and switching of capacitors.

Switching produces unidirectional or oscillatory impulses with durations of 5000–20,000 μsec. The amplitude of the overvoltage varies between 1.8 and 2.5 per unit. Some modern circuit breakers use pre-insertion resistance, which reduces the overvoltage amplitude to 1.5–1.8 per unit. The base is the crest value of the rated voltage.

Switching overvoltages are calculated from computer simulations that can provide the distribution and standard deviation of the switching overvoltages. Figure 4.23 shows typical switching impulse voltages. Switching surge performance of the insulators is determined by flashover tests. The test is performed by applying a standard impulse with a time to crest of 250 μsec and time to half value of 5000 μsec. The test is repeated 20 times at different voltage levels and the number of flashovers is counted at each voltage level. These represent the statistical distribution of the switching surge impulse flashover probability. The correlation of the flashover probability with the calculated switching impulse voltage distribution gives the probability, or risk, of failure. The measure of the risk of failure is the number of flashovers expected by switching surges per year.

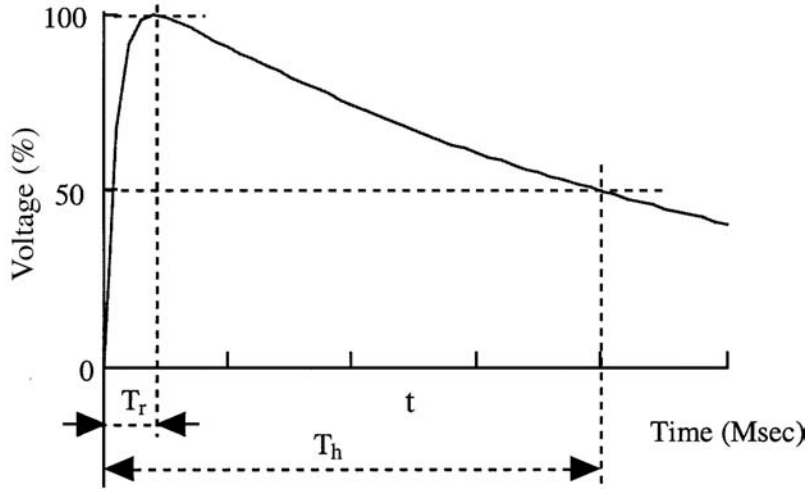

FIGURE 4.24 Lightning overvoltages. T_r = 0.1–20 μsec, T_h 20–200 μsec, where T_r is the time-to-crest value and T_h is the time-to-half value.

Lightning Overvoltages

Lightning overvoltages are caused by lightning strikes:

1. to the phase conductors
2. to the shield conductor (the large current-caused voltage drop in the grounding resistance may cause flashover to the conductors [back flash]).
3. to the ground close to the line (the large ground current induces voltages in the phase conductors).

Lighting strikes cause a fast-rising, short-duration, unidirectional voltage pulse. The time-to-crest is between 0.1–20 μsec. The time-to-half value is 20–200 μsec.

The peak amplitude of the overvoltage generated by a direct strike to the conductor is very high and is practically limited by the subsequent flashover of the insulation. Shielding failures and induced voltages cause somewhat less overvoltage. Shielding failure caused overvoltage is around 500 kV–2000 kV. The lightning-induced voltage is generally less than 400 kV. The actual stress on the insulators is equal to the impulse voltage.

The insulator BIL is determined by using standard lightning impulses with a time-to-crest value of 1.2 μsec and time-to-half value of 50 μsec. This is a measure of the insulation strength for lightning. Figure 4.24 shows a typical lightning pulse.

When an insulator is tested, peak voltage of the pulse is increased until the first flashover occurs. Starting from this voltage, the test is repeated 20 times at different voltage levels and the number of flashovers are counted at each voltage level. This provides the statistical distribution of the lightning impulse flashover probability of the tested insulator.

Environmental Stresses

Most environmental stress is caused by weather and by the surrounding environment, such as industry, sea, or dust in rural areas. The environmental stresses affect both mechanical and electrical performance of the line.

Temperature

The temperature in an outdoor station or line may fluctuate between –50°C and +50°C, depending upon the climate. The temperature change has no effect on the electrical performance of outdoor insulation. It is believed that high temperatures may accelerate aging. Temperature fluctuation causes an increase of mechanical stresses, however it is negligible when well-designed insulators are used.

UV Radiation

UV radiation accelerates the aging of nonceramic composite insulators, but has no effect on porcelain and glass insulators. Manufacturers use fillers and modified chemical structures of the insulating material to minimize the UV sensitivity.

Rain

Rain wets porcelain insulator surfaces and produces a thin conducting layer most of the time. This reduces the flashover voltage of the insulators. As an example, a 230-kV line may use an insulator string with 12 standard ball-and-socket-type insulators. Dry flashover voltage of this string is 665 kV and the wet flashover voltage is 502 kV. The percentage reduction is about 25%.

Nonceramic polymer insulators have a water-repellent hydrophobic surface that reduces the effects of rain. As an example, with a 230-kV composite insulator, dry flashover voltage is 735 kV and wet flashover voltage is 630 kV. The percentage reduction is about 15%. The insulator's wet flashover voltage must be higher than the maximum temporary overvoltage.

Icing

In industrialized areas, conducting water may form ice due to water-dissolved industrial pollution. An example is the ice formed from acid rain water. Ice deposits form bridges across the gaps in an insulator string that result in a solid surface. When the sun melts the ice, a conducting water layer will bridge the insulator and cause flashover at low voltages. Melting ice-caused flashover has been reported in the Quebec and Montreal areas.

Pollution

Wind drives contaminant particles into insulators. Insulators produce turbulence in airflow, which results in the deposition of particles on their surfaces. The continuous depositing of the particles increases the thickness of these deposits. However, the natural cleaning effect of wind, which blows loose particles away, limits the growth of deposits. Occasionally, rain washes part of the pollution away. The continuous depositing and cleaning produces a seasonal variation of the pollution on the insulator surfaces. However, after a long time (months, years), the deposits are stabilized and a thin layer of solid deposit will cover the insulator. Because of the cleaning effects of rain, deposits are lighter on the top of the insulators and heavier on the bottom. The development of a continuous pollution layer is compounded by chemical changes. As an example, in the vicinity of a cement factory, the interaction between the cement and water produces a tough, very sticky layer. Around highways, the wear of car tires produces a slick, tar-like carbon deposit on the insulator's surface.

Moisture, fog, and dew wet the pollution layer, dissolve the salt, and produce a conducting layer, which in turn reduces the flashover voltage. The pollution can reduce the flashover voltage of a standard insulator string by about 20–25%.

Near the ocean, wind drives salt water onto insulator surfaces, forming a conducting salt-water layer which reduces the flashover voltage. The sun dries the pollution during the day and forms a white salt layer. This layer is washed off even by light rain and produces a wide fluctuation in pollution levels.

The Equivalent Salt Deposit Density (ESDD) describes the level of contamination in an area. Equivalent Salt Deposit Density is measured by periodically washing down the pollution from selected insulators using distilled water. The resistivity of the water is measured and the amount of salt that produces the same resistivity is calculated. The obtained mg value of salt is divided by the surface area of the insulator. This number is the ESDD. The pollution severity of a site is described by the average ESDD value, which is determined by several measurements.

Table 4.2 shows the criteria for defining site severity.

The contamination level is light or very light in most parts of the U.S. and Canada. Only the seashores and heavily industrialized regions experience heavy pollution.

TABLE 4.2 Site Severity (IEEE Definitions)

Description	ESDD (mg/cm^2)
Very light	0–0.03
Light	0.03–0.06
Moderate	0.06–0.1
Heavy	<0.1

TABLE 4.3 Typical Sources of Pollution

Pollution Type	Source of Pollutant	Deposit Characteristics	Area
Rural areas	Soil dust	High resitivity layer, effective rain washing	Large areas
Desert	Sand	Low resistivity	Large areas
Coastal area	Sea salt	Very low resistivity, easily washed by rain	10–20 km from the sea
Industrial	Steel mill, coke plants, chemical plants, generating stations, quarries	High conductivity, extremely difficult to remove, insoluble	Localized to the plant area
Mixed	Industry, highway, desert	Very adhesive, medium resistivity	Localized to the plant area

Typically, the pollution level is very high in Florida and on the southern coast of California. Heavy industrial pollution occurs in the industrialized areas and near large highways. Table 4.3 gives a summary of the different sources of pollution.

The flashover voltage of polluted insulators has been measured in laboratories. The correlation between the laboratory results and field experience is weak. The test results provide guidance, but insulators are selected using practical experience.

Altitude

The insulator's flashover voltage is reduced as altitude increases. Above 1500 feet, an increase in the number of insulators should be considered. A practical rule is a 3% increase of clearance or insulator strings' length per 1000 ft as the elevation increases.

Mechanical Stresses

Suspension insulators need to carry the weight of the conductors and the weight of occasional ice and wind loading.

In northern areas and in higher elevations, insulators and lines are frequently covered by ice in the winter. The ice produces significant mechanical loads on the conductor and on the insulators. The transmission line insulators need to support the conductor's weight and the weight of the ice in the adjacent spans. This may increase the mechanical load by 20–50%.

The wind produces a horizontal force on the line conductors. This horizontal force increases the mechanical load on the line. The wind-force-produced load has to be added vectorially to the weight-produced forces. The design load will be the larger of the combined wind and weight, or ice and wind load.

The dead-end insulators must withstand the longitudinal load, which is higher than the simple weight of the conductor in the half span.

A sudden drop in the ice load from the conductor produces large-amplitude mechanical oscillations, which cause periodic oscillatory insulator loading (stress changes from tension to compression and back).

The insulator's one-minute tension strength is measured and used for insulator selection. In addition, each cap-and-pin or ball-and-socket insulator is loaded mechanically for one minute and simultaneously energized. This mechanical and electrical (M&E) value indicates the quality of insulators. The maximum load should be around 50% of the M&E load.

The Bonneville Power Administration uses the following practical relation to determine the required M&E rating of the insulators.

1. M&E > 5* Bare conductor weight/span
2. M&E > Bare conductor weight + Weight of 3.81 cm (1.5 in) of ice on the conductor (3 lb/sq ft)
3. M&E > 2* (Bare conductor weight + Weight of 0.63 cm (1/4 in) of ice on the conductor and loading from a wind of 1.8 kg/sq ft (4 lb/sq ft)

The required M&E value is calculated from all equations above and the largest value is used.

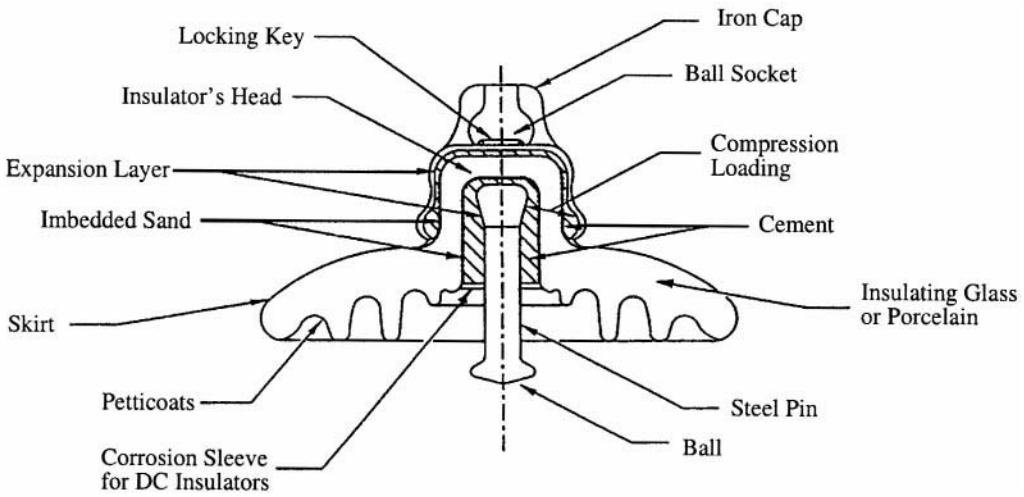

FIGURE 4.25 Cross-section of a standard ball-and-socket insulator.

Ceramic (Porcelain and Glass) Insulators

Materials

Porcelain is the most frequently used material for insulators. Insulators are made of wet, processed porcelain. The fundamental materials used are a mixture of feldspar (35%), china clay (28%), flint (25%), ball clay (10%), and talc (2%). The ingredients are mixed with water. The resulting mixture has the consistency of putty or paste and is pressed into a mold to form a shell of the desired shape. The alternative method is formation by extrusion bars that are machined into the desired shape. The shells are dried and dipped into a glaze material. After glazing, the shells are fired in a kiln at about 1200°C. The glaze improves the mechanical strength and provides a smooth, shiny surface. After a cooling-down period, metal fittings are attached to the porcelain with Portland cement.

Toughened glass is also frequently used for insulators. The melted glass is poured into a mold to form the shell. Dipping into hot and cold baths cools the shells. This thermal treatment shrinks the surface of the glass and produces pressure on the body, which increases the mechanical strength of the glass. Sudden mechanical stresses, such as a blow by a hammer or bullets, will break the glass into small pieces. The metal end-fitting is attached by alumina cement.

Insulator Strings

Most high-voltage lines use ball-and-socket-type porcelain or toughened glass insulators. These are also referred to as "cap and pin." The cross section of a ball-and-socket-type insulator is shown in Fig. 4.25. The porcelain skirt provides insulation between the iron cap and steel pin. The upper part of the porcelain is smooth to promote rain washing and cleaning of the surface. The lower part is corrugated, which prevents wetting and provides a longer protected leakage path. Portland cement attaches the cup and pin. Before the application of the cement, the porcelain is sandblasted to generate a rough surface. A thin expansion layer (e.g., bitumen) covers the metal surfaces. The loading compresses the cement and provides high mechanical strength. The basic technical data of a standard ball-and-socket insulator is as follows:

TABLE 4.4 Technical Data of a Standard Insulator

Diameter	25.4 cm	(10 in.)
Spacing	14.6 cm	(5-3/4 in.)
Leakage distance	305 cm	(12 ft)
Typical operating voltage	10 kV	
Mechanical strength	75 kN	(15 klb)

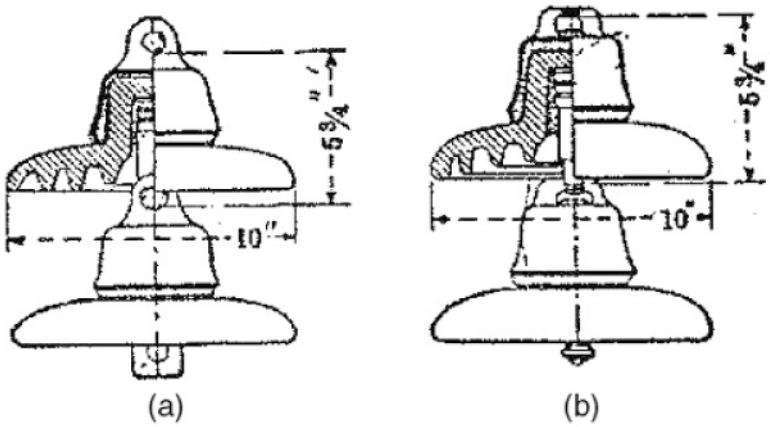

FIGURE 4.26 Insulator string: (a) clevis type, (b) ball-and-socket type.

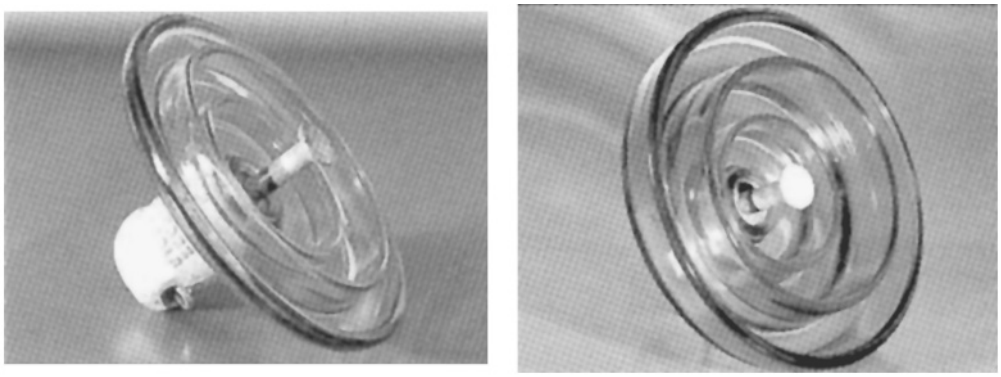

FIGURE 4.27 Standard and fog-type insulators. (Courtesy of Sediver, Inc., Nanterre Cedex, France.)

The metal parts are designed to fail before the porcelain fails as the mechanical load increases. This acts as a mechanical fuse protecting the tower structure.

The ball-and-socket insulators are attached to each other by inserting the ball in the socket and securing the connection with a locking key. Several insulators are connected together to form an insulator string. Figure 4.26 shows a ball-and-socket insulator string and the clevis-type string, which is used less frequently for transmission lines.

Fog-type, long leakage distance insulators are used in polluted areas, close to the ocean, or in industrial environments. Figure 4.27 shows representative fog-type insulators, the mechanical strength of which is higher than standard insulator strength. As an example, a 6 1/2 × 12 1/2 fog-type insulator is rated to 180 kN (40 klb) and has a leakage distance of 50.1 cm (20 in.).

Insulator strings are used for high-voltage transmission lines and substations. They are arranged vertically on support towers and horizontally on dead-end towers. Table 4.5 shows the typical number of insulators used by utilities in the U.S. and Canada in lightly polluted areas.

TABLE 4.5 Typical Number of Standard (5-1/4 ft × 10 in.) Insulators at Different Voltage Levels

Line Voltage (kV)	Number of Standard Insulators
69	4–6
115	7–9
138	8–10
230	12
287	15
345	18
500	24
765	30–35

Post-Type Insulators

Post-type insulators are used for medium- and low-voltage transmission lines, where insulators replace the cross-arm (Fig. 4.23). However, the majority of post insulators are used in substations where insulators support conductors, bus bars, and equipment. A typical example is the interruption chamber of a live tank circuit breaker. Typical post-type insulators are shown in Fig. 4.28.

Older post insulators are built somewhat similar to cap-and-pin insulators, but with hardware that permits stacking of the insulators to form a high-voltage unit. These units can be found in older stations. Modern post insulators consist of a porcelain column, with weather skirts or corrugation on the outside surface to increase leakage distance. For indoor use, the outer surface is corrugated. For outdoor use, a deeper weather shed is used. The end-fitting seals the inner part of the tube to prevent water penetration. Figure 4.28 shows a representative unit used at a substation. Equipment manufacturers use the large post-type insulators to house capacitors, fiber-optic cables and electronics, current transformers, and operating mechanisms. In some cases, the insulator itself rotates and operates disconnect switches.

Post insulators are designed to carry large compression loads, smaller bending loads, and small tension stresses.

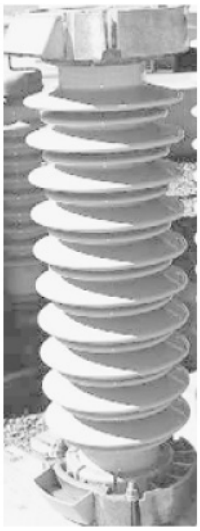

FIGURE 4.28 Post insulators.

Long Rod Insulators

The long rod insulator is a porcelain rod with an outside weather shed and metal end fittings. The long rod is designed for tension load and is applied on transmission lines in Europe. Figure 4.29 shows a typical long rod insulator. These insulators are not used in the U.S. because vandals may shoot the insulators, which will break and cause outages. The main advantage of the long rod design is the elimination of metal parts between the units, which reduces the insulator's length.

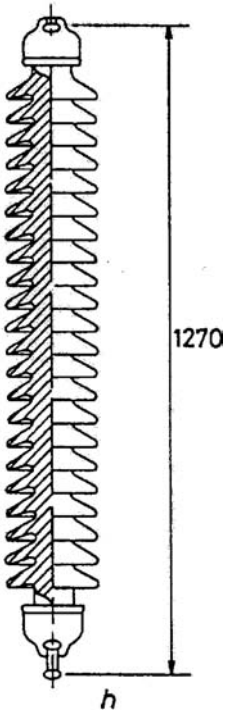

FIGURE 4.29 Long rod insulator.

Nonceramic (Composite) Insulators

Nonceramic insulators use polymers instead of porcelain. High-voltage composite insulators are built with mechanical load-bearing fiberglass rods, which are covered by polymer weather sheds to assure high electrical strength.

The first insulators were built with bisphenol epoxy resin in the mid-1940s and are still used in indoor applications. Cycloaliphatic epoxy resin insulators were introduced in 1957. Rods with weather sheds were molded and cured to form solid insulators. These insulators were tested and used in England for several years. Most of them were exposed to harsh environmental stresses and failed. However, they have been successfully used indoors. The first composite insulators, with fiberglass rods and rubber weather sheds, appeared in the mid-1960s. The advantages of these insulators are:

- Lightweight, which lowers construction and transportation costs.
- More vandalism resistant.

- Higher strength-to-weight ratio, allowing longer design spans.
- Better contamination performance.
- Improved transmission line aesthetics, resulting in better public acceptance of a new line.

However, early experiences were discouraging because several failures were observed during operation. Typical failures experienced were:

- Tracking and erosion of the shed material, which led to pollution and caused flashover.
- Chalking and crazing of the insulator's surface, which resulted in increased contaminant collection, arcing, and flashover.
- Reduction of contamination flashover strength and subsequent increased contamination-induced flashover.
- Deterioration of mechanical strength, which resulted in confusion in the selection of mechanical line loading.
- Loosening of end fittings.
- Bonding failures and breakdowns along the rod-shed interface.
- Water penetration followed by electrical failure.

As a consequence of reported failures, an extensive research effort led to second- and third-generation nonceramic transmission line insulators. These improved units have tracking free sheds, better corona resistance, and slip-free end fittings. A better understanding of failure mechanisms and of mechanical strength-time dependency has resulted in newly designed insulators that are expected to last 20–30 years. Increased production quality control and automated manufacturing technology has further improved the quality of these third-generation nonceramic transmission line insulators.

Composite Suspension Insulators

A cross-section of a third-generation composite insulators is shown in Fig. 4.30. The major components of a composite insulator are:

- End fittings
- Corona ring(s)
- Fiberglass-reinforced plastic rod
- Interface between shed and sleeve
- Weather shed

End Fittings

End fittings connect the insulator to a tower or conductor. It is a heavy metal tube with an oval eye, socket, ball, tongue, and a clevis ending. The tube is attached to a fiberglass rod. The duty of the end fitting is to provide a reliable, non-slip attachment without localized stress in the fiberglass rod. Different manufacturers use different technologies. Some methods are:

1. The ductile galvanized iron-end fitting is wedged and glued with epoxy to the rod.
2. The galvanized forged steel-end fitting is swaged and compressed to the rod.
3. The malleable cast iron, galvanized forged steel, or aluminous bronze-end fitting is attached to the rod by controlled swaging. The material is selected according to the corrosion resistance requirement. The end fitting coupling zone serves as a mechanical fuse and determines the strength of the insulator.
4. High-grade forged steel or ductile iron is crimped to the rod with circumferential compression.

The interface between the end fitting and the shed material must be sealed to avoid water penetration. Another technique, used mostly in distribution insulators, involves the weather shed overlapping the end fitting.

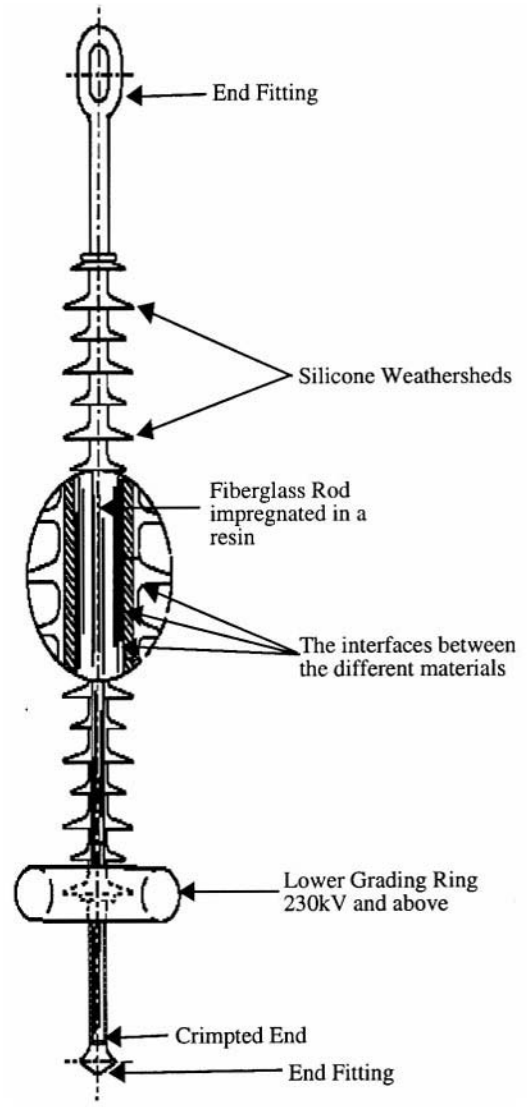

FIGURE 4.30 Cross-section of a typical composite insulator. (*Toughened Glass Insulators.* Sediver, Inc., Nanterre Cedex, France. With permission.)

Corona Ring(s)

Electrical field distribution along a nonceramic insulator is nonlinear and produces very high electric fields near the end of the insulator. High fields generate corona and surface discharges, which are the source of insulator aging. Above 230 kV, each manufacturer recommends aluminum corona rings be installed at the line end of the insulator. Corona rings are used at both ends at higher voltages (>500 kV).

Fiberglass-Reinforced Plastic Rod

The fiberglass is bound with epoxy or polyester resin. Epoxy produces better-quality rods but polyester is less expensive. The rods are manufactured in a continuous process or in a batch mode, producing the required length. The even distribution of the glass fibers assures equal loading, and the uniform impregnation assures good bonding between the fibers and the resin. To improve quality, some manufacturers use E-glass to avoid brittle fractures. Brittle fracture can cause sudden shattering of the rod.

Interfaces Between Shed and Fiberglass Rod

Interfaces between the fiberglass rod and weather shed should have no voids. This requires an appropriate interface material that assures bonding of the fiberglass rod and weather shed. The most frequently used techniques are:

1. The fiberglass rod is primed by an appropriate material to assure the bonding of the sheds.
2. Silicon rubber or ethylene propylene diene monomer (EPDM) sheets are extruded onto the fiberglass rod, forming a tube-like protective covering.
3. The gap between the rod and the weather shed is filled with silicon grease, which eliminates voids.

Weather Shed

All high-voltage insulators use rubber weather sheds installed on fiberglass rods. The interface between the weather shed, fiberglass rod, and the end fittings are carefully sealed to prevent water penetration. The most serious insulator failure is caused by water penetration to the interface.

The most frequently used weather shed technologies are:

1. Ethylene propylene copolymer (EPM) and silicon rubber alloys, where hydrated-alumina fillers are injected into a mold and cured to form the weather sheds. The sheds are threaded to the fiberglass rod under vacuum. The inner surface of the weather shed is equipped with O-ring type grooves filled with silicon grease that seals the rod-shed interface. The gap between the end-fittings and the sheds is sealed by axial pressure. The continuous slow leaking of the silicon at the weather shed junctions prevents water penetration.
2. High-temperature vulcanized silicon rubber (HTV) sleeves are extruded on the fiberglass surface to form an interface. The silicon rubber weather sheds are injection-molded under pressure and placed onto the sleeved rod at a predetermined distance. The complete subassembly is vulcanized at high temperatures in an oven. This technology permits the variation of the distance between the sheds.
3. The sheds are directly injection-molded under high pressure and high temperature onto the primed rod assembly. This assures simultaneous bonding to both the rod and the end-fittings. Both EPDM and silicon rubber are used. This one-piece molding assures reliable sealing against moisture penetration.
4. One piece of silicon or EPDM rubber shed is molded directly to the fiberglass rod. The rubber contains fillers and additive agents to prevent tracking and erosion.

Composite Post Insulators

The construction and manufacturing method of post insulators is similar to that of suspension insulators. The major difference is in the end fittings and the use of a larger diameter fiberglass rod. The latter is necessary because bending is the major load on these insulators. The insulators are flexible, which permits bending in case of sudden overload. A typical post-type insulator used for 69-kV lines is shown in Fig. 4.31.

Post-type insulators are frequently used on transmission lines. Development of station-type post insulators has just begun. The major problem is the fabrication of high strength, large diameter fiberglass tubes and sealing of the weather shed.

Insulator Failure Mechanism

Porcelain Insulators

Cap-and-pin porcelain insulators are occasionally destroyed by direct lightning strikes, which generate a very steep wave front. Steep-front waves break down the porcelain in the cap, cracking the porcelain. The penetration of moisture results in leakage currents and short circuits of the unit.

Mechanical failures also crack the insulator and produce short circuits. The most common cause is water absorption by the Portland cement used to attach the cap to the porcelain. Water absorption

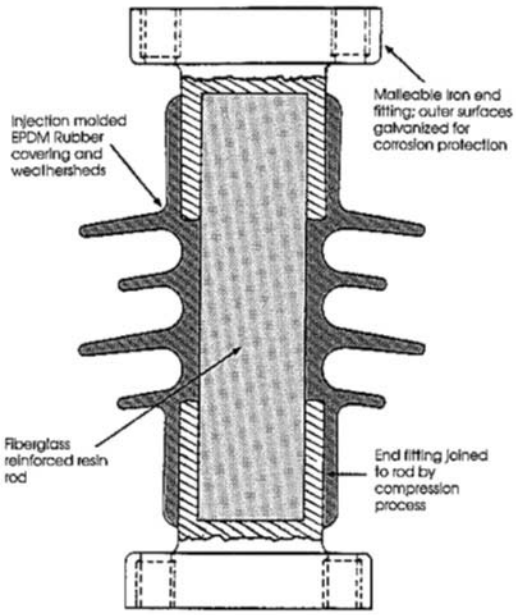

FIGURE 4.31 Post-type composite insulator. (*Toughened Glass Insulators.* Sediver, Inc., Nanterre Cedex, France. With permission.)

expands the cement, which in turn cracks the porcelain. This reduces the mechanical strength, which may cause separation and line dropping.

Short circuits of the units in an insulator string reduce the electrical strength of the string, which may cause flashover in polluted conditions.

Glass insulators use alumina cement, which reduces water penetration and the head-cracking problem. A great impact, such as a bullet, can shatter the shell, but will not reduce the mechanical strength of the unit.

The major problem with the porcelain insulators is pollution, which may reduce the flashover voltage under the rated voltages. Fortunately, most areas of the U.S. are lightly polluted. However, some areas with heavy pollution experience flashover regularly.

Insulator Pollution

Insulation pollution is a major cause of flashovers and of long-term service interruptions. Lightning-caused flashovers produce short circuits. The short circuit current is interrupted by the circuit breaker and the line is reclosed successfully. The line cannot be successfully reclosed after pollution-caused flashover because the contamination reduces the insulation's strength for a long time. Actually, the insulator must dry before the line can be reclosed.

Ceramic Insulators

Pollution-caused flashover is an involved process that begins with the pollution source. Some sources of pollution are: salt spray from an ocean, salt deposits in the winter, dust and rubber particles during the summer from highways and desert sand, industrial emissions, engine exhaust, fertilizer deposits, and generating station emissions. Contaminated particles are carried in the wind and deposited on the insulator's surface. The speed of accumulation is dependent upon wind speed, line orientation, particle size, material, and insulator shape. Most of the deposits lodge between the insulator's ribs and behind the cap because of turbulence in the airflow in these areas (Fig. 4.32).

The deposition is continuous, but is interrupted by occasional rain. Rain washes the pollution away and high winds clean the insulators. The top surface is cleaned more than the ribbed bottom. The

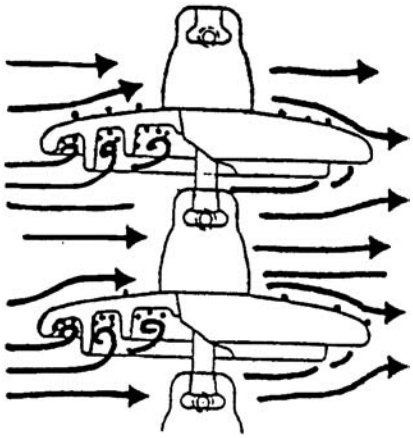

FIGURE 4.32 Deposit accumulation. (*Application Guide for Composite Suspension Insulators.* Sediver, Inc., York, SC, 1993. With permission.)

horizontal and V strings are cleaned better by the rain than the I strings. The deposit on the insulator forms a well-dispersed layer and stabilizes around an average value after longer exposure times. However, this average value varies with the changing of the seasons.

Fog, dew, mist, or light rain wets the pollution deposits and forms a conductive layer. Wetting is dependent upon the amount of dissolvable salt in the contaminant, the nature of the insoluble material, duration of wetting, surface conditions, and the temperature difference between the insulator and its surroundings. At night, the insulators cool down with the low night temperatures. In the early morning, the air temperature begins increasing, but the insulator's temperature remains constant. The temperature difference accelerates water condensation on the insulator's surface. Wetting of the contamination layer starts leakage currents.

Leakage current density depends upon the shape of the insulator's surface. Generally, the highest current density is around the pin. The current heats the conductive layer and evaporates the water at the areas with high current density. This leads to the development of dry bands around the pin. The dry bands modify the voltage distribution along the surface. Because of the high resistance of the dry bands, it is across them that most of the voltages will appear. The high voltage produces local arcing. Short arcs (Fig. 4.33) will bridge the dry bands.

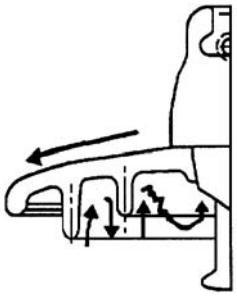

FIGURE 4.33 Dry-band arcing. (*Application Guide for Composite Suspension Insulators.* Sediver, Inc., York, SC, 1993. With permission.)

Leakage current flow will be determined by the voltage drop of the arcs and by the resistance of the wet layer in series with the dry bands. The arc length may increase or decrease, depending on the layer resistance. Because of the large layer resistance, the arc first extinguishes, but further wetting reduces the resistance, which leads to increases in arc length. In adverse conditions, the level of contamination is high and the layer resistance becomes low because of intensive wetting. After several arcing periods, the length of the dry band will increase and the arc will extend across the insulator. This contamination causes flashover.

In favorable conditions when the level of contamination is low, layer resistance is high and arcing continues until the sun or wind dries the layer and stops the arcing. Continuous arcing is harmless for ceramic insulators, but it ages nonceramic and composite insulators.

The mechanism described above shows that heavy contamination and wetting may cause insulator flashover and service interruptions. Contamination in dry conditions is harmless. Light contamination and wetting causes surface arcing and aging of nonceramic insulators.

Nonceramic Insulators

Nonceramic insulators have a dirt and water repellent (hydrophobic) surface that reduces pollution accumulation and wetting. The different surface properties slightly modify the flashover mechanism.

Contamination buildup is similar to that in porcelain insulators. However, nonceramic insulators tend to collect less pollution than ceramic insulators. The difference is that in a composite insulator, the diffusion of low-molecular-weight silicone oil covers the pollution layer after a few hours. Therefore, the pollution layer will be a mixture of the deposit (dust, salt) and silicone oil. A thin layer of silicone oil, which provides a hydrophobic surface, will also cover this surface.

Wetting produces droplets on the insulator's hydrophobic surface. Water slowly migrates to the pollution and partially dissolves the salt in the contamination. This process generates high resistivity in the wet region. The connection of these regions starts leakage current. The leakage current dries the surface and increases surface resistance. The increase of surface resistance is particularly strong on the shaft of the insulator where the current density is higher.

Electrical fields between the wet regions increase. These high electrical fields produce spot discharges on the insulator's surface. The strongest discharge can be observed at the shaft of the insulator. This discharge reduces hydrophobicity, which results in an increase of wet regions and an intensification of the discharge. At this stage, dry bands are formed at the shed region. In adverse conditions, this phenomenon leads to flashover. However, most cases of continuous arcing develop as the wet and dry regions move on the surface.

The presented flashover mechanism indicates that surface wetting is less intensive in nonceramic insulators. Partial wetting results in higher surface resistivity, which in turn leads to significantly higher flashover voltage. However, continuous arcing generates local hot spots, which cause aging of the insulators.

Effects of Pollution

The flashover mechanism indicates that pollution reduces flashover voltage. The severity of flashover voltage reduction is shown in Fig. 4.34. This figure shows the surface electrical stress (field), which causes flashover as a function of contamination, assuming that the insulators are wet. This means that the salt in the deposit is completely dissolved. The Equivalent Salt Deposit Density (ESDD) describes the level of contamination.

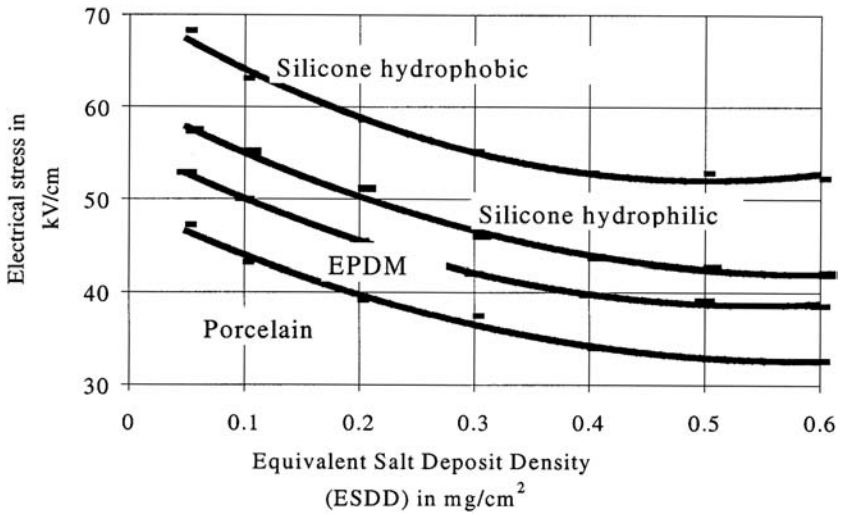

FIGURE 4.34 Surface electrical stress vs. ESDD of fully wetted insulators (laboratory test results). (*Application Guide for Composite Suspension Insulators.* Sediver, Inc., York, SC, 1993. With permission.)

TABLE 4.6 Number of Standard Insulators for Contaminated Areas

System Voltage kV	Level of Contamination			
	Very light	Light	Moderate	Heavy
138	6/6	8/7	9/7	11/8
230	11/10	14/12	16/13	19/15
345	16/15	21/17	24/19	29/22
500	25/22	32/27	37/29	44/33
765	36/32	47/39	53/42	64/48

Note: First number is for I-string; second number is for V-string.

These results show that the electrical stress, which causes flashover, decreases by increasing the level of pollution on all of the insulators. This figure also shows that nonceramic insulator performance is better than ceramic insulator performance. The comparison between EPDM and silicone shows that flashover performance is better for the latter.

Table 4.6 shows the number of standard insulators required in contaminated areas. This table can be used to select the number of insulators, if the level of contamination is known.

Pollution and wetting cause surface discharge arcing, which is harmless on ceramic insulators, but produces aging on composite insulators. Aging is a major problem and will be discussed in the next section.

Composite Insulators

The Electric Power Research Institute (EPRI) conducted a survey analyzing the cause of composite insulator failures and operating conditions. The survey was based on the statistical evaluation of failures reported by utilities.

Results show that a majority of insulators (48%) are subjected to very light pollution and only 7% operate in heavily polluted environments. Figure 4.35 shows the typical cause of composite insulator failures. The majority of failures are caused by deterioration and aging. Most electrical failures are caused by water penetration at the interface, which produces slow tracking in the fiberglass rod surface. This tracking produces a conduction path along the fiberglass surface and leads to internal breakdown of the insulator. Water penetration starts with corona or erosion-produced cuts, holes on the weather shed, or mechanical load-caused separation of the end-fitting and weather shed interface.

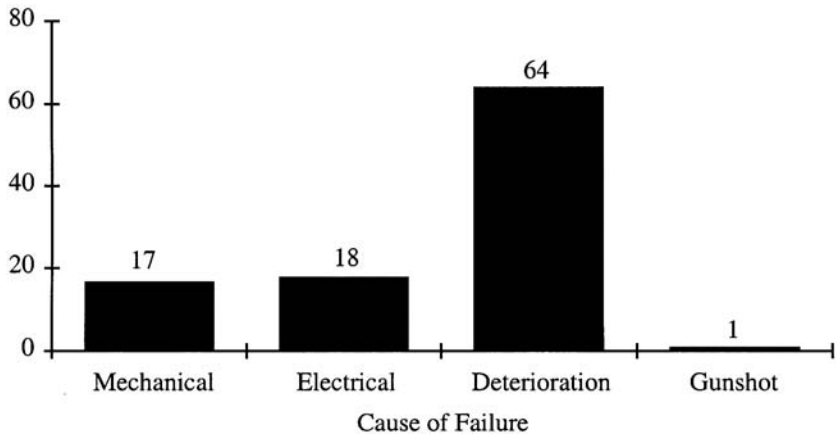

FIGURE 4.35 Cause of composite insulator failure. (Schneider et al., Nonceramic insulators for transmission lines, *IEEE Transaction on Power Delivery,* 4(4), 2214-2221, April, 1989.)

Most of the mechanical failures are caused by breakage of the fiberglass rods in the end fitting. This occurs because of local stresses caused by inappropriate crimping. Another cause of mechanical failures is brittle fracture. Brittle fracture is initiated by the penetration of water containing slight acid from pollution. The acid may be produced by electrical discharge and acts as a cathalizator, attacking the bonds and the glass fibers to produce a smooth fracture. The brittle fractures start at high mechanical stress points, many times in the end fitting.

Aging of Composite Insulators

Most technical work concentrates on the aging of nonceramic insulators and the development of test methods that simulate the aging process. Transmission lines operate in a polluted atmosphere. Inevitably, insulators will become polluted after several months in operation. Fog and dew cause wetting and produce uneven voltage distribution, which results in surface discharge. Observations of transmission lines at night by a light magnifier show that surface discharge occurs in nearly every line in wet conditions. UV radiation and surface discharge cause some level of deterioration after long-term operation. These are the major causes of aging in composite insulators which also lead to the uncertainty of an insulator's life span. If the deterioration process is slow, the insulator can perform well for a long period of time. This is true of most locations in the U.S. and Canada. However, in areas closer to the ocean or areas polluted by industry, deterioration may be accelerated and insulator failure may occur after a few years of exposure. Surveys indicate that some insulators operate well for 18–20 years and others fail after a few months. An analysis of laboratory data and literature surveys permit the formulation of the following aging hypothesis:

1. Wind drives dust and other pollutants into the composite insulator's water-repellent surface. The combined effects of mechanical forces and UV radiation produces slight erosion of the surface, increasing surface roughness and permitting the slow buildup of contamination.
2. Diffusion drives polymers out of the bulk skirt material and embeds the contamination. A thin layer of polymer will cover the contamination, assuring that the surface maintains hydrophobicity.
3. High humidity, fog, dew, or light rain produce droplets on the hydrophobic insulator surface. Droplets may roll down from steeper areas. In other areas, contaminants diffuse through the thin polymer layer and droplets become conductive.
4. Contamination between the droplets is wetted slowly by the migration of water into the dry contaminant. This generates a high resistance layer and changes the leakage current from capacitive to resistive.
5. The uneven distribution and wetting of the contaminant produces an uneven voltage stress distribution along the surface. Corona discharge starts around the droplets at the high stress areas. Additional discharge may occur between the droplets.
6. The discharge consumes the thin polymer layer around the droplets and destroys hydrophobicity.
7. The deterioration of surface hydrophobicity results in dispersion of droplets and the formation of a continuous conductive layer in the high stress areas. This increases leakage current.
8. Leakage current produces heating, which initiates local dry band formation.
9. At this stage, the surface consists of dry regions, highly resistant conducting surfaces, and hydrophobic surfaces with conducting droplets. The voltage stress distribution will be uneven on this surface.
10. Uneven voltage distribution produces arcing and discharges between the different dry bands. These cause further surface deterioration, loss of hydrophobicity, and the extension of the dry areas.
11. Discharge and local arcing produces surface erosion, which ages the insulator's surface.
12. A change in the weather, such as the sun rising, reduces the wetting. As the insulator dries, the discharge diminishes.
13. The insulator will regain hydrophobicity if the discharge-free dry period is long enough. Typically, silicon rubber insulators require 6–8 h; EPDM insulators require 12–15 h to regain hydrophobicity.

14. Repetition of the described procedure produces erosion on the surface. Surface roughness increases and contamination accumulation accelerates aging.
15. Erosion is due to discharge-initiated chemical reactions and a rise in local temperature. Surface temperature measurements, by temperature indicating point, show local hot-spot temperatures between 260°C and 400°C during heavy discharge.

The presented hypothesis is supported by the observation that the insulator life spans in dry areas are longer than in areas with a wetter climate. Increasing contamination levels reduce an insulator's life span. The hypothesis is also supported by observed beneficial effects of corona rings on insulator life.

DeTourreil et al. (1990) reported that aging reduces the insulator's contamination flashover voltage. Different types of insulators were exposed to light natural contamination for 36–42 months at two different sites. The flashover voltage of these insulators was measured using the "quick flashover salt fog" technique, before and after the natural aging. The quick flashover salt fog procedure subjects the insulators to salt fog (80 kg/m^3 salinity). The insulators are energized and flashed over 5–10 times. Flashover was obtained by increasing the voltage in 3% steps every 5 min from 90% of the estimated flashover value until flashover. The insulators were washed, without scrubbing, before the salt fog test. The results show that flashover voltage on the new insulators was around 210 kV and the aged insulators flashed over around 184–188 kV. The few years of exposure to light contamination caused a 10–15% reduction of salt fog flashover voltage.

Natural aging and a follow-up laboratory investigation indicated significant differences between the performance of insulators made by different manufacturers. Natural aging caused severe damage on some insulators and no damage at all on others.

Methods for Improving Insulator Performance

Contamination caused flashovers produce frequent outages in severely contaminated areas. Lines closer to the ocean are in more danger of becoming contaminated. Several countermeasures have been proposed to improve insulator performance. The most frequently used methods are:

1. **Increasing leakage distance by increasing the number of units or by using fog-type insulators.** The disadvantages of the larger number of insulators are that both the polluted and the impulse flashover voltages increase. The latter jeopardizes the effectiveness of insulation coordination because of the increased strike distance, which increases the overvoltages at substations.
2. **Application insulators are covered with a semiconducting glaze.** A constant leakage current flows through the semiconducting glaze. This current heats the insulator's surface and reduces the moisture of the pollution. In addition, the resistive glaze provides an alternative path when dry bands are formed. The glaze shunts the dry bands and reduces or eliminates surface arcing. The resistive glaze is exceptionally effective near the ocean.
3. **Periodic washing of the insulators with high-pressure water.** The transmission lines are washed by a large truck carrying water and pumping equipment. Trained personnel wash the insulators by aiming the water spray toward the strings. Substations are equipped with permanent washing systems. High-pressure nozzles are attached to the towers and water is supplied from a central pumping station. Safe washing requires spraying large amounts of water at the insulators in a short period of time. Fast washing prevents the formation of dry bands and pollution-caused flashover. However, major drawbacks of this method include high installation and operational costs.
4. **Periodic cleaning of the insulators by high pressure driven abrasive material, such as ground corn cobs or walnut shells.** This method provides effective cleaning, but cleaning of the residual from the ground is expensive and environmentally undesirable.
5. **Replacement of porcelain insulators with nonceramic insulators.** Nonceramic insulators have better pollution performance, which eliminates short-term pollution problems at most sites. However, insulator aging may affect the long-term performance.

6. **Covering the insulators with a thin layer of room-temperature vulcanized (RTV) silicon rubber coating.** This coating has a hydrophobic and dirt-repellent surface, with pollution performance similar to nonceramic insulators. Aging causes erosion damage to the thin layer after 5–10 years of operation. When damage occurs, it requires surface cleaning and a reapplication of the coating. Cleaning by hand is very labor intensive. The most advanced method is cleaning with high pressure driven abrasive materials like ground corn cobs or walnut shells. The coating is sprayed on the surface using standard painting techniques.
7. **Covering the insulators with a thin layer of petroleum or silicon grease.** Grease provides a hydrophobic surface and absorbs the pollution particles. After one or two years of operation, the grease saturates the particles and it must be replaced. This requires cleaning of the insulator and application of the grease, both by hand. Because of the high cost and short life span of the grease, it is not used anymore.

References

Application Guide for Composite Suspension Insulators, Sediver Inc., York, SC, 1993.

DeTourreil, C.H. and Lambeth, P.J., Aging of composite insulators: Simulation by electrical tests, *IEEE Trans. on Power Delivery,* 5(3), 1558-1567, July, 1990.

Fink, D.G. and Beaty, H.W., *Standard Handbook for Electrical Engineers,* 11th ed., McGraw-Hill, New York, 1978.

Gorur, R.S., Karady, G.G., Jagote, A., Shah, M., and Yates, A., Aging in silicon rubber used for outdoor insulation, *IEEE Transaction on Power Delivery,* 7(2), 525-532, March, 1992.

Hall, J.F., History and bibliography of polymeric insulators for outdoor application, *IEEE Transaction on Power Delivery,* 8(1), 376-385, January, 1993.

Karady, G.G., Outdoor insulation, *Proceedings of the Sixth International Symposium on High Voltage Engineering,* New Orleans, LA, September, 1989, 30.01-30.08.

Karady, G.G., Rizk, F.A.M., and Schneider, H.H., Review of CIGRE and IEEE Research into Pollution Performance of Nonceramic Insulators: Field Aging Effect and Laboratory Test Techniques, in *International Conference on Large Electric High Tension Systems (CIGRE), Group 33,* (33-103), Paris, 1-8, August, 1994.

Looms, J.S.T., *Insulators for High Voltages,* Peter Peregrinus Ltd., London, 1988.

Schneider, H., Hall, J.F., Karady, G., and Rendowden, J., Nonceramic insulators for transmission lines, *IEEE Transaction on Power Delivery,* 4(4), 2214-2221, April, 1989.

Toughened Glass Insulators. Sediver Inc., Nanterre Cedex, France.

Transmission Line Reference Book (345 kV and Above), 2nd ed., EL 2500 Electric Power Research Institute (EPRI), Palo Alto, CA, 1987.

4.4 Transmission Line Construction and Maintenance

Wilford Caulkins and Kristine Buchholz

The information herein was derived from personal observation and participation in the construction of overhead transmission lines for over 35 years. Detailed information, specific tools and equipment have been provided previously and are available in IEEE Standard 524-1992 and IEEE Standard 524A-1993.

The purpose of this section is to give a general overview of the steps that are necessary in the planning and construction of a typical overhead transmission line, to give newcomers to the trade a general format to follow, and assist transmission design engineers in understanding how such lines are built.

Stringing overhead conductors in transmission is a very specialized type of construction requiring years of experience, as well as equipment and tools that have been designed, tried, and proven to do the work. Because transmission of electrical current is normally at higher voltages (69 kV and above), conductors must be larger in diameter and span lengths must be longer than in normal distribution.

Although proximity to other energized lines may be limited on the right-of-way, extra care must be exercised to protect the conductor so that when energized, power loss and corona are not a problem.

There are four methods that can be used to install overhead transmission conductors:

1. Slack stringing
2. Semi-tension stringing
3. Full-tension stringing
4. Helicopter stringing

Slack stringing can only be utilized if it is not necessary to keep the conductor off of the ground, and if no energized lines lie beneath the line being strung. In this method the pulling lines are pulled out on the ground, threaded through the stringing blocks, and the conductor is pulled in with less tension than is required to keep it off the ground. This is not considered to be an acceptable method when demands involve maximum utilization of transmission requirements.

Semi-tension methods are merely an upgrading of slack stringing, but do not necessarily keep the conductor completely clear of the ground, or the lines used to pull.

Full-tension stringing is a method of installing the conductors and overhead groundwire in which sufficient pulling capabilities on one end and tension capabilities on the other, keep the wires clear of any obstacles during the movement of the conductor from the reel to its final sag position. This ensures that these current-carrying cables are "clipped" into the support clamps in the best possible condition, which is the ultimate goal of the work itself.

Stringing with helicopters, which is much more expensive per hour of work, can be much less expensive when extremely arduous terrain exists along the right-of-way and when proper pre-planning is utilized. Although pulling conductors themselves with a helicopter can be done, it is limited and normally not practical. Maximum efficiency can be achieved when structures are set and pilot lines are pulled with the helicopter, and then the conductor stringing is done in a conventional manner. Special tools (such as stringing blocks) are needed if helicopters are used.

So that maximum protection of the conductor is realized and maximum safety of personnel is attained, properly designed and constructed tools and equipment are tantamount to a successful job. Because the initial cost of these tools and equipment represent such a small percentage of the overall cost of the project, the highest quality should be used, thus minimizing "down time" and possible failure during the course of construction.

Tools

Basic tools needed to construct overhead transmission lines are as follows:

1. Conductor blocks
2. Overhead groundwire blocks
3. Catch-off blocks
4. Sagging blocks
5. Pulling lines
6. Pulling grips
7. Catch-off grips
8. Swivels
9. Running boards
10. Conductor lifting hooks
11. Hold-down blocks

Conductor blocks are made in the following configurations:

1. Single conductor
2. Multiple conductor
3. Multiversal type (can be converted from bundle to single, and vice versa)
4. Helicopter

Conductor blocks should be large enough to properly accommodate the conductor and be lined with a resilient liner such as neoprene or polyurethane and constructed of lightweight, high-strength materials. Sheaves should be mounted on anti-friction ball bearings to reduce the tension required in stringing and facilitate proper sagging. Conductor blocks are available for stringing single conductors or multiple conductors. Some are convertible, thus enhancing their versatility. When stringing multiple conductors, it is desirable to pull all conductors with a single pulling line so that all conductors in the bundle have identical tension history. The running board makes this possible. Pulling lines are divided into two categories:

1. Steel cable
2. Synthetic rope

Because of the extra high tension required in transmission line construction, steel pulling lines and pilot lines are most practical to use. Torque-resistant, stranded, and swagged cable are used so that ball bearing swivels can be utilized to prevent torque buildup from being transferred to the conductor. Some braided or woven steel cables are also used. If synthetic ropes are utilized, the most important features should include:

1. No torque
2. Very minimum elongation
3. No "kinking"
4. Easily spliced
5. High strength/small diameter
6. Excellent dielectric properties

Stringing overhead groundwires does not normally require the care of current-carrying conductors. Most overhead groundwires are stranded steel construction and the use of steel wire with a fiber-optic core for communications has become a common practice. Special care should be taken to ensure that excessive bending does not occur when erecting overhead groundwires with fiber-optic centers, such as OPT-GW (Optical Power Telecommunications — Ground Wire) and ADSS (All Dielectric Self-Supporting Cable). Special instructions are available from the manufacturer, which specify minimum sheave and bullwheel diameter for construction. OPT-GW should be strung using an antirotational device to prevent the cable from twisting.

Equipment

Pullers are used to bring in the main pulling line. Multidrum pullers, called pilot line winders, are used to tension string the heavy pulling cable.

Primary pullers are used to tension string the conductors. These pullers are either drum type or bullwheel type. The drum type is used more extensively in many areas of North America because the puller and pulling cable are stored on one piece of equipment, but it is not practical in other areas because it is too heavy. Thus, the bullwheel type is used allowing the puller and pulling cable to be separated onto two pieces of equipment. Also, the pulling cable can be separated into shorter lengths to allow easier handling, especially if manual labor is preferred.

Tensioners should be bullwheel type using multigroove wheels for more control. Although V groove machines are used on some lighter, smaller conductors, they are not recommended in transmission work because of the crushing effect on the conductor. Tensioners are either mounted on a truck or trailer.

Reel stands are used to carry the heavy reels of conductor and are equipped with brakes to hold "tailing tension" on the conductor as it is fed into the bullwheel tensioner. These stands are usually mounted on a trailer separated from the tensioner.

Helicopters are normally used to fly in a light line which can be used to pull in the heavier cable.

Procedures

Once the right-of-way has been cleared, the following are normal steps taken in construction:

1. Framing
2. Pulling
3. Pulling overhead groundwire up to sag and installation
4. Pulling in main line with pilot line
5. Stringing conductors
6. Sagging conductors
7. Clipping in conductors
8. Installing spacer or spacer dampers where applicable

Framing normally consists of erecting poles, towers, or other structures, including foundations and anchors on guyed structures. It is desirable for the stringing blocks to be installed, with finger lines, on the ground before structures are set, to eliminate an extra climb later. Helicopters are used to set structures, especially where rough terrain exists or right-of-way clearances are restricted.

Once structures are secure, overhead groundwire and pilot lines are pulled in together with a piece of equipment such as a caterpillar or other track vehicle. A helicopter is also used to fly in these lines. Once the overhead groundwires are in place, they are sagged and secured, thus giving the structures more stability for the stringing of the conductors. This is especially important for guyed structures.

Normally the three pilot lines (typically 3/8 in. diameter swagged steel cable) pull in the heavier pulling line (typically 3/4 in. diameter or 7/8 in. diameter swagged steel) under tension. The main pulling line is then attached to the conductor which is strung under full tension. Once the conductor is "caught off," the main pulling line is returned for pulling of the next phase.

Once the conductors are in place, they are then brought up to final sag and clipped into the conductor clamps provided. If the conductor is a part of a bundle per phase, the spacers or spacer dampers are installed, using a spacer cart which is either pulled along from the ground or self-propelled.

Coordination between design engineers and construction personnel is very important in the planning and design of transmission lines. Although it is sometimes impossible to accommodate the most efficient capabilities of the construction department (or line contractor), much time and money can be conserved if predesign meetings are held to discuss items such as the clearances needed for installing overhead groundwire blocks, hardware equipped with "work" holes to secure lifting hooks or blocks, conductor reel sizes compatible with existing reel stands, length of pull most desirable, or towers equipped to facilitate climbing.

For maximum safety of personnel constructing transmission lines, proper and effective grounding procedures should be utilized. Grounding can be accomplished by:

1. adequate grounding of conductors being strung and pulling cables being used, or
2. fully insulating equipment and operator, or
3. isolating equipment and personnel.

All equipment, conductors, anchors, and structures within a defined work area must be bonded together and connected to the ground source. The recommended procedures of personnel protection are the following:

1. Establish equipotential work zones.
2. Select grounding equipment for the worst-case fault.
3. Discontinue all work when the possibility of lightning exists which may affect the work site.

In addition to the grounding system, the best safety precaution is to treat all equipment as if it could become energized.

Helicopters

As already mentioned, the use of helicopters is another option that is being chosen more frequently for transmission system construction and maintenance. There are a wide variety of projects where helicopters become involved, making the projects easier, safer, or more economical. When choosing any construction or maintenance method, identify the work to be accomplished, analyze the potential safety aspects, list the possible alternatives, and calculate the economics. Helicopters add a new dimension to this analytical process by adding to the alternatives, frequently reducing the risks of accident or injury, and potentially reducing costs. The most critical consideration in the use of a helicopter is the ability to safely position the helicopter and line worker at the work location.

Conductor Stringing

Helicopters are used for conductor stringing on towers through the use of pilot lines. Special stringing blocks are installed at each tower and a helicopter is brought in and attached to a pilot line. The helicopter flies along the tower line and slips the pilot line in through each stringing block until it reaches the end of the set of towers for conductor pulling, where it disconnects and the pilot line is transferred to a ground crew. The ground crew then proceeds to pull the conductor in the conventional manner (Caulkins, 1987). The helicopter may also be used to monitor the conductor pulling and is readily available to assist if the conductor stalls at any tower location.

Structure and Material Setting

The most obvious use of helicopters is in the setting of new towers and structures. Helicopters are frequently used in rough terrain to fly in the actual tower to a location where a ground crew is waiting to spot the structure into a preconstructed foundation. In addition, heavy material can be transported to remote locations, as well as the construction crew.

The use of helicopters can be especially critical if the tower line is being replaced following a catastrophe or failure. Frequently, roads and even construction paths are impassable or destroyed following natural disasters. Helicopters can carry crews and materials with temporary structures that can be erected within hours to restore tower lines. Again, depending on the terrain and current conditions, whether the existing structure is repaired or temporary tower structures are utilized, the helicopter is invaluable to carry in the needed supplies and personnel.

Insulator Replacement

A frequent maintenance requirement on a transmission system is replacing insulators. This need is generated for various reasons, including line upgrading, gunshots, environmental damage, or defects in the original insulator manufacturing. With close coordinated crews, helicopters can maximize the efficiency of the replacement project.

Crews are located at several towers to perform the actual insulator removal and installation. The crews will do the required setup for a replacement, but the helicopter can be used to bring in the necessary tools and equipment. The crew removes the old insulator string and sets it to one side of the work location. When the crews are ready, the helicopter flies in the new insulator string to each tower. The crew on the tower detaches the new insulator string from the helicopter, positions it, and then attaches the old string to the helicopter, which removes the string to the staging area. With a well-coordinated team of helicopters and experienced line workers, it is not unusual to achieve a production rate of replacing all insulators on four three-phase structures per crew per day. Under ideal conditions, crews are able to replace the insulators on a structure in one hour (Buchholz, 1987).

Replacing Spacers

One of the first uses of helicopters in live-line work was the replacement of spacers in the early 1980s. This method was a historic step in live-line work since it circumvented the need for hot sticks or insulated aerial lift devices.

The first projects involved a particular spacer wearing into the conductor strands, causing the separation of the conductor. Traditionally, the transmission line would have been de-energized, grounded, and either a line worker would have utilized a spacer cart to move out on the line to replace the spacer, or the line would have been lowered and the spacer replaced and the conductor strengthened. The obvious safety dilemma was whether the conductor could support a line worker on a spacer cart or whether it was physically able to withstand the tensions of lowering it to the ground. By utilizing a helicopter and bare-hand work methods, the spacers were able to be replaced and the conductor strengthened where necessary with full-tension compression splices while providing total safety to the line workers and a continuous supply of energy over the transmission lines. One of the early projects achieved a replacement and installation of 25,000 spacers without a single accident or injury. A typical spacer replacement required about 45 sec, including the travel time between work locations (Buchholz, 1987).

Insulator Washing

Another common practice is to utilize helicopters for insulator washing. Again, this is a method that allows for the line to remain energized during the process. The helicopter carries a water tank that is refilled at a staging area near the work location. A hose and nozzle are attached to a structure on the helicopter and are operated by a qualified line worker who directs the water spray and adequately cleans the insulator string. Again, with the ease of access afforded by the helicopter, the speed of this operation can result in a typical three-phase tower being cleaned in a few minutes.

Inspections

Helicopters are invaluable for tower line and structure inspections. Due to the ease of the practice and the large number of inspections that can be accomplished, utilities have increased the amount of maintenance inspections being done, thus promoting system reliability.

Helicopters typically carry qualified line workers who utilize stabilizing binoculars to visually inspect the transmission tower for signs of rusting or weakness and the transmission hardware and conductor for damage and potential failure. Infrared inspections and photographic imaging can also be accomplished from the helicopter, either by mounting the cameras on the helicopter or through direct use by the crew. During these inspections, the helicopter provides a comfortable situation for accomplishing the necessary recording of specific information, tower locations, etc. In addition, inspections from helicopters are required following a catastrophic event or system failure. It is the only logical method of quickly inspecting a transmission system for the exact location and extent of damage.

Helicopter Method Considerations

The ability to safely position a helicopter and worker at the actual work site is the most critical consideration when deciding if a helicopter method can be utilized for construction or maintenance. The terrain and weather conditions are obvious factors, as well as the physical spacing needed to position the helicopter and worker in the proximity required for the work method. If live-line work methods are to be utilized, the minimum approach distance required for energized line work must be calculated very carefully for every situation. The geometry of each work structure, the geometry of the individual helicopter, and the positioning of the helicopter and worker for the specific work method must be analyzed. There are calculations that are available to analyze the approach distances (IEEE Task Force 15.07.05.05, 1999).

When choosing between construction and maintenance work methods, the safety of the line workers is the first consideration. Depending on circumstances, a helicopter method may be the safest work method. Terrain has always been a primary reason for choosing helicopters to assist with projects since the ability to drive to each work site may not be possible. However, helicopters may still be the easiest and most economic alternative when the terrain is open and flat, especially when there are many individual tower locations that will be contacted. Although helicopters may seem to be expensive on a per person basis, the ability to quickly position workers and easily move material can drastically reduce

costs. When live-line methods can be utilized, the positioning of workers, material, and equipment becomes comparatively easier.

Finally, if the safe use of the helicopter allows the transmission systems to remain energized throughout the project, the helicopter may be the only possible alternative. Since the transmission system is a major link in the competitive energy markets, transmission operation will have reliability performance measures which must be achieved. Purchasing replacement energy through alternate transmission paths, as was done in the regulated world, is no longer an option. Transmission system managers are required to keep systems operational and will be fined if high levels of performance are not attained. The option of de-energizing systems for maintenance practices may be too costly in the deregulated world.

References

Buchholz, F., Helicopter application in transmission system maintenance and repair, in *IEEE/CSEE Joint Conference on High-Voltage Transmission Systems in China,* October, 1987.

Caulkins, III., W., Practical applications and experiences in the installation of overhead transmission line conductors, in *IEEE/CSEE Joint Conference on High-Voltage Transmission Systems in China*, October, 1987.

Guide to Grounding During the Installation of Overhead Transmission Line Conductors: Supplement to IEEE Guide to the Installation of Overhead Transmission Line Conductors, IEEE 524A-1993, 1998.

Guide to the Installation of Overhead Transmission Line Conductors, IEEE 524-1992, 1998.

IEEE Task Force 15.07.05.05, PE 046 PRD (04-99), Recommended Practices for Helicopter Bonding Procedures for Live Line Work.

4.5 Insulated Power Cables for High-Voltage Applications

Carlos V. Núñez-Noriega and Felimón Hernandez

The choice of transmitting and distributing electric power through underground vs. overhead systems requires consideration of economical, technical, and environmental issues. Underground systems have traditionally been favored when distributing electric power to densely populated areas and when reliability or aesthetics is important. Underground distribution systems provide superior reliability because they are not exposed to wind, lightning, vandalism, or vehicle damage. These factors are the main contributors to failures of overhead electric power distribution systems. When designed and installed properly, underground distribution systems also require less preventive maintenance. The main disadvantage of underground transmission and distribution systems as compared with overhead lines is its higher cost.

Underground transmission and distribution of electric power is done through the use of insulated power cables. Cable designs vary widely depending on many factors such as voltage, power rating, application, etc.; however, all cables have certain common components. This section presents an overview of insulated electric power cables, standard usage practices, and common formulas used to calculate electric parameters important for the design of underground electric power systems.

Typical Cable Description

The basic function of an insulated power cable is to transmit electric power at a predetermined current and voltage. A typical single-core insulated power cable consists of a copper or aluminum conductor and several layers of insulation. The constructional design of power cables is more complex for cables designed for higher voltages. A cable for voltage in the tens of kilovolts may also include a metallic shield to provide a moisture barrier, an extruded semiconductive screen, and a metallic mesh or sheath which provides a path for the return currents and a reference to ground for the voltage.

Since insulated cables present no voltage at the external protecting jacket while in operation, they can be installed either directly buried (in direct contact with ground) or in a duct bank. Power insulated

FIGURE 4.36 Elements of typical (a) single-core and (b) three-core, steel armored, insulated power cables.

cables are designed to endure different types of stresses such as electrical stress caused by the rated voltage and by transient overvoltages, mechanical stress due to tension and compression during the installation, thermal stress produced during normal operation, and chemical stress caused by the reaction with the environment that may occur when the cable is installed in aggressive soils or in the presence of some chemicals. An insulated power cable typically consists of the following elements: a) a central conductor (or conductors), through which the electric current flows, b) the insulation, which withstands the applied voltage to ground, c) the shielding, consisting of a semiconductor shield that uniformly distributes the electric field around the insulation, d) a metallic sheath that provides a reference for the voltage and a path for the return and short-circuit currents, and e) an external cover that provides mechanical protection. Figure 4.36(a) illustrates a single-core insulated power cable rated at 1 kV with several layers of insulation and a metallic shield. Figure 4.36(b) shows a typical three-core, steel wire armored cable designed for voltages up to 15 kV.

Conductor

The conductor of a typical power cable is made of copper or aluminum. A single-core cable with a *concentric* configuration consists of a single central wire around which concentric layers of wire are built. An alternative configuration is the *shaped compact* single-core cable. The compacted cable is obtained

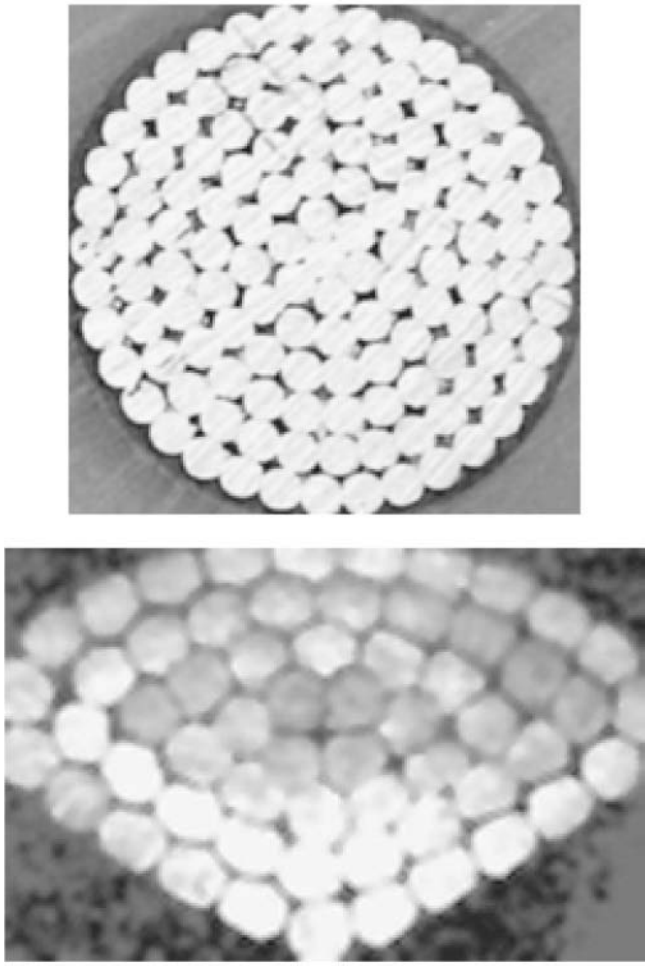

FIGURE 4.37 Cross-section view of (a) a concentric cable and (b) a single sector of a compact-shaped three-sector conductor.

by passing the cable through compacting machines to obtain its form. Because of compacting ratios of 85 to 90%, more current capacity per unit of transversal section is achieved with compact cables, and they are therefore sometimes preferred over regular concentric cables. Figure 4.37 illustrates (a) a cross-section view of a concentric cable and (b) a single section of a compact-shaped three-sector cable. For voltages of 1 kV or less, cables with solid conductors are sometimes used. Solid conductors have the disadvantage of reduced flexibility. This is partially overcome by using three or more sectors per core.

Insulation

Paper and natural rubbers were used for many years as insulating materials in underground power cables. Presently, synthetic materials are preferred for insulation of cables. The chemical composition of such materials can be altered to produce polymers with specific chemical, electrical, and mechanical properties. Although the list of materials used as cable insulation is extensive, ethylene propylene (*EP* or *EPR*) and cross-linked polyethylene (*XLP* or *XLPE*) are by far the most popular. EP and XLP insulation have similar insulating characteristics and expected long life under the same operational conditions. Some companies prefer the XLP to the EP because the former is transparent and phenomena like treeing, which is a common cause of power cable failures, can be easily analyzed under the microscope. Other insulating

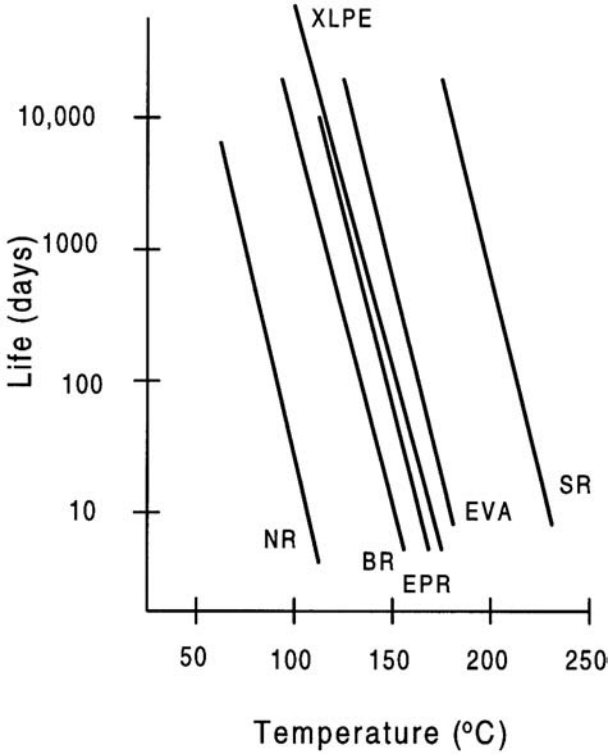

FIGURE 4.38 Life vs. temperature for different insulating materials.

materials used in cables include natural rubber (NR), silicone rubber (SR), ethyl vinyl acetate (EVA), and butyl rubber (BR).

An important consideration in the selection of insulating material is made by comparing aging performance as it relates to the maximum operating temperature of the cable, typically 60°C. This relation is obtained by using the Arrhenius reaction rate equation. A graph of life in days vs. temperature in °C is obtained. A typical comparison for different materials is illustrated in Fig. 4.38.

Semiconducting Shield

In a typical high-voltage cable, two layers of semiconductor material surround the metallic core. The first layer, placed directly around the conductor, has the following purposes:

1. To distribute the electric field uniformly around the conductor.
2. To prevent the formation of ionized voids in the conductor.
3. To dampen impulse currents traveling over the conductor surface.

The second layer of semiconductor material is placed around the first insulating layer and has the following purposes:

1. To reduce the surface voltage to zero.
2. To confine the electric field to the insulation, eliminating tangential stresses.
3. To offer a direct path to ground for short-circuit current if the shield is grounded.

Metallic Sheath

The metallic sheath surrounding insulated cables serves several purposes: as an electrostatic shield, as a ground fault current conductor, and as a neutral wire.

1. The metallic sheath designed for electrostatic purpose should be made of non-magnetic tape or non-magnetic wires. Copper is usually used for these sheaths.
2. When properly grounded, this sheath provides a path for short-circuit current.
3. With appropriate dimensions, the metallic sheath can be used as a system neutral, as in residential distribution cables where single-phase transformers are common. When single-core cables are used in three-phase systems, the grounded sheath provides a path for unbalanced currents.

When high-voltage underground cables require some type of moisture insulating barrier, a metallic pipe surrounds the current-carrying cable. The materials most commonly used as moisture barriers are lead and aluminum. The electric currents carried by the high-voltage cable will induce a voltage in the metallic shield that surrounds the conductor, and in the shields of other surrounding cables. These induced voltages, in turn, will generate an induced current flow with its associated heat losses. In the case of steel shields, the losses will include magnetization and hysteresis losses.

External Layer

The purpose of the external layer in insulated power cables is to provide mechanical protection against the environment during the installation and operation of the power cable. Currently, materials commonly used as the external layer for extruded power cables include PVC and polyethylene of low and high density. These materials are used for their ability to withstand the cable operating temperature, their resistance to excessive degradation when in contact with some chemicals typical of some operating environments, and their excellent mechanical properties for undergoing stresses during transportation, or compression and tension during installation and operation.

Overview of Electric Parameters of Underground Power Cables

Cable Electrical Resistance

The cable operation parameters determine the cable behavior under emergency and normal operating conditions. The cable impedance, $(R + jX_L)$, is useful for calculating regulation and losses under normal conditions and short-circuit current magnitude under short-circuit fault conditions. Alterations in parameters due to temperature and length variations include the change of resistance. In order to simplify the selection of a power cable for a given application, the maximum cable operating temperature is determined based on engineering calculations and laboratory tests. In the case of single wires, which are stranded together following a helical path to form a cable, a factor must be added to account for the extra length. In multi-core cables, the extra length due to the layout of the individual cores must also be accounted for. To simplify the calculation of electrical parameters, graphs of conductor size vs. resistance in ohm/kilometer can be developed and are provided by the manufacturer. Typically, manufacturers provide AC and DC resistance values which are temperature dependent. In general, the DC resistance is given by:

$$R_{t_c} = R_{20}\left[1+\alpha_{20}\left(t_c - 20\right)\right] \tag{4.4}$$

where

R_{tc} = conductor resistance at temperature t_c°C (in ohms)
R_{20} = conductor resistance at temperature 20°C (in ohms)
α_{20} = temperature coefficient of resistance of conductor material at 20°C
t_c = conductor temperature (in °C)

The AC resistance of cables is important because it affects the current-carrying capacity. The AC resistance of cables is affected mainly by skin effect and proximity effect. The analysis of these effects is complicated and graphs and tables provided by the cable manufacturer should be used to simplify any

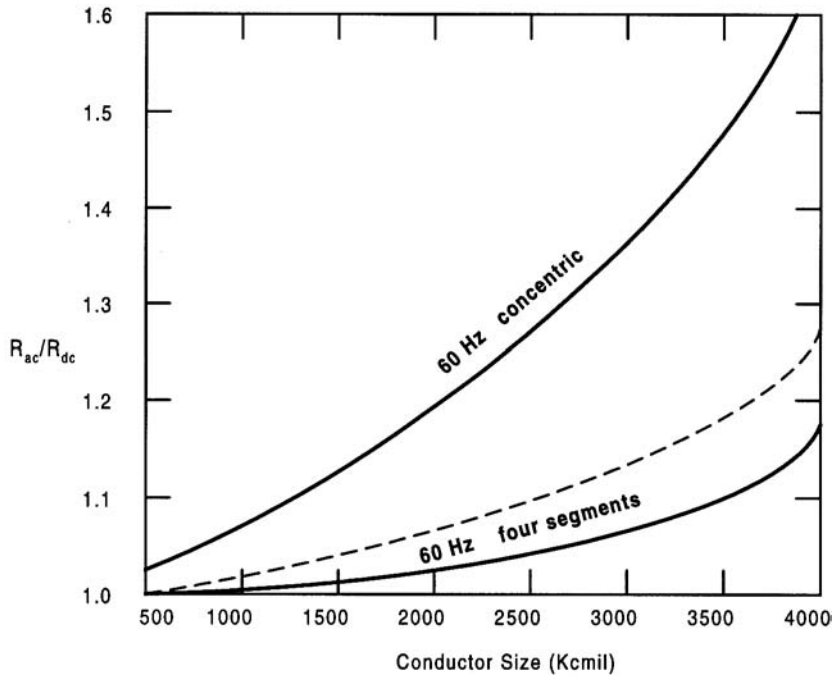

FIGURE 4.39 Conductor size vs. resistance.

calculations. Figure 4.39 illustrates a typical chart of AC/DC resistance vs. cable size for two different types of cable cores.

Cable Inductance

A variable magnetic field is created when an electric alternating current passes through a conductor. This field interacts with the magnetic field of other adjacent current-carrying conductors. The time-varying magnetic field divided by the time-varying current is called inductance. The total cable inductance is composed of the self (or internal) inductance and the mutual (or external) inductance. The mutual inductance is caused by the interaction of adjacent conductors carrying an alternating current. The inductance L per core of either a three-core cable or three single-core cables is obtained from

$$L = K + 0.2 \ln \frac{2S}{d} \quad \left(\text{in mH/km}\right) \tag{4.5}$$

where

K = a constant that accounts for the number of wires in the core (see Table 4.7)
S = distance between conductors in mm for trefoil spacing, or
= 1.26 × spacing for single-core cables in flat configuration (in mm)
d = equivalent conductor diameter (in mm)

Cable Capacitance

The capacitance between two conductors is defined as the charge between the conductors divided by the difference in voltage between them. The capacitance of power cables is affected by several factors, including geometry of the construction (if single-core or triplex), existence of metallic shielding, and type and thickness of insulating material.

TABLE 4.7 Approximate Values of K for Stranded Conductors

Number of Wires in Conductor	K
3	0.078
7	0.064
19	0.055
37	0.053
61	0.051

For a single-core cable, the capacitance per meter is given by:

$$C = \frac{q}{V} \tag{4.6}$$

or

$$C = \frac{\varepsilon_r}{18 \ln\left(D/d\right)} \tag{4.7}$$

where

D = diameter over insulation (in meters)
d = diameter over conductor (in meters)
ε_r = relative permitivity

The relative permitivity is a function of the insulating material of the cables and can be safely neglected for cables operating at 60 Hz and at normal operating temperatures.

For three-core type cables, the capacitance between one conductor and the other conductors can be approximated using the previous equation where D becomes the diameter of one conductor plus the thickness of the insulation between conductors plus the thickness of insulation between any conductor and the metallic shield.

Shield Bonding Methods and Electric Parameters

Effect of Shield Bonding Method in the Electric Parameters

Metallic shields of cables can be grounded in several ways, depending on national or regional practices, safety issues, and practical considerations. The grounding method employed is important since induced and return currents may potentially flow through grounded shields, effectively derating the cable. A single current-carrying conductor inside its shield can be modeled as shown in Fig. 4.40. For simplicity it is assumed that the conductor and shield are of infinite length. Three shield bonding methods will be discussed in this section. In the first method of shield bonding, the shield is not grounded or it is grounded at one end only; in the second method, the shield is grounded at each end; and in the third method, the shields are grounded and transposed at multiple locations throughout the length of the cable. In each case, a three-phase system composed of three single-core cables is assumed.

Ungrounded and Single-Point Grounded Shields

When the shield is not grounded, the current flowing in the center conductor will induce electric and magnetic fields in the surrounding shield and in the conductors and shields of adjacent cables. Because induction is maximum in the shield wall closest to the inner conductor, and minimum in the outer wall of the shield, a current flow is driven by the difference in electromagnetic fields. The losses associated

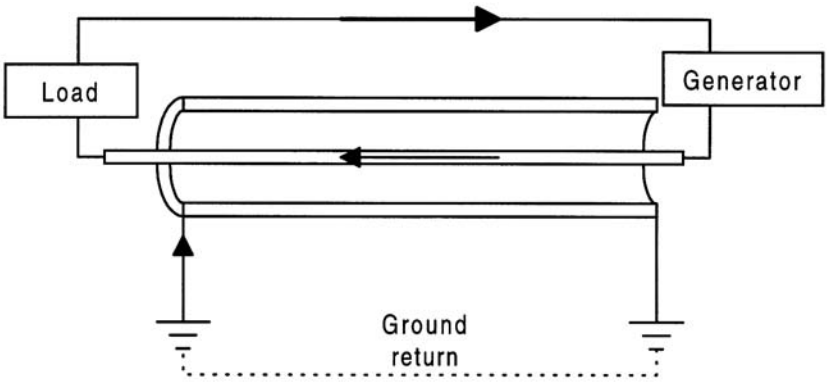

FIGURE 4.40 Model of a current carrying conductor within a metallic shield.

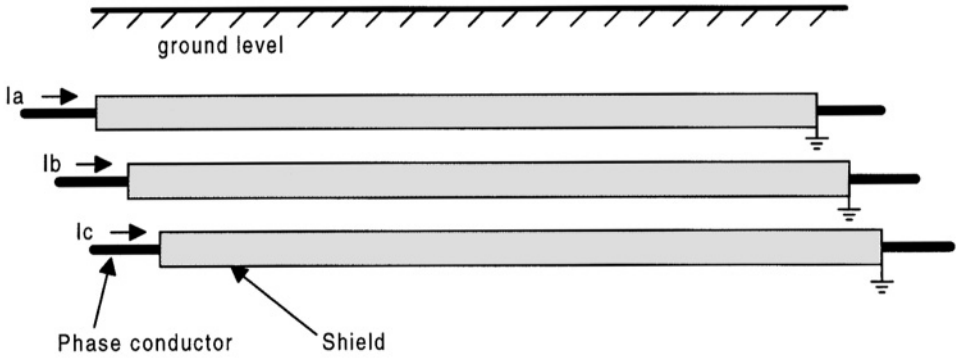

FIGURE 4.41 Single-point grounded shield system.

with these currents are described as *eddy current* losses. In single-core lead-shield conductors, eddy current losses are normally small when compared with conductor losses, and are therefore neglected. In the case of more than one conductor with aluminum shield, losses may become significant, especially when the shielded cables are in close proximity.

The single-point grounded shield system is the simplest form of bonding a cable shield. The single-point grounded system consists of connecting and grounding the shield of each cable at a single point along its length, usually at one end as shown in Fig. 4.41. In this condition, the shield circuit is not closed and therefore no shield current will flow. If the phase currents are unbalanced, a return current will flow through the earth (and the ground wires, if installed) but no return current will flow through the shield. In the ungrounded and single-point grounded shield systems, only eddy currents flow through the shields.

Multigrounded Shields

When the shields of a cable are connected at both ends, the system is said to be multigrounded (or multipoint grounded). A multigrounded system is illustrated in Fig. 4.42. In this system a closed path exists for the shield currents to flow through. The shield circulating currents produce a magnetic field that tends to cancel the magnetic field generated by the phase current. This cancellation occurs in single-phase underground systems such as those feeding individual homes in some residential areas. The reason for the cancellation is that phase current and return current flow in opposite directions. In multicircuit three-phase systems, however, the magnetic field cancellation rarely occurs, mainly due to mutual inductance and unpredicted current unbalances.

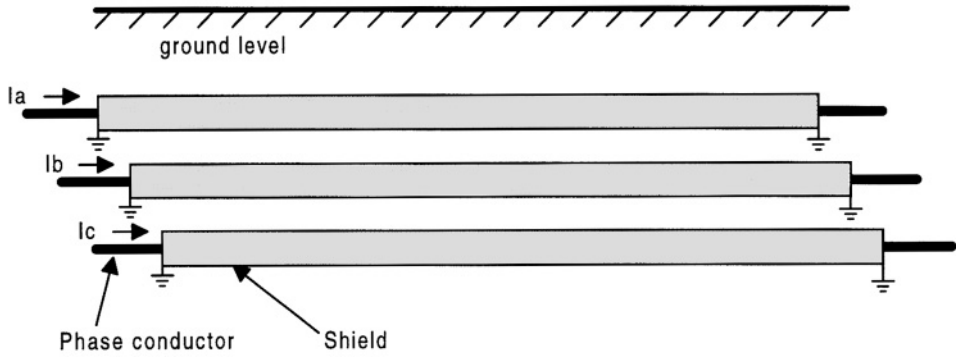

FIGURE 4.42 Multigrounded shield system.

It is important to note that multigrounded systems, such as the one depicted in Fig. 4.42, are rarely used since the shield circulating currents increases the joule losses, therefore decreasing the ampere rating of the cable.

Cross-Bonded with Transposition and Sectionalized with Transposition

A third method of bonding cable shields is known as cross-bonded with transposition and is illustrated in Fig. 4.43. In this method, the shields are divided into three or more sections and grounded at each end of the route. A route consists of three or a multiple of three sections. The conductor shields are then adequately transposed, minimizing the induced shield currents and consequent losses. The shields are isolated from ground using polyethylene or other plastic material. A variant of this method calls for sectionalizing the shields and grounding at both ends, each section of the shield further canceling the shield circulating currents. It is common practice to cross-bond cables at the splices. That is, the total length of cable that can normally be stored in a reel is the cross-bonding length. For long cable runs, the number of cross-bonding sections must be a multiple of three, making a ground connection at every third station. Cross-bonding with transposition and the sectionalizing with transposition techniques reduce the induced shield currents to zero or to values low enough to be safely neglected.

The most prevalent practice for sheath bonding in the U.S., Canada, and Great Britain has been either to use single-point grounded or sectionalized cross-bonded sheath to minimize sheath losses. A secondary benefit of these bonding practices associated with the reduction of sheath circulating currents is a drastic reduction of the magnetic field generated by unbalanced currents, especially at large distances from the lines.

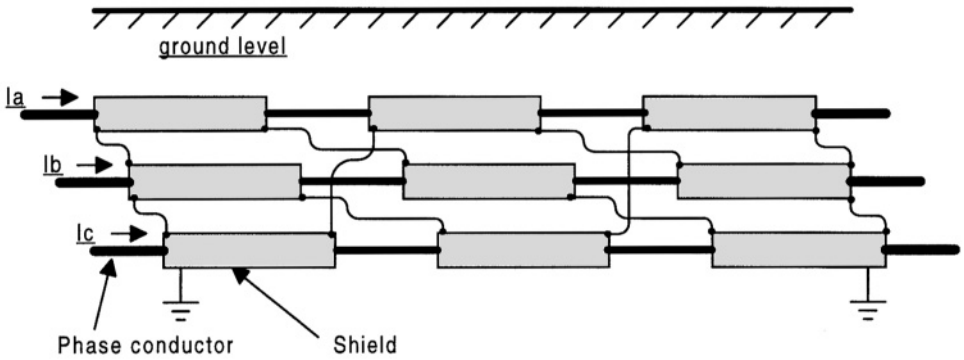

FIGURE 4.43 Multipoint grounded with transposition system.

Calculation of Losses

When the sheath is grounded or bonded to earth at more than one point, current flows through the sheath due to the emf induced in it by the alternating current in the central conductor. The mechanism of induction is the same as the mechanism of induction in a transformer. The induced voltage in the sheath of such conductor is:

$$E_s = I X_m \tag{4.8}$$

where I = conductor current in amperes and

$$X_m = 2\pi f M\, 10^{-3} \quad (\text{in ohms/km}) \tag{4.9}$$

where the mutual inductance between conductors and sheath is:

$$M = 0.2 \log_e \frac{2S}{d_m} \quad (\text{in mH/km}) \tag{4.10}$$

The impedance of the sheath is given by:

$$Z_s = \sqrt{R_s^2 + X_m^2} \quad (\text{in ohms/km}) \tag{4.11}$$

where R_s is the sheath resistance.

The sheath current is therefore:

$$I_s = \frac{E_s}{\sqrt{R_s^2 + X_m^2}} \tag{4.12}$$

or

$$I_s = \frac{IX_m}{\sqrt{R_s^2 + X_m^2}} \tag{4.13}$$

Finally, the sheath current losses per phase is given by:

$$I_s^2 R_s = \frac{I^2 X_m^2 R_s}{R_s^2 + X_m^2} \quad (\text{in watts/km}) \tag{4.14}$$

The calculations described above assume that voltage induction by nearby conductors and nearby sheaths is negligible.

Underground Layout and Construction

Residential Distribution Layout

In general, the design of underground distribution systems feeding residential areas is similar to overhead distribution systems. As in overhead systems, a primary main is installed from which distribution transformers supply consumers at a lower voltage (120–240 V). There are two widely used circuit

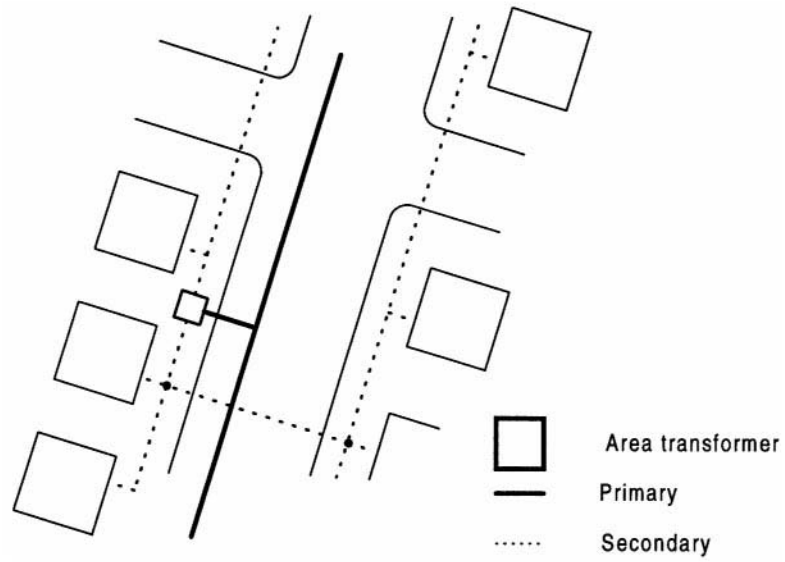

FIGURE 4.44 Underground layout with area transformer.

configurations preferred in underground systems for residential areas. The selection between these two is a matter of simple economics.

In the first case, the design is such that the primary main supplies a step-down transformer from which several secondary mains connect to consumers. This design configuration is illustrated in Fig. 4.44. In the second design, the primary main supplies the consumer directly through individual transformers placed next to the consumer service entrance. In this design pattern, the secondary mains are eliminated. This design configuration is illustrated in Fig. 4.45.

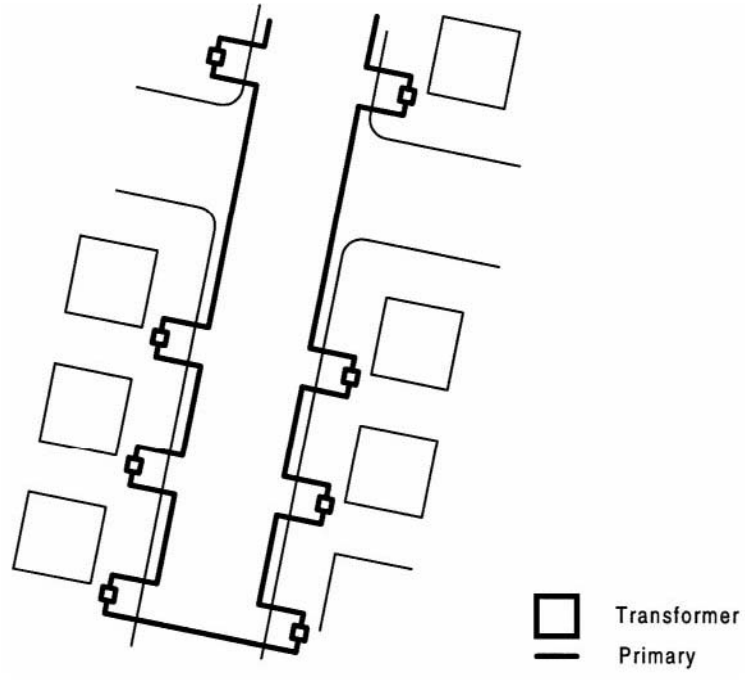

FIGURE 4.45 Underground layout with individual transformers.

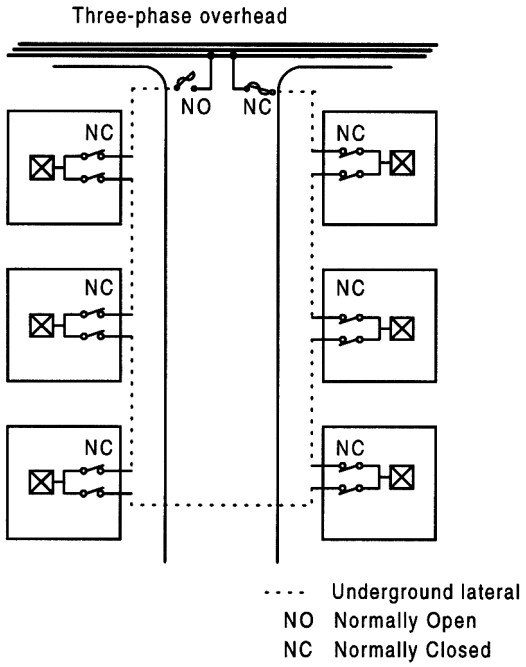

FIGURE 4.46 Open-loop design with NO and NC switches.

In each case, the primary feeder radiates from a substation, and laterals are connected, usually through adequate protective devices. The purpose of these devices is to protect the feeder from faults occurring in the lateral circuits.

Because faults in underground systems are often difficult to locate and repair, an open loop design is frequently used in these systems. As seen in Fig. 4.46, this design consists of a primary main, from which a lateral supplies a group of consumers through an open loop. In the case of a fault in the primary feeder, the faulted section is open at both ends and service to the lateral is re-established by closing the loop through the normally open switch.

Commercial and Industrial Layout

Commercial and industrial consumers are treated differently than residential. Commercial and industrial loads require three-phase supply and a more reliable service. In distribution circuits serving these loads, a neutral wire is installed to carry the unbalanced current. Because digging in these areas may be restricted, the cables and equipment are installed in ducts and manholes, improving maintenance and repair time.

Economics and quality of service required are factors to consider during the design phase of underground distribution systems for commercial and industrial consumers. In general, two designs are favored. In the first design, illustrated in Fig. 4.47, the load is connected through a transformer, the primary of which is connected to an automatic throw-over device. In case of a fault in the main feeder, to which the load is connected, the device automatically switches over to an alternate main feeder.

The second design is more complex and expensive, but provides superior reliability. In this design, several primary feeders connect the primary of a group of transformers. The secondaries of the transformers are connected together through fuses and protectors, forming a low-voltage network. In the event of failure in one of the primary feeders, the appropriate protective device opens, and power distribution continues through the other primaries without interruption.

Direct Buried Cables

Underground distribution power cables can be installed directly in a trench (direct burial) or in a duct. In some instances, power cables can be installed with telephone, gas, water, or other facilities. Direct

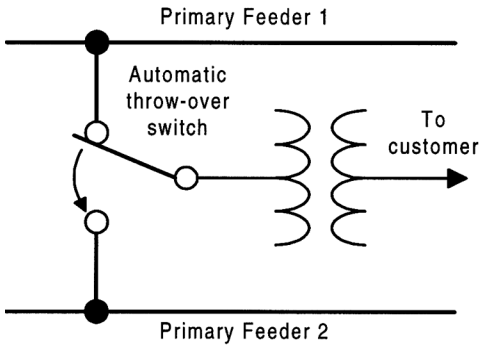

FIGURE 4.47 Diagram of throw-over switch and two supplies for extra reliability.

burial of power cables is commonly used in low-density residential areas. The main advantage of direct burial installation is cost, since conduits and manholes are eliminated. The National Electrical Safety Code (NESC) provides minimum requirements for width and depth of the trench as well as the number and types of facilities that can be installed together with the power cable. The direct burial of cables is divided into several stages, which commonly include surveying the land and digging trial holes to determine soil characteristics. In the U.S., mechanized equipment is commonly used for the installation of directly buried cable. Such equipment performs the trenching, cable lying, and backfilling in a single operation.

Cable in Ducts

Ducts or conduits are normally used under roadways, or in locations where mechanical or other types of damage may be expected. Conduit installation is expensive and complex and the conduit type should be selected carefully. The conduit materials most commonly used for underground cables are precast concrete, plastic, fiber, and iron. Because iron pipes are so costly, their use is normally limited to places where only very shallow digging is possible and mechanical rigidity is required. Conduits used under roads and railways are commonly encased in concrete.

All pipes and ducts must be installed and joined according to the manufacturer's specifications. It is common practice to seal the duct to prevent foreign materials from entering the conduit. Another practice consists of including a noncorroding draw line in the duct prior to sealing it. This is a beneficial provision, especially in long lengths between manholes. Finally, it is not uncommon to install spare ducts for future use during the construction stage.

Manholes

Manholes are typically built at the splices as a way for workers to install cables or other equipment, provide test points, and perform routine or emergency maintenance operations. The dimensions of the manholes should accommodate the conduits and cables entering the manhole and any equipment installed, such as transformers or protective equipment. Finally, the manhole should be big enough to provide adequate headroom for workers.

In less than perfect soils, manholes should be provided with adequate drainage. In extreme cases of wet soil, and if sewer connections are possible, appropriate connections should be made from the manholes to the sewer lines. If sewer connections are not possible, manholes should be constructed with waterproof concrete. This is a necessary requirement where the natural water table is higher than the bottom of the manhole.

Testing, Troubleshooting, and Fault Location

Testing of insulated cables is performed for a variety of reasons. When completed at the factory, tests are usually an integral part of the manufacturing process. These tests aim at measuring important parameters such as thickness of insulation, conductivity, etc. After installation, tests are performed almost exclusively

to detect the location of failures. This section presents an overview of some commonly performed pre- and post-installation tests.

Four types of tests are performed on cables:

1. Routine tests performed on every cable to ensure compliance with specifications and the integrity of every cable.
2. Sample tests performed periodically on cable samples to ensure manufacturing consistency.
3. Experimental tests performed to determine characteristics of newly developed materials.
4. Site tests performed after installation in the field.

Tests 1 through 3 provide insight into cable dimensions, insulation resistance and capacitance. In addition, high voltage, impulse voltage, and measurement of partial discharge trials are performed as part of these tests.

Impulse Test

The purpose of the impulse voltage test is to check the cable under conditions of transient overvoltages or other temporary high-voltage surges normally associated with switching operations or atmospheric discharges. Such conditions are often encountered during the regular operation of a cable. During a typical impulse voltage test, the cable is first subjected to mechanical stresses typically found in a routine installation procedure, such as bending. A set of negative and positive impulses at the withstand level are applied to the cable which has been heated at the maximum conductor temperature. After the impulses are applied, the cable may be subjected to a high-voltage test.

High-Voltage Test

High-voltage tests are performed to locate defects in insulated cables. The selection of voltage level is extremely important: if the voltage is too high, it may cause incipient damage of the cable, affecting future service life. On the other hand, the breakdown of the insulation under high voltage is also time dependent and therefore a number of voltage/time to breakdown tests are performed. These tests are important for developmental purposes but have little use as predictors of service life.

Partial Discharge Test

Gas-filled voids are found in the insulation and at the juncture of dielectric and conductive sheaths of cables. The breakdown of this gas produces a phenomenon known as partial discharge. Partial discharge occurs at these voids because the breakdown strength of the gas within voids is much less than that of the typical cable insulation material. In fact, discharges may occur at voltages lower than the operating voltage of the cable. The level of voltage at which partial discharge occurs first is called the discharge inception voltage.

Incidence of Faults and Fault Location

The major causes of faults in underground cables (listed below) are an indication of some of the hazards to which cables are exposed: accidental contact, aging, faulty installation, lightning, and others. Depending on the location, accidental contact and aging account for more than 50% of all faults. Because accidental contacts with cables often produce only minor damage, there is a time lapse until the cable deteriorates enough to produce failure and operation of protective equipment. When there is accidental contact with cables, failures may occur as a result of prolonged exposure to moisture, loss of dielectric material, corrosion, etc.

An effective location of faults in an underground cable system requires a systematic approach. Typically, the following steps are followed to successfully locate a fault:

1. The existence and type of fault is first determined. This requires the determination of damage to the shield and or changes in continuity of the conductor.
2. Once the existence of the fault is assured, it is necessary to diagnose the cause of the fault. This can be determined in several ways, including ruling out faulty operation of protective equipment. A Megger may be used to check continuity.

3. In the case of intermittent faults, preconditioning of the cable may be required to produce a "stable" fault. This step may or may not be required, depending on the type of equipment available for fault location. The most common preconditioning technique used consists of allowing current to pass through the fault to carbonize the insulation.
4. Once a consistent fault is observed, procedures for fault prelocation are followed. This is known as pinpointing the fault location. This step assures that the location and repair of a faulted underground cable will be accomplished in one single excavation. Most modern instruments used to pinpoint faults are based on traveling waves theory.

References

Ametani, A., A general formulation of impedance and admittance of cables, *IEEE Trans. PAS-99*, 3, 902-910, May/June 1980.

Densley, R. J., An investigation into the growth of electrical trees in XLPE cable insulation, *IEEE Trans. EI-14*, 148-158, June 1979.

Gale, P. F., Cable fault location by impulse current method, *Proc. IEEE 122*, 403-408, April 1975.

Graneau, P., *Underground Power Transmission: The Science, Technology, and Economics of High Voltage Cables*, John Wiley & Sons, New York, 1979.

IEEE Guide for the Application of Sheath-Bonding Methods for Single-Conductor Cable and the Calculation of Induced Voltages and Currents in Cable Sheaths. *ANSI/IEEE Std. 575-1988.*

Kalsi, S. S. and Minnich, S. H., Calculation of circulating current losses in cable conductors, *IEEE Trans. PAS-99*, March/April, 1980.

Kojima, K. et al., Development and commercial use of 275 kV XLPE power cable, *IEEE Trans. PAS-100*, 1, 203-210.

McAllister, D., *Electric Cables Handbook*, Granada Publishing Ltd., Great Britain, 1982.

Milne, A. G. and Mochlinski, K., Characteristics of soil affecting cable ratings, *Proc. IEEE 111* (5), 1964.

Pansini, A., *Guide to Electrical Power Distribution Systems*, Pennwell Books, Tulsa, OK, 1996.

Transmission cable magnetic field research, *EPRI EL-6759-D, Project 7898-21, Final Report*, April 1990.

4.6 Transmission Line Parameters

Manuel Reta-Hernández

The power transmission line is one of the major components of an electric power system. Its major function is to transport electric energy, with minimal losses, from the power sources to the load centers, usually separated by long distances. The three basic electrical parameters of a transmission line are:

1. Series resistance
2. Series inductance
3. Shunt capacitance

Once evaluated, the parameters are used to model the line and to perform design calculations. The arrangement of the parameters (equivalent circuit) representing the line depends upon the length of the line.

Equivalent Circuit

A transmission line is defined as a short-length line if its length is less than 80 km (50 mi). In this case, the capacitive effect is negligible and only the resistance and inductive reactance are considered. Assuming balanced conditions, the line can be represented by the equivalent circuit of a single phase with resistance R, and inductive reactance X_L in series, as shown in Fig. 4.48.

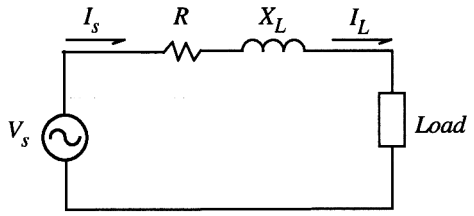

FIGURE 4.48 Equivalent circuit of a short-length transmission line.

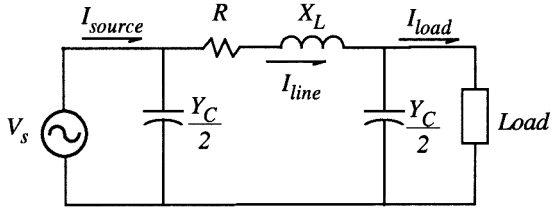

FIGURE 4.49 Equivalent circuit of a medium-length transmission line.

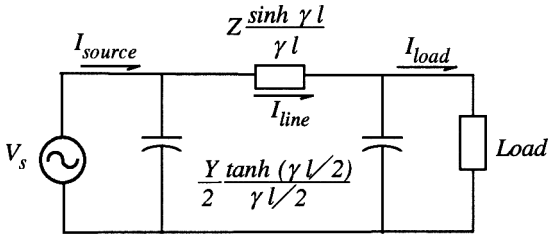

FIGURE 4.50 Equivalent circuit of a long-length transmission line.

If the line is between 80 km (50 mi) and 240 km (150 mi) long, the line is considered a medium-length line and its single-phase equivalent circuit can be represented in a nominal π circuit configuration. The shunt capacitance of the line is divided into two equal parts, each placed at the sending and receiving ends of the line. Figure 4.49 shows the equivalent circuit for a medium-length line.

Both short- and medium-length transmission lines use approximated lumped-parameter models. However, if the line is more than 240 km long, the model must consider parameters uniformly distributed along the line. The appropriate series impedance and shunt capacitance are found by solving the corresponding differential equations, where voltages and currents are described as a function of distance and time. Figure 4.50 shows the equivalent circuit for a long line,

where $Z = z\,l$ = equivalent total series impedance (Ω)
$Y = y\,l$ = total shunt admittance (S)
z = series impedance per unit length (Ω/m)
y = shunt admittance per unit length (S/m)

$\gamma = \sqrt{z\,y}$ = propagation constant

Detailed methods for calculating the three basic transmission line parameters are presented in the next sections.

Resistance

The AC resistance of a conductor in a transmission line is based on the calculation of its DC resistance. If DC is flowing along a round cylindrical conductor, the current is uniformly distributed over its cross-section area and the DC resistance is evaluated by:

$$R_{dc} = \frac{\rho l}{A} \quad [\Omega] \tag{4.15}$$

where ρ = conductor resistivity at a given temperature (Ω-m)
l = conductor length (m)
A = conductor cross-section area (m^2)

If AC current is flowing, rather than DC current, the conductor effective resistance is higher due to the skin effect (presented in the next section).

Frequency Effect

The frequency of the AC voltage produces a second effect on the conductor resistance due to the nonuniform distribution of the current. This phenomenon is known as skin effect. As frequency increases, the current tends to go toward the surface of the conductor and the current density decreases at the center. Skin effect reduces the effective cross-section area used by the current and thus the effective resistance increases. Also, although in small amount, a further resistance increase occurs when other current-carrying conductors are present in the immediate vicinity. A skin correction factor k, obtained by differential equations and Bessel functions, is considered to reevaluate the AC resistance. For 60 Hz, k is estimated around 1.02:

$$R_{ac} = R_{ac}\, k \tag{4.16}$$

Other variations in resistance are caused by:

- temperature
- spiraling of stranded conductors
- bundle conductors arrangement

Temperature Effect

The resistivity of any metal varies linearly over an operating temperature, and therefore the resistance of any conductor suffers the same variations. As temperature rises, the resistance increases linearly, according to the following equation:

$$R_2 = R_1 \left(\frac{T + t_2}{T + t_1} \right) \tag{4.17}$$

where R_2 = resistance at second temperature t_2 (°C)
R_1 = resistance at initial temperature t_1 (°C)
T = temperature coefficient for the particular material (°C)

Resistivity (ρ) and temperature coefficient (T) constants depend on the particular conductor material. Table 4.8 lists resistivity and temperature coefficients of some typical conductor materials.

Spiraling and Bundle Conductor Effect

There are two types of transmission line conductors: overhead and underground. Overhead conductors, made of naked metal and suspended on insulators, are preferred over underground conductors because of the lower cost and ease of maintenance.

TABLE 4.8 Resistivity and Temperature Coefficient of Some Materials

Material	Resistivity at 20°C (Ω-m)	Temperature Coefficient (°C)
Silver	1.59×10^{-8}	243.0
Annealed copper	1.72×10^{-8}	234.5
Hard-drawn copper	1.77×10^{-8}	241.5
Aluminum	2.83×10^{-8}	228.1

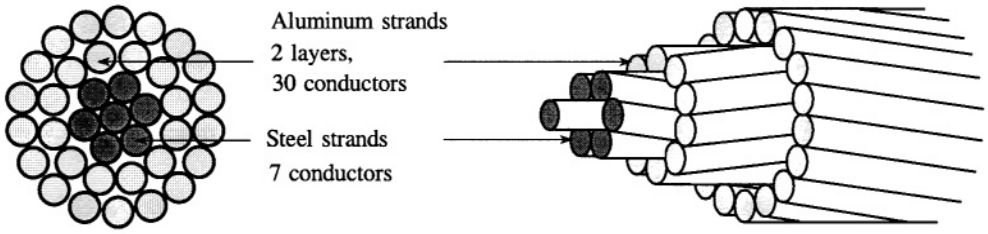

FIGURE 4.51 Stranded aluminum conductor with stranded steel core (ACSR).

In overhead transmission lines, aluminum is a common material because of the lower cost and lighter weight compared to copper, although more cross-section area is needed to conduct the same amount of current. The aluminum conductor, steel-reinforced (ACSR), is one of the most used conductors. It consists of alternate layers of stranded conductors, spiraled in opposite directions to hold the strands together, surrounding a core of steel strands as shown in Fig. 4.51. The purpose of introducing a steel core inside the stranded aluminum conductors is to obtain a high strength-to-weight ratio. A stranded conductor offers more flexibility and is easier to manufacture than a solid large conductor. However, the total resistance is increased because the outside strands are larger than the inside strands due to the spiraling.

The resistance of each wound conductor at any layer, per unit length, is based on its total length as follows:

$$R_{cond} = \frac{\rho}{A}\sqrt{1+\left(\pi\frac{1}{p}\right)^2} \quad [\Omega \text{ m}] \tag{4.18}$$

where R_{cond} = resistance of wound conductor (**Ω**)

$\sqrt{1+\left(\pi\frac{1}{p}\right)^2}$ = length of wound conductor (m)

$p_{cond} = \frac{l_{turn}}{2r_{layer}}$ = relative pitch of wound conductor

l_{turn} = length of one turn of the spiral (m)

$2r_{layer}$ = diameter of the layer (m)

The parallel combination of n conductors with the same diameter per layer gives the resistance per layer as follows:

$$R_{layer} = \frac{1}{\sum_{i=1}^{n}\frac{1}{R_i}} \quad [\Omega/\text{m}]. \tag{4.19}$$

Similarly, the total resistance of the stranded conductor is evaluated by the parallel combination of resistances per layer.

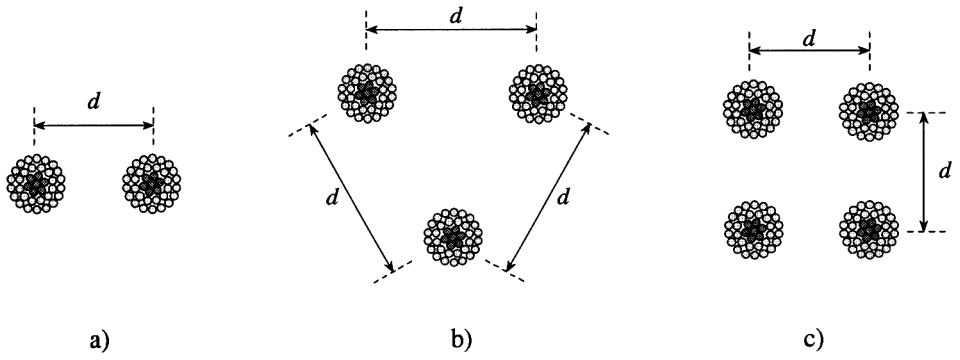

FIGURE 4.52 Stranded conductors arranged in bundles of (a) two, (b) three, and (c) four.

In high-voltage transmission lines, there may be more than one conductor per phase. This is a bundle configuration used to increase the current capability and to reduce corona discharge. By increasing the number of conductors per phase, the current capacity is increased, and the total AC resistance is proportionally decreased with respect to the number of conductors per bundle. Corona occurs when high electric field strength along the conductor surface causes ionization of the surrounding air, producing conducting atmosphere and thus producing corona losses, audible noise, and radio interference. Although corona losses depend on meteorological conditions, their evaluation takes into account the conductance between conductors and between conductors and ground. Conductor bundles may be applied to any voltage but are always used at 345 kV and above to limit corona. To maintain the distance between bundle conductors, spacers are used which are made of steel or aluminum bars. Figure 4.52 shows some arrangements of stranded bundle configurations.

Current-Carrying Capacity (Ampacity)

In overhead transmission lines, the current-carrying capacity is determined mostly by the conductor resistance and the heat dissipated from its surface. The heat generated in a conductor (I^2R) is dissipated from its surface area by convection and by radiation:

$$I^2R = S\left(w_c + w_r\right) \quad [\text{W}] \tag{4.20}$$

where R = conductor resistance (Ω)
I = conductor current-carrying (A)
S = conductor surface area (sq. in.)
w_c = convection heat loss (W/sq. in.)
w_r = radiation heat loss (W/sq. in.)

Dissipation by convection is defined as:

$$w_c = \frac{0.0128\sqrt{pv}}{T_{air}^{0.123}\sqrt{d_{cond}}}\,\Delta t \quad \left[\text{W}\right] \tag{4.21}$$

where p = atmospheric pressure (atm)
v = wind velocity (ft/sec)
d_{cond} = conductor diameter (in.)
T_{air} = air temperature (Kelvin)
Δt = $T_c - T_{air}$ = temperature rise of the conductor (°C)

Dissipation by radiation is obtained from the Stefan-Boltzmann law and is defined as:

$$w_r = 36.8\,E\left[\left(\frac{T_c}{1000}\right)^4 - \left(\frac{T_{air}}{1000}\right)^4\right] \quad \left[\text{W/sq. in.}\right] \tag{4.22}$$

where w_r = radiation heat loss (W/sq. in.)
E = emissivity constant (1 for the absolute black body and 0.5 for oxidized copper)
T_c = conductor temperature (°C)
T_{air} = ambient temperature (°C)

Substituting Eqs. (4.21) and (4.22) in (4.20) we can obtain the conductor ampacity at given temperatures.

$$I = \sqrt{\frac{\left(w_c + w_r\right) S}{R}} \quad \left[\text{A}\right] \tag{4.23}$$

$$I = \sqrt{\frac{S}{R}\left(\left(\frac{\Delta t\left(0.0128\sqrt{pv}\right)}{T_{air}^{0.123}\sqrt{d_{cond}}}\right) + \left(36.8\,E\left(\frac{T_c^4 - T_{air}^4}{1000^4}\right)\right)\right)} \quad \left[\text{A}\right] \tag{4.24}$$

Some approximated current-carrying capacity values for overhead aluminum and aluminum reinforced conductors are presented in the section "Characteristics of Overhead Conductors."

Inductance and Inductive Reactance

The magnetic flux generated by the current in transmission line conductors produces a total inductance whose magnitude depends on the line configuration. To determine the inductance of the line, it is necessary to calculate, as in any magnetic circuit with permeability μ:

1. the magnetic field intensity H,
2. the magnetic field density B, and
3. the flux linkage λ.

Inductance of a Solid, Round, Infinitely Long Conductor

Consider a long, solid, cylindrical conductor with radius r, carrying current I as shown in Fig. 4.53. If the conductor is a nonmagnetic material, and the current is assumed to be uniformly distributed (no skin effect), then the generated internal and external magnetic field lines are concentric circles around the conductor with direction defined by the right-hand rule.

Internal Inductance

To obtain the internal inductance, a magnetic field at radius x inside the conductor is chosen as shown in Fig. 4.54.

The fraction of the current I_x enclosed in the area of the circle is determined by:

$$I_x = \frac{\pi x^2}{\pi r^2}\, I \quad \left[\text{A}\right]. \tag{4.25}$$

Ampere's law determines the magnetic field intensity Hx constant at any point along the circle contour:

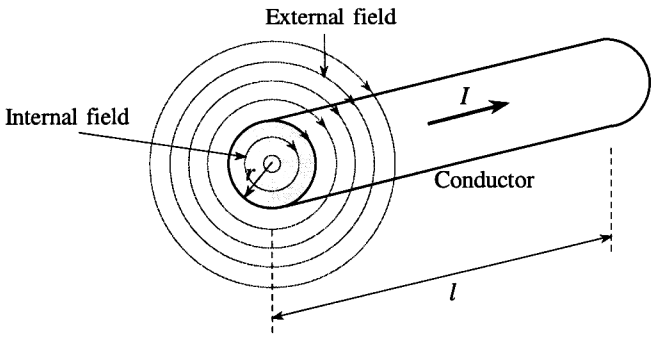

FIGURE 4.53 External and internal concentric magnetic flux lines around the conductor.

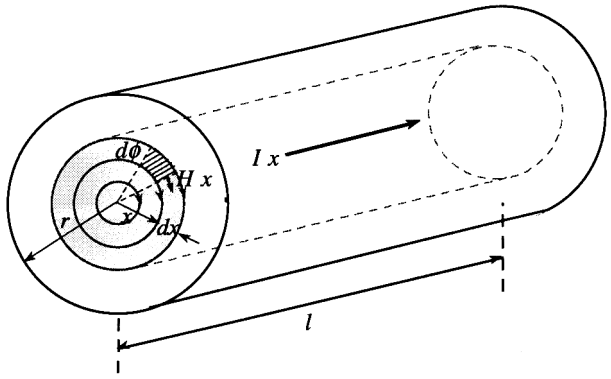

FIGURE 4.54 Internal magnetic flux.

$$H_x = \frac{I_x}{2\pi x} = \frac{I}{2\pi r^2} x \quad \left[\text{A/m}\right]. \tag{4.26}$$

The magnetic flux density B_x is obtained by

$$B_x = \mu H_x = \frac{\mu_0}{2\pi}\left(\frac{I\,x}{r^2}\right) \quad \left[\text{T}\right] \tag{4.27}$$

where $\mu = \mu_0 = 4\,\pi \times 10^{-7}$ (H/m) for a nonmagnetic material.

The differential flux $d\phi$ enclosed in a ring of thickness dx for a 1-m length of conductor, and the differential flux linkage $d\lambda$ in the respective area are

$$d\phi = B_x\,dx = \frac{\mu_0}{2\pi}\left(\frac{I\,x}{r^2}\right)dx \quad \left[\text{Wb/m}\right] \tag{4.28}$$

$$d\lambda = \frac{\pi x^2}{\pi r^2} d\phi = \frac{\mu_0}{2\pi}\left(\frac{I\,x^3}{r^4}\right)dx \quad \left[\text{Wb-turn/m}\right]. \tag{4.29}$$

The internal flux linkage is obtained by integrating the differential flux linkage from $x = 0$ to $x = r$

$$\lambda_{\text{int}} = \int_0^r d\lambda = \frac{\mu_0}{8\pi} I \quad \left[\text{Wb-turn}/\text{m}\right]. \tag{4.30}$$

The inductance due to internal flux linkage per-unit length becomes

$$L_{\text{int}} = \frac{\lambda_{\text{int}}}{I} = \frac{\mu_0}{8\pi} \quad \left[\text{H}/\text{m}\right]. \tag{4.31}$$

External Inductance

The external inductance is evaluated assuming that the total current I is concentrated at the conductor surface (maximum skin effect). At any point on an external magnetic field circle of radius y (Fig. 4.55), the magnetic field intensity H_y and the magnetic field density B_y are

$$H_y = \frac{I}{2\pi y} \quad \left[\text{A}/\text{m}\right] \quad \text{and} \tag{4.32}$$

$$B_y = \mu H_y = \frac{\mu_0}{2\pi} \frac{I}{y} \quad \left[\text{T}\right]. \tag{4.33}$$

The differential flux $d\phi$ enclosed in a ring of thickness dy, from point D_1 to point D_2, for a 1-m length of conductor is

$$d\phi = B_y\, dy = \frac{\mu_0}{2\pi} \frac{I}{y} dy \quad \left[\text{Wb}/\text{m}\right]. \tag{4.34}$$

As the total current I flows in the surface conductor, then the differential flux linkage $d\lambda$ has the same magnitude as the differential flux $d\phi$.

$$d\lambda = d\phi = \frac{\mu_0}{2\pi} \frac{I}{y} dy \quad \left[\text{Wb-turn}/\text{m}\right] \tag{4.35}$$

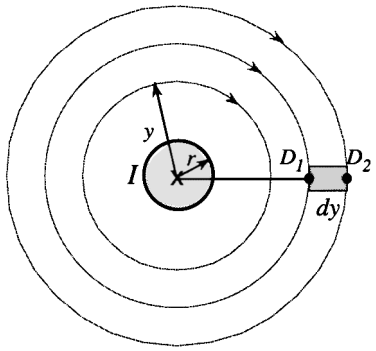

FIGURE 4.55 External magnetic flux.

The total external flux linkage enclosed by the ring is obtained by integrating from D_1 to D_2

$$\lambda_{1-2} = \int_{D_1}^{D_2} d\lambda = \frac{\mu_0}{2\pi} I \int_{D_1}^{D_2} \frac{dy}{y} = \frac{\mu_0}{2\pi} I \ln\left(\frac{D_1}{D_2}\right) \quad \left[\text{Wb-turn}/\text{m}\right]. \tag{4.36}$$

In general, the external flux linkage from the surface of the conductor to any point D is

$$\lambda_{\text{ext}} = \int_{r}^{D} d\lambda = \frac{\mu_0}{2\pi} I \ln\left(\frac{D}{r}\right) \quad \left[\text{Wb-turn}/\text{m}\right]. \tag{4.37}$$

The summation of the internal and external flux linkage at any point D permits evaluation of the total inductance of the conductor L_{tot} per-unit length as follows,

$$\lambda_{\text{intl}} + \lambda_{\text{ext}} = \frac{\mu_0}{2\pi} I \left[\frac{1}{4} + \ln\left(\frac{D}{r}\right)\right] = \frac{\mu_0}{2\pi} I \ln\left(\frac{D}{e^{-1/4} r}\right) \quad \left[\text{Wb-turn}/\text{m}\right] \tag{4.38}$$

$$L_{\text{tot}} = \frac{\lambda_{\text{int}} + \lambda_{\text{ext}}}{I} = \frac{\mu_0}{2\pi} \ln\left(\frac{D}{GMR}\right) \quad \left[\text{H}/\text{m}\right] \tag{4.39}$$

where GMR (geometric mean radius) = $e^{-1/4} r = 0.7788\, r$.

Inductance of a Two-Wire, Single-Phase Line

Consider a two-wire, single-phase line with conductors *A* and *B* with the same radius *r*, separated by a distance $D > r_A$ and r_B, and conducting the same current *I* as shown in Fig. 4.56. The current flows from the source to the load in conductor *A* and returns in conductor *B* ($I_A = -I_B$).

The magnetic flux generated by one conductor links the second conductor. The total flux linking conductor *A*, for instance, has two components: (a) the flux generated by conductor *A*, and (b) the flux generated by conductor *B* which links conductor *A*.

As shown in Fig. 4.57, the total flux linkage from conductors *A* and *B* at point *P* is

$$\lambda_{AP} = \lambda_{AAP} + \lambda_{ABP} \tag{4.40}$$

$$\lambda_{BP} = \lambda_{BAP} + \lambda_{BBP} \tag{4.41}$$

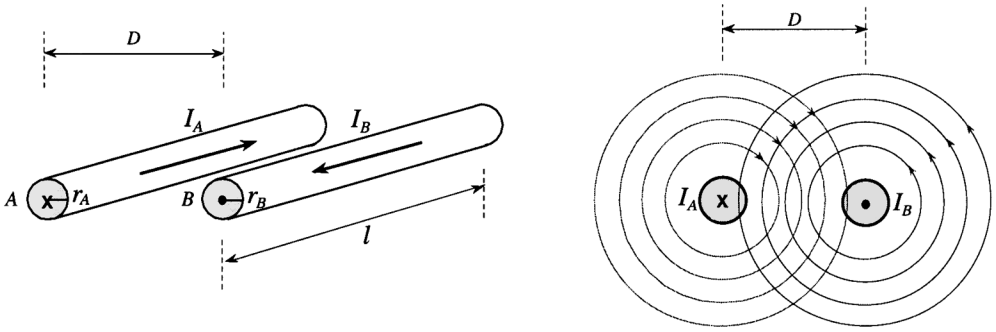

FIGURE 4.56 External magnetic flux around conductors in a two-wire, single-phase line.

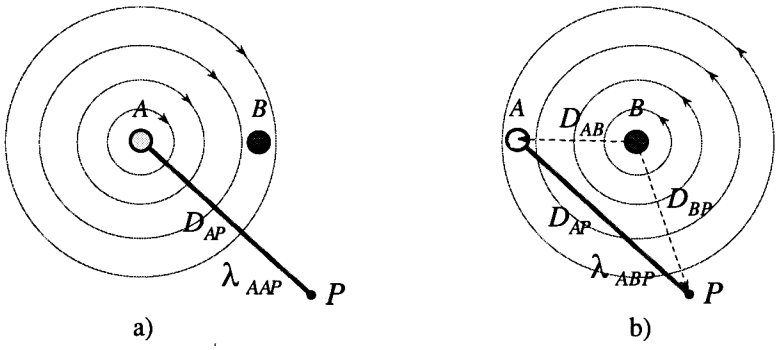

FIGURE 4.57 Flux linkage of (a) conductor *A* at point *P*, and (b) conductor *B* on conductor *A* at point *P*. Single-phase.

where λ_{AAP} = flux linkage from magnetic field of conductor *A* at point *P*
λ_{ABP} = flux linkage from magnetic field of conductor *B* on conductor *A* at point *P*
λ_{BAP} = flux linkage from magnetic field of conductor *A* on conductor *B* at point *P*
λ_{BBP} = flux linkage from magnetic field of conductor *B* at point *P*

A graphical description of flux linkages λ_{AAP} and λ_{ABP} is shown in Fig. 4.57.

The equations of the different flux linkage above are found by analyzing the flux linkage in a single conductor.

$$\lambda_{AAP} = \frac{\mu_0}{2\pi} I \ln\left(\frac{D_{AP}}{GMR_A}\right) \tag{4.42}$$

$$\lambda_{ABP} = \int_D^{D_{BP}} B_{BP}\, dP = -\frac{\mu_0}{2\pi} I \ln\left(\frac{D_{BP}}{D}\right) \tag{4.43}$$

$$\lambda_{BAP} = \int_D^{D_{AP}} B_{AP}\, dP = \frac{\mu_0}{2\pi} I \ln\left(\frac{D_{AP}}{D}\right) \tag{4.44}$$

$$\lambda_{BBP} = -\frac{\mu_0}{2\pi} I \ln\left(\frac{D_{BP}}{GMR_B}\right) \tag{4.45}$$

The total flux linkage of the system at point *P* is the algebraic summation of λ_{AP} and λ_{BP}

$$\lambda_P = \lambda_{AP} + \lambda_{BP} = \left(\lambda_{AAP} + \lambda_{ABP}\right) - \left(\lambda_{BAP} + \lambda_{BBP}\right) \tag{4.46}$$

$$\lambda_P = \frac{\mu_0}{2\pi} I \ln\left[\left(\frac{D_{AP}}{GMR_A}\right)\left(\frac{D}{D_{BP}}\right)\left(\frac{D_{BP}}{GMR_B}\right)\left(\frac{D}{D_{AP}}\right)\right] = \frac{\mu_0}{2\pi} I \ln\left(\frac{D^2}{GMR_A\, GMR_B}\right) \tag{4.47}$$

If the conductors have the same radius, $r_A = r_B = r$, and the point *P* is shifted to infinity, then the total flux leakage of the system is

$$\lambda = \frac{\mu_0}{\pi} I \ln\left(\frac{D}{GMR}\right) \quad \left[\text{Wb-turn}/\text{m}\right], \tag{4.48}$$

and the total inductance per-unit length becomes

$$L_{\text{1–phase system}} = \frac{\lambda}{I} = \frac{\mu_0}{\pi} \ln\left(\frac{D}{GMR}\right) \quad \left[\text{H}/\text{m}\right]. \tag{4.49}$$

It can be seen that the inductance of the single-phase system is twice the inductance of a single conductor.

For a line with stranded conductors, the inductance is determined using a new *GMR* value (GMR_{stranded}) evaluated according to the number of conductors. Generally, the GMR_{stranded} for any particular cable can be found in conductors tables. Additionally, if the line is composed of bundle conductors, the inductance is reevaluated taking into account the number of bundle conductors and the separation among them. The GMR_{bundle} is introduced to determine the final inductance value.

Assuming the same separation among bundles, the equation for GMR_{bundle}, up to three conductors per bundle, is defined as

$$GMR_{\text{n bundle conductors}} = \left(d^{n-1}\, GMR_{\text{stranded}}\right)^{1/n} \tag{4.50}$$

where n = number of conductors per bundle
GMR_{stranded} = *GMR* of the stranded conductor
d = distance between bundle conductors

Inductance of a Three-Phase Line

The derivations for the inductance in a single-phase system can be extended to obtain the inductance per phase in a three-phase system. Consider a three-phase, three-conductor system as shown in Fig. 4.58. The currents I_A, I_B, and I_C circulate along conductors with radius r_A, r_B, and r_C, and the separation between conductors are D_{AB}, D_{BC}, and D_{CA} (where $D > r$).

The flux linkage calculation of conductor *A* at point *P*, is calculated as

$$\lambda_{AP} = \lambda_{AAP} + \lambda_{ABP} + \lambda_{ACP} \tag{4.51}$$

$$\lambda_{AAP} = \frac{\mu_0}{2\pi} I_A \ln\left(\frac{D_{AP}}{GMR_A}\right) \tag{4.52}$$

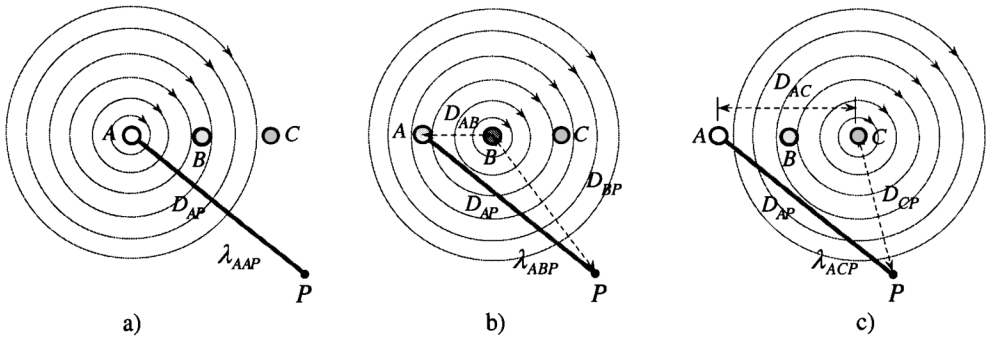

FIGURE 4.58 Flux linkage of (a) conductor *A* at point *P*, (b) conductor *B* on conductor *A* at point *P*, and (c) conductor C on conductor A at point P. Three-phase.

$$\lambda_{ABP} = \int_{D_{AB}}^{D_{BP}} B_{BP}\, dP = \frac{\mu_0}{2\pi} I_B \ln\left(\frac{D_{BP}}{D_{AB}}\right) \tag{4.53}$$

$$\lambda_{ACP} = \int_{D_{AC}}^{D_{CP}} B_{CP}\, dP = \frac{\mu_0}{2\pi} I_C \ln\left(\frac{D_{CP}}{D_{AC}}\right) \tag{4.54}$$

where λ_{AP} = total flux linkage of conductor A at point P
λ_{AAP} = flux linkage from magnetic field of conductor A at point P
λ_{ABP} = flux linkage from magnetic field of conductor B on conductor A at point P
λ_{ACP} = flux linkage from magnetic field of conductor C on conductor B at point P

The flux linkages of conductors B and C to point P have expressions similar to those for conductor A. All flux linkages expressions are

$$\lambda_{AP} = \frac{\mu_0}{2\pi}\left[I_A \ln\left(\frac{D_{AP}}{GMR_A}\right) + I_B \ln\left(\frac{D_{BP}}{D_{AB}}\right) + I_C \ln\left(\frac{D_{CP}}{D_{AC}}\right)\right] \tag{4.55}$$

$$\lambda_{BP} = \frac{\mu_0}{2\pi}\left[I_A \ln\left(\frac{D_{AP}}{D_{BA}}\right) + I_B \ln\left(\frac{D_{BP}}{GMR_B}\right) + I_C \ln\left(\frac{D_{CP}}{D_{BC}}\right)\right] \tag{4.56}$$

$$\lambda_{CP} = \frac{\mu_0}{2\pi}\left[I_A \ln\left(\frac{D_{AP}}{D_{CA}}\right) + I_B \ln\left(\frac{D_{BP}}{D_{CB}}\right) + I_C \ln\left(\frac{D_{CP}}{GMR_C}\right)\right] \tag{4.57}$$

Rearranging the expressions, we have

$$\begin{aligned}\lambda_{AP} = {} & \frac{\mu_0}{2\pi}\left[I_A \ln\left(\frac{1}{GMR_A}\right) + I_B \ln\left(\frac{1}{D_{AB}}\right) + I_C \ln\left(\frac{1}{D_{AC}}\right)\right] \\ & + \frac{\mu_0}{2\pi}\left[I_A \ln\left(D_{AP}\right) + I_B \ln\left(D_{BP}\right) + I_C \ln\left(D_{CP}\right)\right]\end{aligned} \tag{4.58}$$

$$\begin{aligned}\lambda_{BP} = {} & \frac{\mu_0}{2\pi}\left[I_A \ln\left(\frac{1}{D_{BA}}\right) + I_B \ln\left(\frac{1}{GMR_B}\right) + I_C \ln\left(\frac{1}{D_{BC}}\right)\right] \\ & + \frac{\mu_0}{2\pi}\left[I_A \ln\left(D_{AP}\right) + I_B \ln\left(D_{BP}\right) + I_C \ln\left(D_{CP}\right)\right]\end{aligned} \tag{4.59}$$

$$\begin{aligned}\lambda_{CP} = {} & \frac{\mu_0}{2\pi}\left[I_A \ln\left(\frac{1}{D_{CA}}\right) + I_B \ln\left(\frac{1}{D_{CB}}\right) + I_C \ln\left(\frac{1}{GMR_C}\right)\right] \\ & + \frac{\mu_0}{2\pi}\left[I_A \ln\left(D_{AP}\right) + I_B \ln\left(D_{BP}\right) + I_C \ln\left(D_{CP}\right)\right]\end{aligned} \tag{4.60}$$

The second part of each equation is zero for practical conditions assuming that point P is shifted to infinity. Therefore, the expressions of the total flux linkage for all conductors are

$$\lambda_A = \frac{\mu_0}{2\pi}\left[I_A \ln\left(\frac{1}{GMR_A}\right) + I_B \ln\left(\frac{1}{D_{AB}}\right) + I_C \ln\left(\frac{1}{D_{AC}}\right)\right] \tag{4.61}$$

$$\lambda_B = \frac{\mu_0}{2\pi}\left[I_A \ln\left(\frac{1}{D_{BA}}\right) + I_B \ln\left(\frac{1}{GMR_B}\right) + I_C \ln\left(\frac{1}{D_{BC}}\right)\right] \tag{4.62}$$

$$\lambda_C = \frac{\mu_0}{2\pi}\left[I_A \ln\left(\frac{1}{D_{CA}}\right) + I_B \ln\left(\frac{1}{D_{CB}}\right) + I_C \ln\left(\frac{1}{GMR_C}\right)\right] \tag{4.63}$$

The flux linkage of each phase conductor depends on the three currents, and therefore the inductance per phase is not only one as in the single-phase system. Instead, three different inductances (self and mutual conductor inductances) exist. Calculating the inductance values from the equations above and arranging the equations in a matrix form, we can obtain the set of inductances in the system

$$\begin{bmatrix}\lambda_A \\ \lambda_B \\ \lambda_C\end{bmatrix} = \begin{bmatrix}L_{AA} & L_{AB} & L_{AC} \\ L_{BA} & L_{BB} & L_{BC} \\ L_{CA} & L_{CB} & L_{CC}\end{bmatrix}\begin{bmatrix}I_A \\ I_B \\ I_C\end{bmatrix} \tag{4.64}$$

where $\lambda_A, \lambda_B, \lambda_C$ = total flux linkage of conductor A, B, and C
L_{AA}, L_{BB}, L_{CC} = self-inductance of conductors A, B, and C field of conductor A at point P
$L_{AB}, L_{BC}, L_{CA}, L_{BA}, L_{CB}, L_{AC}$ = mutual inductance among conductors

With nine different inductances in a simple three-phase system, the analysis could be a little more complicated. A single inductance per phase can be obtained, however, if the three conductors are arranged with the same separation among them $D = D_{AB} = D_{BC} = D_{CA}$ (triangle configuration). In this case the flux linkage of conductor A per-unit length is

$$\lambda_A = \frac{\mu_0}{2\pi}\left[I_A \ln\left(\frac{1}{GMR_A}\right) + I_B \ln\left(\frac{1}{D}\right) + I_C \ln\left(\frac{1}{D}\right)\right]. \tag{4.65}$$

Assuming a balanced system ($I_A + I_B + I_C = 0$, or $I_A = -I_B - I_C$), then the flux linkage is

$$\lambda_A = \frac{\mu_0}{2\pi} I_A \ln\left(\frac{D}{GMR_A}\right) \quad \left[\text{Wb-turn}/\text{m}\right]. \tag{4.66}$$

If the GMR value is the same in all phase conductors, the total flux linkage expression is the same for all phases. Therefore, the equivalent inductance per phase is

$$L_{\text{phase}} = \frac{\mu_0}{2\pi} \ln\left(\frac{D}{GMR_{cond}}\right) \quad \left[\text{H}/\text{m}\right]. \tag{4.67}$$

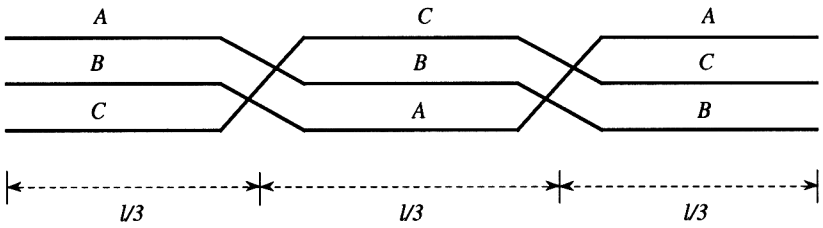

FIGURE 4.59 Arrangement of conductors in a transposed line.

Inductance of Transposed Three-Phase Transmission Lines

In actual transmission lines, the phase conductors generally do not have a symmetrical (triangular) arrangement. However, if the phase conductors are transposed, an average distance *GMD* (geometrical mean distance) is substituted for distance *D*, and the calculation of the phase inductance derived for symmetrical arrangement is still valid. In a transposed system, each phase conductor occupies the location of the other two phases for one third of the total line length as shown in Fig. 4.59.

The inductance per phase per unit length in a transmission line is

$$L_{\text{phase}} = \frac{\mu_0}{2\pi} \ln\left(\frac{GMD}{GMR_{\text{cond}}}\right) \quad \left[\text{H}/\text{m}\right] \tag{4.68}$$

where $GMD = \sqrt[3]{D_{AB} D_{BC} D_{CA}}$ = geometrical mean distance for a three-phase line.

Once the inductance per phase is obtained, the inductive reactance can be evaluated as

$$X_{\text{L}_{\text{phase}}} = 2\pi f L_{\text{phase}} = \mu_0 \, f \ln\left(\frac{GMD}{GMR_{\text{cond}}}\right) \quad \left[\Omega/\text{m}\right]. \tag{4.69}$$

For bundle conductors, the GMR_{bundle} value is determined, as in the single-phase transmission line case, by the number of conductors, and by the number of conductors per bundle and the separation among them. The expression for the total inductive reactance per phase is

$$X_{\text{L}_{\text{phase}}} = \mu_0 \, f \ln\left(\frac{GMD}{GMR_{\text{bundle}}}\right) \quad \left[\Omega/\text{m}\right] \tag{4.70}$$

where $GMR_{\text{bundle}} = (d^{n-1} \, GMR_{\text{stranded}})^{1/n}$ = geometric mean radius of bundle conductors
- GMD = geometric mean distance
- GMR_{stranded} = geometric mean radius of stranded conductor
- d = distance between bundle conductors
- n = number of conductors per bundle
- f = frequency (60 Hz)

Capacitance and Capacitive Reactance

To evaluate the capacitance between conductors in a surrounding medium with permitivity ε, it is necessary to first determine the voltage between the conductors, and the electric field strength of the surrounding.

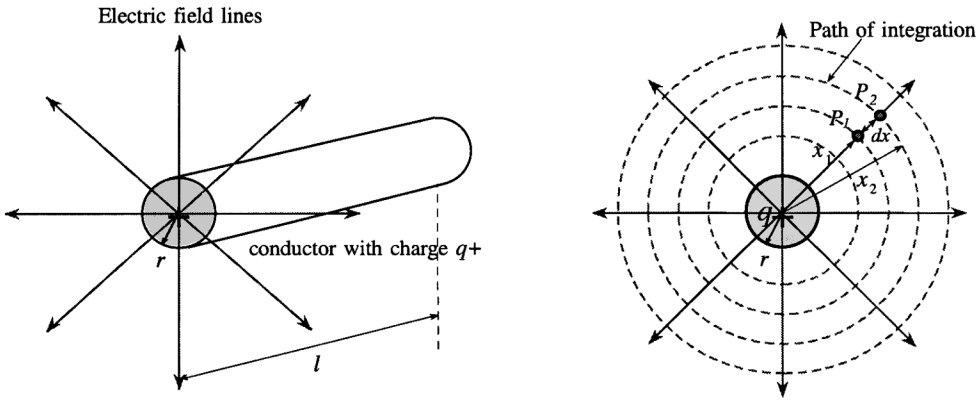

FIGURE 4.60 Electric field produced from a single conductor.

Capacitance of a Single Solid Conductor

Consider a solid, cylindrical, long conductor with radius r, in a free space with permitivity ε_0, and with a charge of $q+$ C per meter uniformly distributed on the surface. There is a constant electric field strength on the surface of cylinder (Fig. 4.60). The resistivity of the conductor is assumed to be zero (perfect conductor), which results in zero internal electric field due to the charge on the conductor.

The charge $q+$ produces an electric field radial to the conductor with equipotential surfaces concentric to the conductor. According to Gauss's law, the total electric flux leaving a closed surface is equal to the total charge inside the volume enclosed by the surface. Therefore, at an outside point P separated x meters from the center of the conductor, the electric field flux density, and the electric field intensity are

$$Density_P = \frac{q}{A} = \frac{q}{2\pi x} \quad \left[\text{C}\right] \quad \text{and} \tag{4.71}$$

$$E_P = \frac{Density_P}{\varepsilon} = \frac{q}{2\pi\varepsilon_0 x} \quad \left[\text{V/m}\right] \tag{4.72}$$

where $Density_P$ = electric flux density at point P
E_P = electric field intensity at point P
A = surface of a concentric cylinder with one-meter length and radius x (m^2)
ε = $\varepsilon_0 = \frac{10^{-9}}{36\pi}$ = permitivity of free space assumed for the conductor (F/m)

The potential difference or voltage difference between two outside points P_1 and P_2 with corresponding distances x_1 and x_2 from the conductor center is defined by integrating the electric field intensity from x_1 to x_2

$$V_{1-2} = \int_{x_1}^{x_2} E_P \frac{dx}{x} = \int_{x_1}^{x_2} \frac{q}{2\pi\varepsilon_0}\frac{dx}{x} = \frac{q}{2\pi\varepsilon_0}\ln\left[\frac{x_2}{x_1}\right] \quad \left[\text{V}\right]. \tag{4.73}$$

Then, the capacitance between points P_1 and P_2 is evaluated as

$$C_{1-2} = \frac{q}{V_{1-2}} = \frac{2\pi\varepsilon_0}{\ln\left[\dfrac{x_2}{x_1}\right]} \quad \left[\mathrm{F/m}\right]. \tag{4.74}$$

If point P_1 is located at the conductor surface ($x_1 = \mathrm{r}$), and point P_2 is located at ground surface below the conductor ($x_2 = H$), then the voltage of the conductor and the capacitance between the conductor and ground are

$$V_{\mathrm{cond}} = \frac{q}{2\pi\varepsilon_0}\ln\left[\frac{H}{r}\right] \quad \left[\mathrm{V}\right] \quad \text{and} \tag{4.75}$$

$$C_{\text{cond-ground}} = \frac{q}{V_{\mathrm{cond}}} = \frac{2\pi\varepsilon_0}{\ln\left[\dfrac{H}{r}\right]} \quad \left[\mathrm{F/m}\right]. \tag{4.76}$$

Capacitance of a Single-Phase Line with Two Wires

Consider a two-wire, single-phase line with conductors A and B with the same radius r, separated by a distance $D > r_A$ and r_B. The conductors are energized by a voltage source such that conductor A has a charge q^+ and conductor B a charge q^- as shown in Fig. 4.61.

The charge on each conductor generates independent electric fields. Charge q^+ on conductor A generates a voltage $V_{AB\text{-}A}$ between both conductors. Similarly, charge q^- on conductor B generates a voltage $V_{AB\text{-}B}$ between conductors.

$V_{AB\text{-}A}$ is calculated by integrating the electric field intensity, due to the charge on conductor A, on conductor B from r_A to D

$$V_{AB-A} = \int_{r_A}^{D} E_A\, dx = \frac{q}{2\pi\varepsilon_0}\ln\left[\frac{D}{r_A}\right]. \tag{4.77}$$

$V_{AB\text{-}B}$ is calculated by integrating the electric field intensity due to the charge on conductor B from D to r_B

$$V_{AB-B} = \int_{D}^{r_B} E_B\, dx = \frac{-q}{2\pi\varepsilon_0}\ln\left[\frac{r_B}{D}\right]. \tag{4.78}$$

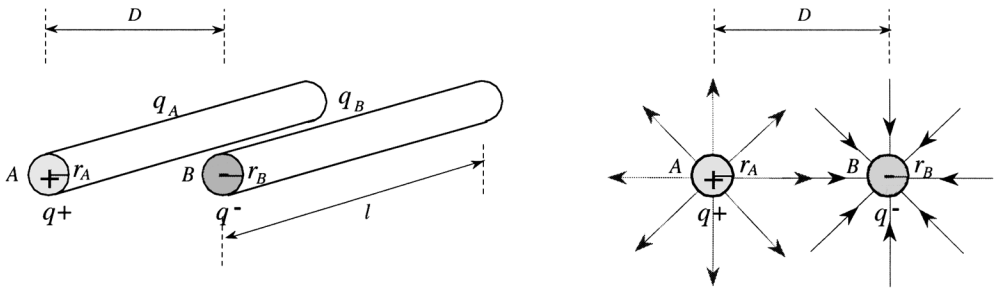

FIGURE 4.61 Electric field produced from a two-wire, single-phase system.

The total voltage is the sum of the generated voltages $V_{AB\text{-}A}$ and $V_{AB\text{-}B}$

$$V_{AB} = V_{AB-A} + V_{AB-B} = \frac{q}{2\pi\varepsilon_0}\ln\left[\frac{D}{r_A}\right] - \frac{q}{2\pi\varepsilon_0}\ln\left[\frac{r_B}{D}\right] = \frac{q}{2\pi\varepsilon_0}\ln\left[\frac{D^2}{r_A r_B}\right]. \tag{4.79}$$

If the conductors have the same radius, $r_A = r_B = r$, then the voltage between conductors V_{AB}, and the capacitance between conductors C_{AB}, for a one-meter line length are

$$V_{AB} = \frac{q}{\pi\varepsilon_0}\ln\left[\frac{D}{r}\right] \quad [\mathrm{V}] \quad \text{and} \tag{4.80}$$

$$C_{AB} = \frac{\pi\varepsilon_0}{\ln\left[\frac{D}{r}\right]} \quad [\mathrm{F/m}]. \tag{4.81}$$

The voltage between each conductor and ground (Fig. 4.62) is one-half of the voltage between the two conductors. Therefore, the capacitance from either line to ground is twice the capacitance between lines

$$V_{AG} = V_{BG} = \frac{V_{AB}}{2} \quad [\mathrm{V}] \tag{4.82}$$

$$C_{AG} = \frac{q}{V_{AG}} = \frac{2\pi\varepsilon_0}{\ln\left[\frac{D}{r}\right]} \quad [\mathrm{F/m}]. \tag{4.83}$$

Capacitance of a Three-Phase Line

Consider a three-phase line with the same voltage magnitude between phases, and assume a balanced system with *abc* (positive) sequence such that $q_A + q_B + q_C = 0$. The conductors have radii r_A, r_B, and r_C, and the spaces between conductors are D_{AB}, D_{BC}, and D_{AC} (where D_{AB}, D_{BC}, and $D_{AC} > r_A$, r_B, and r_C). Also, the effect of earth and neutral conductors is neglected.

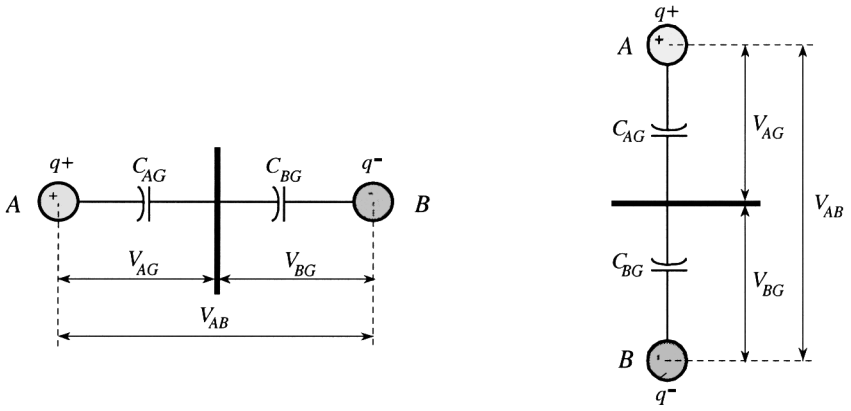

FIGURE 4.62 Capacitance between line-to-ground in a two-wire, single-phase line.

The expression for voltage between two conductors in a single-phase system can be extended to obtain the voltages between conductors in a three-phase system. The expressions for V_{AB} and V_{AC} are

$$V_{AB} = \frac{1}{2\pi\varepsilon_0}\left[q_A \ln\left[\frac{D_{AB}}{r_A}\right] + q_B \ln\left[\frac{r_B}{D_{AB}}\right] + q_C \ln\left[\frac{D_{BC}}{D_{AC}}\right]\right] \quad \text{and} \tag{4.84}$$

$$V_{AC} = \frac{1}{2\pi\varepsilon_0}\left[q_A \ln\left[\frac{D_{CA}}{r_A}\right] + q_B \ln\left[\frac{D_{BC}}{D_{AB}}\right] + q_C \ln\left[\frac{r_C}{D_{AC}}\right]\right] \tag{4.85}$$

If the three-phase system has a triangular arrangement with equidistant conductors such that $D_{AB} = D_{BC} = D_{AC} = D$, with the same radii for the conductors such that $r_A = r_B = r_C = r$ (where $D > r$), the expressions for V_{AB} and V_{AC} are

$$\begin{aligned} V_{AB} &= \frac{1}{2\pi\varepsilon_0}\left[q_A \ln\left[\frac{D}{r}\right] + q_B \ln\left[\frac{r}{D}\right] + q_C \ln\left[\frac{D}{D}\right]\right] \\ &= \frac{1}{2\pi\varepsilon_0}\left[q_A \ln\left[\frac{D}{r}\right] + q_B \ln\left[\frac{r}{D}\right]\right] \quad [\text{V}] \end{aligned} \tag{4.86}$$

$$\begin{aligned} V_{AC} &= \frac{1}{2\pi\varepsilon_0}\left[q_A \ln\left[\frac{D}{r}\right] + q_B \ln\left[\frac{D}{D}\right] + q_C \ln\left[\frac{r}{D}\right]\right] \\ &= \frac{1}{2\pi\varepsilon_0}\left[q_A \ln\left[\frac{D}{r}\right] + q_C \ln\left[\frac{r}{D}\right]\right] \quad [\text{V}] \end{aligned} \tag{4.87}$$

Balanced line-to-line voltages with sequence *abc*, expressed in terms of the line-to-neutral voltage are: $V_{AB} = \sqrt{3}\, V_{AN} \angle 30°$, and $V_{AC} = -V_{CA} = \sqrt{3}\, V_{AN} \angle -30°$; where V_{AN} is the line-to-neutral voltage. Therefore, V_{AN} can be expressed in terms of V_{AB} and V_{AC} as

$$V_{AN} = \frac{V_{AB} + V_{AC}}{3} \tag{4.88}$$

and thus, substituting V_{AB} and V_{AC} from Eqs. (4.81) and (4.82), we have

$$\begin{aligned} V_{AN} &= \frac{1}{6\pi\varepsilon_0}\left[\left[q_A \ln\left[\frac{D}{r}\right] + q_B \ln\left[\frac{r}{D}\right]\right] + \left[q_A \ln\left[\frac{D}{r}\right] + q_C \ln\left[\frac{r}{D}\right]\right]\right] \\ &= \frac{1}{6\pi\varepsilon_0}\left[2q_A \ln\left[\frac{D}{r}\right] + \left(q_B + q_C\right)\ln\left[\frac{r}{D}\right]\right]. \end{aligned} \tag{4.89}$$

Under balanced conditions ($q_A + q_B + q_C = 0$, or $-q_A = (q_B + q_C)$ then, the final expression for the line-to-neutral voltage is

$$V_{AN} = \frac{1}{2\pi\varepsilon_0} q_A \ln\left[\frac{D}{r}\right] \quad [\mathrm{V}]. \tag{4.90}$$

The positive sequence capacitance per unit length between phase *A* and neutral can now be obtained. The same result is obtained for capacitance between phases *B* and *C* to neutral.

$$C_{AN} = \frac{q_A}{V_{AN}} = \frac{2\pi\varepsilon_0}{\ln\left[\frac{D}{r}\right]} \quad \left[\mathrm{F/m}\right] \tag{4.91}$$

Capacitance of Stranded Bundle Conductors

The calculation of the capacitance in the equation above is based on:

1. solid conductors with zero resistivity (zero internal electric field)
2. distributed charge uniformly
3. equilateral spacing of phase conductors

In actual transmission lines, the resistivity of the conductors produces a small internal electric field and, therefore, the electric field at the conductor surface is smaller than estimated. However, the difference is negligible for practical purposes. Because of the presence of other charged conductors, the charge distribution is nonuniform, and therefore the estimated capacitance is different. However, this effect is negligible for most practical calculations. In a line with stranded conductors, the capacitance is evaluated assuming a solid conductor with the same radius as the outside radius of the stranded conductor. This produces a negligible difference.

Most transmission lines do not have equilateral spacing of phase conductors. This causes differences between the line-to-neutral capacitances of the three phases. However, transposing the phase conductors balances the system, resulting in equal line-to-neutral capacitance for each phase and is developed in the following manner.

Consider a transposed three-phase line with conductors having the same radius *r*, and with space between conductors D_{AB}, D_{BC}, and D_{AC}, where D_{AB}, D_{BC}, and $D_{AC} > r$. Assuming *abc* positive sequence, the expressions for V_{AB} on the first, second, and third sections of the transposed line are

$$V_{AB\,\text{first}} = \frac{1}{2\pi\varepsilon_0}\left[q_A \ln\left[\frac{D_{AB}}{r}\right] + q_B \ln\left[\frac{r}{D_{AB}}\right] + q_C \ln\left[\frac{D_{AB}}{D_{AC}}\right]\right] \tag{4.92}$$

$$V_{AB\,\text{second}} = \frac{1}{2\pi\varepsilon_0}\left[q_A \ln\left[\frac{D_{BC}}{r}\right] + q_B \ln\left[\frac{r}{D_{BC}}\right] + q_C \ln\left[\frac{D_{AC}}{D_{AB}}\right]\right] \tag{4.93}$$

$$V_{AB\,\text{third}} = \frac{1}{2\pi\varepsilon_0}\left[q_A \ln\left[\frac{D_{AC}}{r}\right] + q_B \ln\left[\frac{r}{D_{AC}}\right] + q_C \ln\left[\frac{D_{AB}}{D_{BC}}\right]\right]. \tag{4.94}$$

Similarly, the expressions for V_{AC} on the first, second, and third sections of the transposed line are

$$V_{AC\,\text{first}} = \frac{1}{2\pi\varepsilon_0}\left[q_A \ln\left[\frac{D_{AC}}{r}\right] + q_B \ln\left[\frac{D_{BC}}{D_{AB}}\right] + q_C \ln\left[\frac{r}{D_{AC}}\right]\right] \tag{4.95}$$

$$V_{AC\,\text{second}} = \frac{1}{2\pi\varepsilon_0}\left[q_A \ln\left[\frac{D_{AB}}{r}\right] + q_B \ln\left[\frac{D_{AC}}{D_{BC}}\right] + q_C \ln\left[\frac{r}{D_{AB}}\right]\right] \tag{4.96}$$

$$V_{AC\,\text{third}} = \frac{1}{2\pi\varepsilon_0}\left[q_A \ln\left[\frac{D_{BC}}{r}\right] + q_B \ln\left[\frac{D_{AB}}{D_{AC}}\right] + q_C \ln\left[\frac{r}{D_{BC}}\right]\right] \tag{4.97}$$

Taking the average value of the three sections, we have the final expressions of V_{AB} and V_{AC} in the transposed line

$$\begin{aligned} V_{AB\,\text{transp}} &= \frac{V_{AB\,\text{first}} + V_{AB\,\text{second}} + V_{AB\,\text{third}}}{3} \\ &= \frac{1}{6\pi\varepsilon_0}\left[q_A \ln\left[\frac{D_{AB}D_{AC}D_{BC}}{r^3}\right] + q_B \ln\left[\frac{r^3}{D_{AB}D_{AC}D_{BC}}\right] + q_C \ln\left[\frac{D_{AC}D_{AC}D_{BC}}{D_{AC}D_{AC}D_{BC}}\right]\right] \end{aligned} \tag{4.98}$$

$$\begin{aligned} V_{AB\,\text{transp}} &= \frac{V_{AC\,\text{first}} + V_{AC\,\text{second}} + V_{AC\,\text{third}}}{3} \\ &= \frac{1}{6\pi\varepsilon_0}\left[q_A \ln\left[\frac{D_{AB}D_{AC}D_{BC}}{r^3}\right] + q_B \ln\left[\frac{D_{AC}D_{AC}D_{BC}}{D_{AB}D_{AC}D_{BC}}\right] + q_C \ln\left[\frac{r^3}{D_{AC}D_{AC}D_{BC}}\right]\right]. \end{aligned} \tag{4.99}$$

For a balanced system where $-q_A = (q_B + q_C)$, the phase-to-neutral voltage V_{AN} (phase voltage) is

$$\begin{aligned} V_{AN\,\text{transp}} &= \frac{V_{AB\,\text{transp}} + V_{AC\,\text{transp}}}{3} \\ &= \frac{1}{18\pi\varepsilon_0}\left[2q_A \ln\left[\frac{D_{AB}D_{AC}D_{BC}}{r^3}\right] + \left(q_B + q_C\right)\ln\left[\frac{r^3}{D_{AB}D_{AC}D_{BC}}\right]\right] \\ &= \frac{1}{6\pi\varepsilon_0} q_A \ln\left[\frac{D_{AB}D_{AC}D_{BC}}{r^3}\right] = \frac{1}{2\pi\varepsilon_0} q_A \ln\left[\frac{GMD}{r}\right] \quad [\text{V}] \end{aligned} \tag{4.100}$$

where $GMD = \sqrt[3]{D_{AB}D_{BC}D_{CA}}$ = geometrical mean distance for a three-phase line.

For bundle conductors, an equivalent radius r_e replaces the radius r of a single conductor and is determined by the number of conductors per bundle and the spacing of conductors. The expression of r_e is similar to GMR_{bundle} used in the calculation of the inductance per phase, except that the actual outside radius of the conductor is used instead of the GMR_{cond}. Therefore, the expression for V_{AN} is

$$V_{AN\,\text{transp}} = \frac{1}{2\pi\varepsilon_0} q_A \ln\left[\frac{GMD}{r_e}\right] \quad [\text{V}] \tag{4.101}$$

where $r_e = (d^{n-1}\, r)^{1/n}$ = equivalent radius for up to three conductors per bundle (m)
d = distance between bundle conductors (m)
n = number of conductors per bundle

Finally, the capacitance and capacitive reactance per unit length from phase to neutral can be evaluated as

$$C_{AN\ \text{transp}} = \frac{q_A}{V_{AN\ \text{transp}}} = \frac{2\pi\varepsilon_0}{\ln\left[\dfrac{GMD}{r_e}\right]} \quad \left[\text{F}/\text{m}\right] \tag{4.102}$$

$$X_{AN\ \text{transp}} = \frac{1}{2\pi\, \text{f}\, C_{AN\ \text{transp}}} = \frac{1}{4\pi \text{f}\,\varepsilon_0} \ln\left[\frac{GMD}{r_e}\right] \quad \left[\Omega/\text{m}\right]. \tag{4.103}$$

Characteristics of Overhead Conductors

Tables 4.9a and 4.9b present general characteristics of aluminum cable steel reinforced conductors (ACSR). The size of the conductors (cross-section area) is specified in square millimeters and kcmil, where a cmil is the cross-section area of a circular conductor with a diameter of 1/1000 inch. Typical values of resistance, inductive reactance, and capacitive reactance are listed. The approximate current-carrying capacity of the conductors is also included assuming 60 Hz, wind speed of 1.4 mi/h, and conductor and air temperatures of 75°C and 25°C, respectively. Similarly, Tables 4.10a and 4.10b present the corresponding characteristics of aluminum conductors (AAC).

References

Barnes, C. C., *Power Cables: Their Design and Installation*, 2nd ed., Chapman and Hall, Ltd., London, 1966.

Electric Power Research Institute, *Transmission Line Reference Book 345 kV and Above,* 2nd ed., Palo Alto, CA, 1987.

Glover J. D., Sarma, M., and Digby, G., *Power System Analysis and Design with Personal Computer Applications*, 2nd ed., PWS Publishing Company, 1994.

Gross, Ch. A., *Power System Analysis*, John Wiley & Sons, New York, 1979.

Gungor, B. R., *Power Systems*, Harcourt Brace Jovanovich, Florida, 1988.

Yamayee, Z. A., and Bala, J. L. Jr., *Electromechanical Energy Devices and Power Systems,* John Wiley & Sons, New York, 1994.

Zaborszky, J., and Rittenhouse, J. W., *Electric Power Transmission: The Power System in the Steady State,* The Ronald Press Company, New York, 1954.

TABLE 4.9a Characteristics of Aluminum Cable Steel Reinforced Conductors (ACSR)

	Cross-Section Area				Diameter			Approx. Current-	Resistance (mΩ/km)					60-Hz Reactances (Dm = 1m)	
	Total	Aluminum		Stranding	Conductor	Core		Carrying Capacity	DC	AC (60 Hz)			GMR	X_L	X_C
Code	(mm^2)	(kcmil)	(mm^2)	A1/Steel	(mm)	(mm)	Layers	(Amp.)*	25°C	25°C	50°C	75°C	(mm)	(Ω/km)	(MΩ/km)
—	1521	2776	1407	84/19	50.80	13.87	4		21.0	4.5	26.2	28.1	20.33	0.294	0.175
Joree	1344	2515	1274	76/19	47.75	10.80	4		22.7	26.0	28.0	30.0	18.93	0.299	0.178
Thrasher	1235	2312	1171	76/19	45.77	10.34	4		24.7	27.7	30.0	32.2	18.14	0.302	0.180
Kiwi	1146	2167	1098	72/7	44.07	8.81	4		26.4	29.4	31.9	34.2	17.37	0.306	0.182
Bluebird	1181	2156	1092	84/19	44.75	12.19	4		26.5	29.0	31.4	33.8	17.92	0.303	0.181
Chukar	9767	1781	902	84/19	40.69	11.10	4		32.1	34.1	37.2	40.1	16.28	0.311	0.186
Falcon	908	1590	806	54/19	39.24	13.08	3	1380	35.9	37.4	40.8	44.3	15.91	0.312	0.187
Lapwing	862	1590	806	45/7	38.20	9.95	3	1370	36.7	38.7	42.1	45.6	15.15	0.316	0.189
Parrot	862	1510	765	54/19	38.23	12.75	3	1340	37.8	39.2	42.8	46.5	15.48	0.314	0.189
Nuthatch	818	1510	765	45/7	37.21	9.30	3	1340	38.7	40.5	44.2	47.9	14.78	0.318	0.190
Plover	817	1431	725	54/19	37.21	12.42	3	1300	39.9	41.2	45.1	48.9	15.06	0.316	0.190
Bobolink	775	1431	725	45/7	36.25	9.07	3	1300	35.1	42.6	46.4	50.3	14.39	0.320	0.191
Martin	772	1351	685	54/19	36.17	12.07	3	1250	42.3	43.5	47.5	51.6	14.63	0.319	0.191
Dipper	732	1351	685	45/7	35.20	8.81	3	1250	43.2	44.9	49.0	53.1	13.99	0.322	0.193
Pheasant	726	1272	645	54/19	35.10	11.71	3	1200	44.9	46.1	50.4	54.8	14.20	0.321	0.193
Bittern	689	1272	644	45/7	34.16	8.53	3	1200	45.9	47.5	51.9	56.3	13.56	0.324	0.194
Grackle	681	1192	604	54/19	34.00	11.33	3	1160	47.9	49.0	53.6	58.3	13.75	0.323	0.194
Bunting	646	1193	604	45/7	33.07	8.28	3	1160	48.9	50.4	55.1	59.9	13.14	0.327	0.196
Finch	636	1114	564	54/19	32.84	10.95	3	1110	51.3	52.3	57.3	62.3	13.29	0.326	0.196
Bluejay	603	1113	564	45/7	31.95	8.00	3	1110	52.4	53.8	58.9	64.0	12.68	0.329	0.197
Curlew	591	1033	523	54/7	31.62	10.54	3	1060	56.5	57.4	63.0	68.4	12.80	0.329	0.198
Ortolan	560	1033	525	45/7	30.78	7.70	3	1060	56.5	57.8	63.3	68.7	12.22	0.332	0.199
Merganser	596	954	483	30/7	31.70	13.60	2	1010	61.3	61.8	67.9	73.9	13.11	0.327	0.198
Cardinal	546	954	483	54/7	30.38	10.13	3	1010	61.2	62.0	68.0	74.0	12.31	0.332	0.200
Rail	517	954	483	45/7	29.59	7.39	3	1010	61.2	62.4	68.3	74.3	11.73	0.335	0.201
Baldpate	562	900	456	30/7	30.78	13.21	2	960	65.0	65.5	71.8	78.2	12.71	0.329	0.199
Canary	515	900	456	54/7	29.51	9.83	3	970	64.8	65.5	72.0	78.3	11.95	0.334	0.201
Ruddy	478	900	456	45/7	28.73	7.19	3	970	64.8	66.0	72.3	78.6	11.40	0.337	0.202
Crane	501	875	443	54/7	29.11	9.70	3	950	66.7	67.5	74.0	80.5	11.80	0.335	0.202
Willet	474	874	443	45/7	28.32	7.09	3	950	66.7	67.9	74.3	80.9	11.25	0.338	0.203

TABLE 4.9a (continued) Characteristics of Aluminum Cable Steel Reinforced Conductors (ACSR)

	Cross-Section Area				Diameter			Approx. Current-	Resistance (mΩ/km)					60-Hz Reactances (Dm = 1m)	
	Total	Aluminum		Stranding	Conductor	Core		Carrying Capacity	DC	AC (60 Hz)			GMR	X_L	X_C
Code	(mm^2)	(kcmil)	(mm^2)	A1/Steel	(mm)	(mm)	Layers	(Amp.)*	25°C	25°C	50°C	75°C	(mm)	(Ω/km)	(MΩ/km)
Skimmer	479	795	403	30/7	29.00	12.40	2	940	73.5	74.0	81.2	88.4	11.95	0.334	0.202
Mallard	495	795	403	30/19	28.96	12.42	2	910	73.5	74.0	81.2	88.4	11.95	0.334	0.202
Drake	469	795	403	26/7	28.14	10.36	2	900	73.3	74.0	81.2	88.4	11.43	0.337	0.203
Condor	455	795	403	54/7	27.74	9.25	3	900	73.4	74.1	81.4	88.6	11.22	0.339	0.204
Cuckoo	455	795	403	24/7	27.74	9.25	2	900	73.4	74.1	81.4	88.5	11.16	0.339	0.204
Tern	431	795	403	45/7	27.00	6.76	3	900	73.4	74.4	81.6	88.8	10.73	0.342	0.205
Coot	414	795	403	36/1	26.42	3.78	3	910	73.0	74.4	81.5	88.6	10.27	0.345	0.206
Buteo	447	715	362	30/7	27.46	11.76	2	840	81.8	82.2	90.2	98.3	11.34	0.338	0.204
Redwing	445	715	362	30/19	27.46	11.76	2	840	81.8	82.2	90.2	98.3	11.34	0.338	0.204
Starling	422	716	363	26/7	26.7	9.82	2	840	81.5	82.1	90.1	98.1	10.82	0.341	0.206
Crow	409	715	362	54/7	26.31	8.76	3	840	81.5	82.2	90.2	98.2	10.67	0.342	0.206

Source: Transmission Line Reference Book 345 kV and Above, 2nd ed., Electronic Power Research Institute, Palo Alto, CA, 1987. With permission.

TABLE 4.9b Characteristics of Aluminum Cable Steel Reinforced Conductors (ACSR)

	Cross-Section Area				Diameter			Approx. Current-	Resistance (mΩ/km)					60-Hz Reactances (Dm = 1m)	
	Total	Aluminum		Stranding	Conductor	Core		Carrying Capacity	DC	AC (60 Hz)			GMR	X_L	X_C
Code	(mm^2)	(kcmil)	(mm^2)	A1/Steel	(mm)	(mm)	Layers	(Amp.)*	25°C	25°C	50°C	75°C	(mm)	(Ω/km)	(MΩ/km)
Stilt	410	716	363	24/7	26.31	8.76	2	840	81.5	82.2	90.2	98.1	10.58	0.343	0.206
Grebe	388	716	363	45/7	25.63	6.4	3	840	81.5	82.5	90.4	98.4	10.18	0.3446	0.208
Gannet	393	666	338	26/7	25.76	9.5	2	800	87.6	88.1	96.6	105.3	10.45	0.344	0.208
Gull	382	667	338	54/7	25.4	8.46	3	800	87.5	88.1	96.8	105.3	10.27	0.345	0.208
Flamingo	382	667	338	24/7	25.4	8.46	2	800	87.4	88.1	96.7	105.3	10.21	0.346	0.208
Scoter	397	636	322	30/7	25.88	11.1	2	800	91.9	92.3	101.4	110.4	10.70	0.342	0.207
Egret	396	636	322	30/19	25.88	11.1	2	780	91.9	92.3	101.4	110.4	10.70	0.342	0.207
Grosbeak	375	636	322	26/7	25.15	9.27	2	780	91.7	92.2	101.2	110.3	10.21	0.346	0.209
Goose	364	636	322	54/7	24.82	8.28	3	770	91.8	92.4	101.4	110.4	10.06	0.347	0.208
Rook	363	636	322	24/7	24.82	8.28	2	770	91.7	92.3	101.3	110.3	10.06	0.347	0.209
Kingbird	340	636	322	18/1	23.88	4.78	2	780	91.2	92.2	101.1	110.0	9.27	0.353	0.211
Swirl	331	636	322	36/1	23.62	3.38	3	780	91.3	92.4	101.3	110.3	9.20	0.353	0.212
Wood Duck	378	605	307	30/7	25.25	10.82	2	760	96.7	97.0	106.5	116.1	10.42	0.344	0.208
Teal	376	605	307	30/19	25.25	10.82	2	770	96.7	97.0	106.5	116.1	10.42	0.344	0.208
Squab	356	605	356	26/7	25.54	9.04	2	760	96.5	97.0	106.5	116.0	9.97	0.347	0.208
Peacock	346	605	307	24/7	24.21	8.08	2	760	96.4	97.0	106.4	115.9	9.72	0.349	0.210
Duck	347	606	307	54/7	24.21	8.08	3	750	96.3	97.0	106.3	115.8	9.81	0.349	0.210
Eagle	348	557	282	30/7	24.21	10.39	2	730	105.1	105.4	115.8	126.1	10.00	0.347	0.210
Dove	328	556	282	26/7	23.55	8.66	2	730	104.9	105.3	115.6	125.9	9.54	0.351	0.212
Parakeet	319	557	282	24/7	23.22	7.75	2	730	104.8	105.3	115.6	125.9	9.33	0.352	0.212
Osprey	298	556	282	18/1	22.33	4.47	2	740	104.4	105.2	115.4	125.7	8.66	0.358	0.214
Hen	298	477	242	30/7	22.43	9.6	2	670	122.6	122.9	134.9	147.0	9.27	0.353	0.214
Hawk	281	477	242	26/7	21.79	8.03	2	670	122.4	122.7	134.8	146.9	8.84	0.357	0.215
Flicker	273	477	273	24/7	21.49	7.16	2	670	122.2	122.7	134.7	146.8	8.63	0.358	0.216
Pelican	255	477	242	18/1	20.68	4.14	2	680	121.7	122.4	134.4	146.4	8.02	0.364	0.218
Lark	248	397	201	30/7	20.47	8.76	2	600	147.2	147.4	161.9	176.4	8.44	0.360	0.218
Ibis	234	397	201	26/7	19.89	7.32	2	590	146.9	147.2	161.7	176.1	8.08	0.363	0.220
Brant	228	398	201	24/7	19.61	6.53	2	590	146.7	147.1	161.6	176.1	7.89	0.365	0.221
Chickadee	213	397	201	18/1	18.87	3.78	2	590	146.1	146.7	161.0	175.4	7.32	0.371	0.222
Oriole	210	336	170	30/7	18.82	8.08	2	530	173.8	174.0	191.2	208.3	7.77	0.366	0.222

TABLE 4.9b (continued) Characteristics of Aluminum Cable Steel Reinforced Conductors (ACSR)

	Cross-Section Area				Diameter			Approx. Current-	Resistance (mΩ/km)					60-Hz Reactances (Dm = 1m)	
	Total	Aluminum		Stranding	Conductor	Core		Carrying Capacity	DC	AC (60 Hz)			GMR	X_L	X_C
Code	(mm^2)	(kcmil)	(mm^2)	A1/Steel	(mm)	(mm)	Layers	(Amp.)*	25°C	25°C	50°C	75°C	(mm)	(Ω/km)	(MΩ/km)
Linnet	198	336	170	26/7	18.29	6.73	2	530	173.6	173.8	190.9	208.1	7.41	0.370	0.224
Widgeon	193	336	170	24/7	18.03	6.02	2	530	173.4	173.7	190.8	207.9	7.5	0.371	0.225
Merlin	180	336	170	18/1	16.46	3.48	2	530	173.0	173.1	190.1	207.1	6.74	0.377	0.220
Piper	187	300	152	30/7	17.78	7.62	2	500	195.0	195.1	214.4	233.6	7.35	0.370	0.225
Ostrich	177	300	152	26/7	17.27	6.38	2	490	194.5	194.8	214.0	233.1	7.01	0.374	0.227
Gadwall	172	300	152	24/7	17.04	5.69	2	490	194.5	194.8	213.9	233.1	6.86	0.376	0.227
Phoebe	160	300	152	18/1	16.41	3.28	2	490	193.5	194.0	213.1	232.1	6.37	0.381	0.229
Junco	167	267	135	30/7	16.76	7.19	2	570	219.2	219.4	241.1	262.6	6.92	0.375	0.228
Partridge	157	267	135	26/7	16.31	5.99	2	460	218.6	218.9	240.5	262.0	6.61	0.378	0.229
Waxwing	143	267	135	18/1	15.47	3.1	2	460	217.8	218.1	239.7	261.1	6.00	0.386	0.232

* For conductor temperature at 75°C, air at 25°C, wind speed at 1.4 mi/hr, frequency at 60 Hz.

Source: Transmission Line Reference Book 345 kV and Above, 2nd ed., Electronic Power Research Institute, Palo Alto, CA, 1987. With permission.

TABLE 4.10a Characteristics of All-Aluminum Conductors (AAC)

Code	Cross-Section Area (mm^2)	Cross-Section Area kcmil or AWG	Stranding	Diameter (mm)	Layers	Approx. Current-Carrying Capacity (Amp.)*	Resistance (mΩ/km) DC 25°C	Resistance (mΩ/km) AC (60 Hz) 25°C	Resistance (mΩ/km) 50°C	Resistance (mΩ/km) 75°C	GMR (mm)	60-Hz Reactances (Dm = 1 m) X_L (Ω/km)	60-Hz Reactances (Dm = 1 m) X_C (MΩ/km)
Coreopsis	806.2	1591	61	36.93	4	1380	36.5	39.5	42.9	46.3	14.26	0.320	0.190
Gladiolus	765.8	1511	61	35.99	4	1340	38.4	41.3	44.9	48.5	13.90	0.322	0.192
Caranation	725.4	1432	61	35.03	4	1300	40.5	43.3	47.1	50.9	13.53	0.324	0.193
Columbine	865.3	1352	61	34.04	4	1250	42.9	45.6	49.6	53.6	13.14	0.327	0.196
Narcissus	644.5	1272	61	33.02	4	1200	45.5	48.1	52.5	46.7	12.74	0.329	0.194
Hawthorn	604.1	1192	61	31.95	4	1160	48.7	51.0	55.6	60.3	12.34	0.331	0.197
Marigold	564.2	1113	61	30.89	4	1110	52.1	54.3	59.3	64.3	11.92	0.334	0.199
Larkspur	524	1034	61	29.77	4	1060	56.1	58.2	63.6	69.0	11.49	0.337	0.201
Bluebell	524.1	1034	37	29.71	3	1060	56.1	58.2	63.5	68.9	11.40	0.337	0.201
Goldenrod	483.7	955	61	28.6	4	1010	60.8	62.7	68.6	74.4	11.03	0.340	0.203
Magnolia	483.6	954	37	28.55	3	1010	60.8	62.7	68.6	74.5	10.97	0.340	0.203
Crocus	443.6	875	61	27.38	4	950	66.3	68.1	74.5	80.9	10.58	0.343	0.205
Anemone	443.5	875	37	27.36	3	950	66.3	68.1	74.5	80.9	10.49	0.344	0.205
Lilac	403.1	796	61	26.11	4	900	73.0	74.6	81.7	88.6	10.09	0.347	0.207
Arbutus	402.9	795	37	26.06	3	900	73.0	74.6	81.7	88.6	10.00	0.347	0.207
Nasturtium	362.5	715	61	24.76	4	840	81.2	82.6	90.5	98.4	9.57	0.351	0.209
Violet	362.8	716	37	24.74	3	840	81.1	82.5	90.4	98.3	9.48	0.351	0.209
Orchid	322.2	636	37	23.32	3	780	91.3	92.6	101.5	110.4	8.96	0.356	0.212
Mistletoe	281.8	556	37	21.79	3	730	104.4	105.5	115.8	126.0	8.38	0.361	0.215
Dahlia	281.8	556	19	21.72	2	730	104.4	105.5	115.8	125.9	8.23	0.362	0.216
Syringa	241.5	477	37	20.19	3	670	121.8	122.7	134.7	146.7	7.74	0.367	0.219
Cosmos	241.9	477	19	20.14	2	670	121.6	122.6	134.5	146.5	7.62	0.368	0.219
Canna	201.6	398	19	18.36	2	600	145.9	146.7	161.1	175.5	6.95	0.376	0.224
Tulip	170.6	337	19	16.92	2	530	172.5	173.2	190.1	207.1	6.40	0.381	0.228
Laurel	135.2	267	19	15.06	2	460	217.6	218.1	239.6	261.0	5.70	0.390	0.233
Daisy	135.3	267	7	14.88	1	460	217.5	218	239.4	260.8	5.39	0.394	0.233
Oxlip	107.3	212 or (4/0)	7	13.26	1	340	274.3	274.7	301.7	328.8	4.82	0.402	0.239
Phlox	85	168 or (3/0)	7	11.79	1	300	346.4	346.4	380.6	414.7	4.27	0.411	0.245
Aster	67.5	133 or (2/0)	7	10.52	1	270	436.1	439.5	479.4	522.5	3.81	0.40	0.25
Poppy	53.5	106 or (1/0)	7	9.35	1	230	550	550.2	604.5	658.8	3.38	0.429	0.256
Pansy	42.4	#1 AWG	7	8.33	1	200	694.2	694.2	763.2	831.6	3.02	0.438	0.261
Iris	33.6	#2 AWG	7	7.42	1	180	874.5	874.5	960.8	1047.9	2.68	0.446	0.267
Rose	21.1	#3 AWG	7	5.89	1	160	1391.5	1391.5	1528.9	1666.3	2.13	0.464	0.278
Peachbell	13.3	#4 AWG	7	4.67	1	140	2214.4	2214.4	2443.2	2652	1.71	0.481	0.289

* For conductor at 75°C, air at 25°C, wind speed at 1.4 mi/hr, frequency at 60 Hz.

Source: *Transmission Line Reference Book 345 kV and Above,* 2nd ed., Electronic Power Research Institute, Palo Alto, CA, 1987. With permission.

TABLE 4.10b Characteristics of All-Aluminum Conductors (AAC)

Code	Cross-Section Area (mm^2)	Cross-Section Area kcmil or AWG	Stranding	Diameter (mm)	Layers	Approx. Current-Carrying Capacity (Amp.)*	Resistance (mΩ/km) DC 25°C	Resistance (mΩ/km) AC (60 Hz) 25°C	Resistance (mΩ/km) 50°C	Resistance (mΩ/km) 75°C	GMR (mm)	60-Hz Reactances (Dm = 1 m) X_L (Ω/km)	60-Hz Reactances (Dm = 1 m) X_C (MΩ/km)
EVEN SIZES													
Bluebonnet	1773.3	3500	7	54.81	6		16.9	22.2	23.6	25.0	21.24	0.290	0.172
Trillium	1520.2	3000	127	50.75	6		19.7	24.6	26.2	27.9	19.69	0.296	0.175
Lupine	1266.0	2499	91	46.30	5		23.5	27.8	29.8	31.9	17.92	0.303	0.180
Cowslip	1012.7	1999	91	41.40	5		29.0	32.7	35.3	38.0	16.03	0.312	0.185
Jessamine	887.0	1750	61	38.74	4		33.2	36.5	39.5	42.5	14.94	0.317	0.188
Hawkweed	506.7	1000	37	29.24	3	1030	58.0	60.0	65.5	71.2	11.22	0.339	0.201
Camelia	506.4	999	61	29.26	4	1030	58.1	60.1	65.5	71.2	11.31	0.338	0.201
Snapdragon	456.3	900	61	27.79	4	970	64.4	66.3	72.5	78.7	10.73	0.342	0.204
Cockscomb	456.3	900	37	27.74	3	970	64.4	66.3	72.5	78.7	10.64	0.343	0.204
Cattail	380.1	750	61	25.35	4	870	77.4	78.9	86.4	93.9	9.78	0.349	0.208
Petunia	380.2	750	37	23.85	3	870	77.4	78.9	86.4	93.9	9.72	0.349	0.208
Flag	354.5	700	61	24.49	4	810	83.0	84.4	92.5	100.6	9.45	0.352	0.210
Verbena	354.5	700	37	24.43	3	810	83.0	84.4	92.5	100.6	9.39	0.352	0.210
Meadowswee	303.8	600	37	2.63	3	740	96.8	98.0	107.5	117.0	8.69	0.358	0.214
Hyacinth	253.1	500	37	20.65	3	690	116.2	117.2	128.5	140.0	7.92	0.365	0.218
Zinnia	253.3	500	19	20.60	2	690	116.2	117.2	128.5	139.9	7.80	0.366	0.218
Goldentuft	228.0	450	19	19.53	2	640	129.0	129.9	142.6	155.3	7.41	0.370	0.221
Daffodil	177.3	350	19	17.25	2	580	165.9	166.6	183.0	199.3	6.52	0.379	0.227
Peony	152.1	300	19	15.98	2	490	193.4	194.0	213.1	232.1	6.04	0.385	0.230
Valerian	126.7	250	19	14.55	2	420	232.3	232.8	255.6	278.6	5.52	0.392	0.235
Sneezewort	126.7	250	7	14.40	1	420	232.2	232.7	255.6	278.4	5.21	0.396	0.235

Source: Transmission Line Reference Book 345 kV and Above, 2nd ed., Electronic Power Research Institute, Palo Alto, CA, 1987. With permission.

4.7 Sag and Tension of Conductor

D.A. Douglass and Ridley Thrash

The energized conductors of transmission and distribution lines must be placed to totally eliminate the possibility of injury to people. Overhead conductors, however, elongate with time, temperature, and tension, thereby changing their original positions after installation. Despite the effects of weather and loading on a line, the conductors must remain at safe distances from buildings, objects, and people or vehicles passing beneath the line at all times. To ensure this safety, the shape of the terrain along the right-of-way, the height and lateral position of the conductor support points, and the position of the conductor between support points under all wind, ice, and temperature conditions must be known.

Bare overhead transmission or distribution conductors are typically quite flexible and uniform in weight along their length. Because of these characteristics, they take the form of a catenary (Ehrenberg, 1935; Winkelmann, 1959) between support points. The shape of the catenary changes with conductor temperature, ice and wind loading, and time. To ensure adequate vertical and horizontal clearance under all weather and electrical loadings, and to ensure that the breaking strength of the conductor is not exceeded, the behavior of the conductor catenary under all conditions must be known before the line is designed. The future behavior of the conductor is determined through calculations commonly referred to as sag-tension calculations.

Sag-tension calculations predict the behavior of conductors based on recommended tension limits under varying loading conditions. These tension limits specify certain percentages of the conductor's rated breaking strength that are not to be exceeded upon installation or during the life of the line. These conditions, along with the elastic and permanent elongation properties of the conductor, provide the basis for determinating the amount of resulting sag during installation and long-term operation of the line.

Accurately determined initial sag limits are essential in the line design process. Final sags and tensions depend on initial installed sags and tensions and on proper handling during installation. The final sag shape of conductors is used to select support point heights and span lengths so that the minimum clearances will be maintained over the life of the line. If the conductor is damaged or the initial sags are incorrect, the line clearances may be violated or the conductor may break during heavy ice or wind loadings.

Catenary Cables

A bare-stranded overhead conductor is normally held clear of objects, people, and other conductors by periodic attachment to insulators. The elevation differences between the supporting structures affect the shape of the conductor catenary. The catenary's shape has a distinct effect on the sag and tension of the conductor, and therefore, must be determined using well-defined mathematical equations.

Level Spans

The shape of a catenary is a function of the conductor weight per unit length, w, the horizontal component of tension, H, span length, S, and the maximum sag of the conductor, D. Conductor sag and span length are illustrated in Fig. 4.63 for a level span.

The exact catenary equation uses hyperbolic functions. Relative to the low point of the catenary curve shown in Fig. 4.63, the height of the conductor, $y(x)$, above this low point is given by the following equation:

$$y\left(x\right)=\frac{H}{w}\cosh\left(\left(\frac{w}{H}x\right)-1\right)=\frac{w\left(x^2\right)}{2H} \tag{4.104}$$

Note that x is positive in either direction from the low point of the catenary. The expression to the right is an approximate parabolic equation based upon a MacLaurin expansion of the hyperbolic cosine.

For a level span, the low point is in the center, and the sag, D, is found by substituting $x = S/2$ in the preceding equations. The exact and approximate parabolic equations for sag become the following:

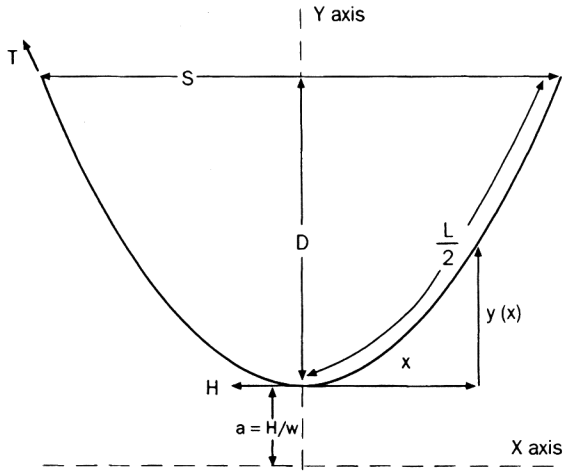

FIGURE 4.63 The catenary curve for level spans.

$$D = \frac{H}{w}\left(\cosh\left(\frac{wS}{2H}\right) - 1\right) = \frac{w\left(S^2\right)}{8H} \tag{4.105}$$

The ratio, *H/w*, which appears in all of the preceding equations, is commonly referred to as the catenary constant. An increase in the catenary constant, having the units of length, causes the catenary curve to become shallower and the sag to decrease. Although it varies with conductor temperature, ice and wind loading, and time, the catenary constant typically has a value in the range of several thousand feet for most transmission-line catenaries.

The approximate or parabolic expression is sufficiently accurate as long as the sag is less than 5% of the span length. As an example, consider a 1000-ft span of Drake conductor ($w = 1.096$ lb/ft) installed at a tension of 4500 lb. The catenary constant equals 4106 ft. The calculated sag is 30.48 ft and 30.44 ft using the hyperbolic and approximate equations, respectively. Both estimates indicate a sag-to-span ratio of 3.4% and a sag difference of only 0.5 in.

The horizontal component of tension, *H*, is equal to the conductor tension at the point in the catenary where the conductor slope is horizontal. For a level span, this is the midpoint of the span length. At the ends of the level span, the conductor tension, *T*, is equal to the horizontal component plus the conductor weight per unit length, *w*, multiplied by the sag, *D*, as shown in the following:

$$T = H + wD \tag{4.106}$$

Given the conditions in the preceding example calculation for a 1000-ft level span of Drake ACSR, the tension at the attachment points exceeds the horizontal component of tension by 33 lb. It is common to perform sag-tension calculations using the horizontal tension component, but the average of the horizontal and support point tension is usually listed in the output.

Conductor Length

Application of calculus to the catenary equation allows the calculation of the conductor length, *L(x)*, measured along the conductor from the low point of the catenary in either direction.

The resulting equation becomes:

$$L\left(x\right) = \frac{H}{w}\text{SINH}\left(\frac{wx}{H}\right) = x\left(1 + \frac{x^2\left(w^2\right)}{6H^2}\right) \tag{4.107}$$

For a level span, the conductor length corresponding to $x = S/2$ is half of the total conductor length and the total length, L, is:

$$L = \left(\frac{2H}{w}\right) \text{SINH}\left(\frac{Sw}{2H}\right) = S\left(1 + \frac{S^2\left(w^2\right)}{24H^2}\right) \tag{4.108}$$

The parabolic equation for conductor length can also be expressed as a function of sag, D, by substitution of the sag parabolic equation, giving:

$$L = S + \frac{8D^2}{3S} \tag{4.109}$$

Conductor Slack

The difference between the conductor length, L, and the span length, S, is called slack. The parabolic equations for slack may be found by combining the preceding parabolic equations for conductor length, L, and sag, D:

$$L - S = S^3\left(\frac{w^2}{24H^2}\right) = D^2\left(\frac{8}{3S}\right) \tag{4.110}$$

While slack has units of length, it is often expressed as the percentage of slack relative to the span length. Note that slack is related to the cube of span length for a given H/w ratio and to the square of sag for a given span. For a series of spans having the same H/w ratio, the total slack is largely determined by the longest spans. It is for this reason that the ruling span is nearly equal to the longest span rather than the average span in a series of suspension spans.

Equation (4.110) can be inverted to obtain a more interesting relationship showing the dependence of sag, D, upon slack, L-S:

$$D = \sqrt{\frac{3S\left(L - S\right)}{8}} \tag{4.111}$$

As can be seen from the preceding equation, small changes in slack typically yield large changes in conductor sag.

Inclined Spans

Inclined spans may be analyzed using essentially the same equations that were used for level spans. The catenary equation for the conductor height above the low point in the span is the same. However, the span is considered to consist of two separate sections, one to the right of the low point and the other to the left as shown in Fig. 4.64 (Winkelmann, 1959). The shape of the catenary relative to the low point is unaffected by the difference in suspension point elevation (span inclination).

In each direction from the low point, the conductor elevation, y(x), relative to the low point is given by:

$$y\left(x\right) = \frac{H}{w}\cosh\left(\left(\frac{w}{H}x\right) - 1\right) = \frac{w\left(x^2\right)}{2H} \tag{4.112}$$

Note that x is considered positive in either direction from the low point.

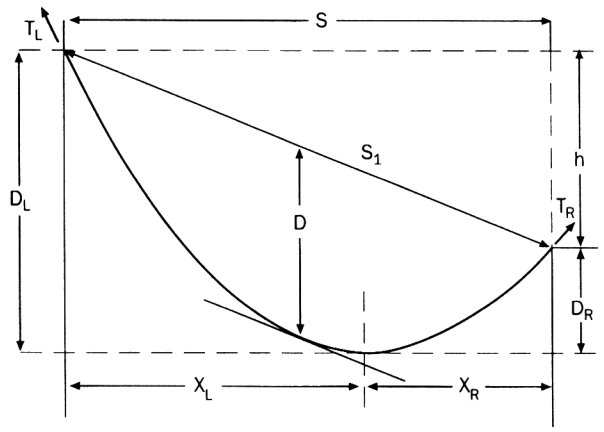

FIGURE 4.64 Inclined catenary span.

The horizontal distance, x_L, from the left support point to the low point in the catenary is:

$$x_L = \frac{S}{2}\left(1 + \frac{h}{4D}\right) \tag{4.113}$$

The horizontal distance, x_R, from the right support point to the low point of the catenary is:

$$x_R = \frac{S}{2}\left(1 - \frac{h}{4D}\right) \tag{4.114}$$

where

S = horizontal distance between support points.
h = vertical distance between support points.
S_1 = straight-line distance between support points.
D = sag measured vertically from a line through the points of conductor support to a line tangent to the conductor.

The midpoint sag, D, is approximately equal to the sag in a horizontal span equal in length to the inclined span, S_1.

Knowing the horizonal distance from the low point to the support point in each direction, the preceding equations for $y(x)$, L, D, and T can be applied to each side of the inclined span.

The total conductor length, L, in the inclined span is equal to the sum of the lengths in the x_R and x_L sub-span sections:

$$L = S + \left(x_R^3 + x_L^3\right)\left(\frac{w^2}{6H^2}\right) \tag{4.115}$$

In each sub-span, the sag is relative to the corresponding support point elevation:

$$D_R = \frac{wx_R^2}{2H} \qquad D_L = \frac{wx_L^2}{2H} \tag{4.116}$$

or in terms of sag, D, and the vertical distance between support points:

$$D_R = D\left(1 - \frac{h}{4D}\right)^2 \qquad D_L = D\left(1 + \frac{h}{4D}\right)^2 \tag{4.117}$$

and the maximum tension is:

$$T_R = H + wD_R \qquad T_L = H + wD_L \tag{4.118}$$

or in terms of upper and lower support points:

$$T_u = T_l + wh \tag{4.119}$$

where

D_R = sag in right sub-span section
D_L = sag in left sub-span section
T_R = tension in right sub-span section
T_L = tension in left sub-span section
T_u = tension in conductor at upper support
T_l = tension in conductor at lower support

The horizontal conductor tension is equal at both supports. The vertical component of conductor tension is greater at the upper support and the resultant tension, T_u, is also greater.

Ice and Wind Conductor Loads

When a conductor is covered with ice and/or is exposed to wind, the effective conductor weight per unit length increases. During occasions of heavy ice and/or wind load, the conductor catenary tension increases dramatically along with the loads on angle and deadend structures. Both the conductor and its supports can fail unless these high-tension conditions are considered in the line design.

The National Electric Safety Code (NESC) suggests certain combinations of ice and wind corresponding to heavy, medium, and light loading regions of the United States. Figure 4.65 is a map of the U.S. indicating those areas (NESC, 1993). The combinations of ice and wind corresponding to loading region are listed in Table 4.11.

The NESC also suggests that increased conductor loads due to high wind loads without ice be considered. Figure 4.66 shows the suggested wind pressure as a function of geographical area for the United States (ASCE Std 7-88).

Certain utilities in very heavy ice areas use glaze ice thicknesses of as much as two inches to calculate iced conductor weight. Similarly, utilities in regions where hurricane winds occur may use wind loads as high as 34 lb/ft^2.

As the NESC indicates, the degree of ice and wind loads varies with the region. Some areas may have heavy icing, whereas some areas may have extremely high winds. The loads must be accounted for in the line design process so they do not have a detrimental effect on the line. Some of the effects of both the individual and combined components of ice and wind loads are discussed in the following.

Ice Loading

The formation of ice on overhead conductors may take several physical forms (glaze ice, rime ice, or wet snow). The impact of lower density ice formation is usually considered in the design of line sections at high altitudes.

The formation of ice on overhead conductors has the following influence on line design:

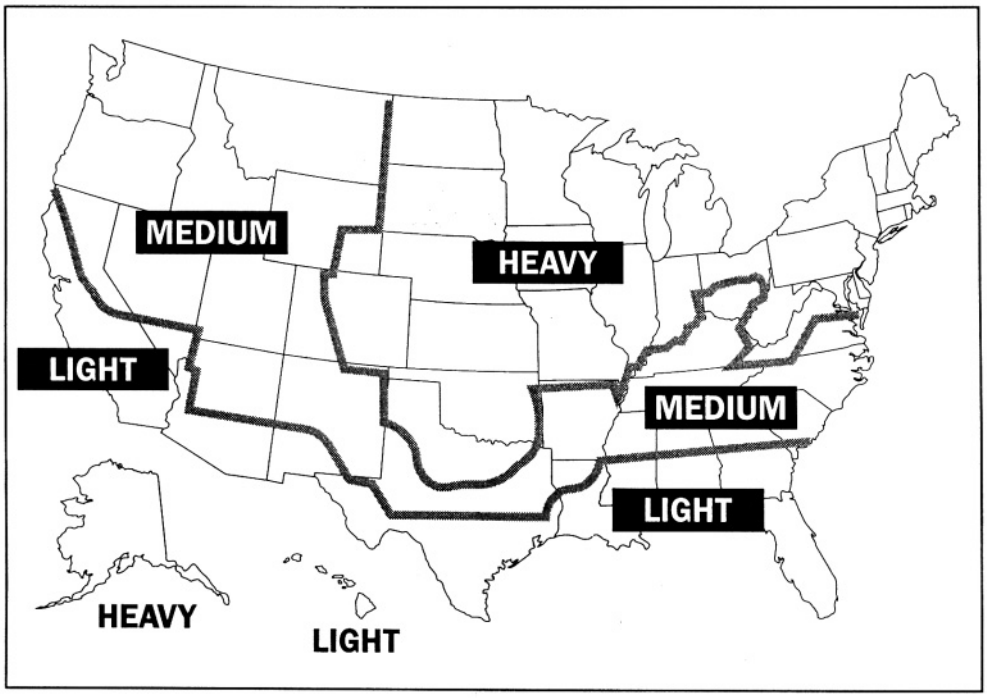

FIGURE 4.65 Ice and wind load areas of the U.S.

TABLE 4.11 Definitions of Ice and Wind Load for NESC Loading Areas

	Loading Districts			
	Heavy	Medium	Light	Extreme Wind Loading
Radial thickness of ice				
(in.)	0.50	0.25	0	0
(mm)	12.5	6.5	0	0
Horizontal wind pressure				
(lb/ft^2)	4	4	9	See Fig. 4.66
(Pa)	190	190	430	
Temperature				
(°F)	0	+15	+30	+60
(°C)	–20	–10	–1	+15
Constant to be added to the resultant for all conductors				
(lb/ft)	0.30	0.20	0.05	0.0
(N/m)	4.40	2.50	0.70	0.0

- Ice loads determine the maximum vertical conductor loads that structures and foundations must withstand.
- In combination with simultaneous wind loads, ice loads also determine the maximum transverse loads on structures.
- In regions of heavy ice loads, the maximum sags and the permanent increase in sag with time (difference between initial and final sags) may be due to ice loadings.

Ice loads for use in designing lines are normally derived on the basis of past experience, code requirements, state regulations, and analysis of historical weather data. Mean recurrence intervals for heavy ice loadings are a function of local conditions along various routings. The impact of varying assumptions concerning ice loading can be investigated with line design software.

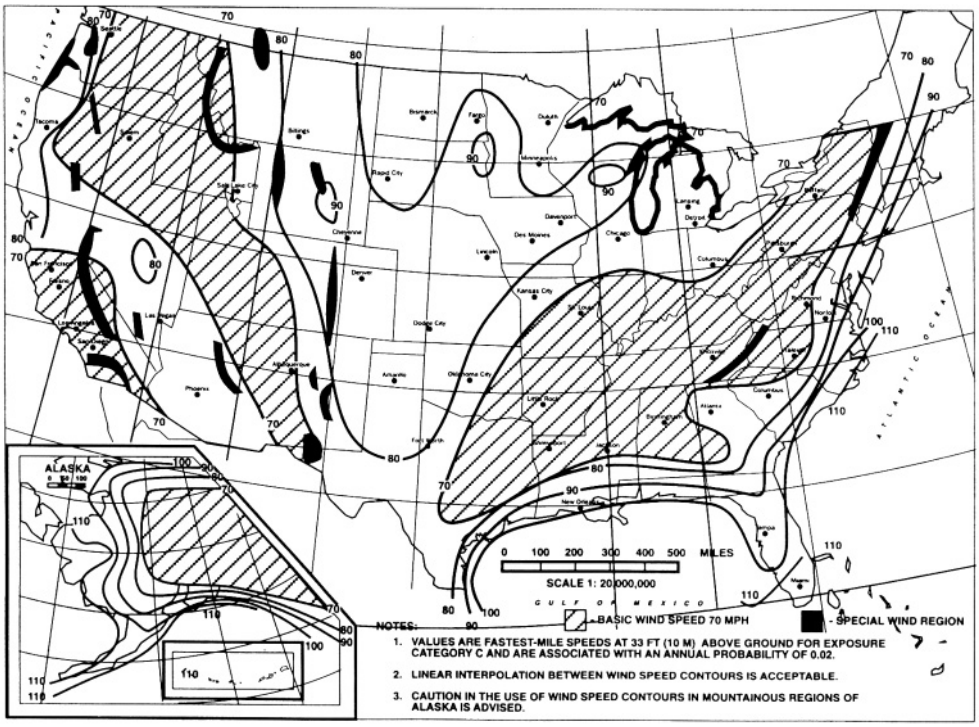

FIGURE 4.66 Wind pressure design values in the United States. (*Source:* Overend, P.R. and Smith, S., Impulse Time Method of Sag Measurement, American Society of Civil Engineers. With permission.)

TABLE 4.12 Ratio of Iced to Bare Conductor Weight

ACSR Conductor	D_c, in.	w_{bare}, lb/ft	w_{ice}, lb/ft	$\frac{w_{bare} + w_{ice}}{w_{bare}}$
#1/0 AWG -6/1 "Raven"	0.398	0.1451	0.559	4.8
477 kcmil-26/7 "Hawk"	0.858	0.6553	0.845	2.3
1590 kcmil-54/19 "Falcon"	1.545	2.042	1.272	1.6

The calculation of ice loads on conductors is normally done with an assumed glaze ice density of 57 lb/ft^3. The weight of ice per unit length is calculated with the following equation:

$$w_{\text{ice}} = 1.244t\left(D_c + t\right) \tag{4.120}$$

where

t = thickness of ice, in.
D_c = conductor outside diameter, in.
w_{ice} = resultant weight of ice, lb/ft

The ratio of iced weight to bare weight depends strongly upon conductor diameter. As shown in Table 4.12 for three different conductors covered with 0.5-in radial glaze ice, this ratio ranges from 4.8 for #1/0 AWG to 1.6 for 1590-kcmil conductors. As a result, small diameter conductors may need to have a higher elastic modulus and higher tensile strength than large conductors in heavy ice and wind loading areas to limit sag.

Wind Loading

Wind loadings on overhead conductors influence line design in a number of ways:

- The maximum span between structures may be determined by the need for horizontal clearance to edge of right-of-way during moderate winds.
- The maximum transverse loads for tangent and small angle suspension structures are often determined by infrequent high wind-speed loadings.
- Permanent increases in conductor sag may be determined by wind loading in areas of light ice load.

Wind pressure load on conductors, P_w, is commonly specified in lb/ft^2. The relationship between P_w and wind velocity is given by the following equation:

$$P_w = 0.0025\left(V_w\right)^2 \tag{4.121}$$

where V_w = the wind speed in miles per hour.

The wind load per unit length of conductor is equal to the wind pressure load, P_w, multiplied by the conductor diameter (including radial ice of thickness t, if any), is given by the following equation:

$$W_w = P_w \frac{\left(D_c + 2t\right)}{12} \tag{4.122}$$

Combined Ice and Wind Loading

If the conductor weight is to include both ice and wind loading, the resultant magnitude of the loads must be determined vectorially. The weight of a conductor under both ice and wind loading is given by the following equation:

$$w_{w+i} = \sqrt{\left(w_b + w_i\right)^2 + \left(W_w\right)^2} \tag{4.123}$$

where

w_b = bare conductor weight per unit length, lb/ft
w_i = weight of ice per unit length, lb/ft
w_w = wind load per unit length, lb/ft
$w_{w\pm i}$ = resultant of ice and wind loads, lb/ft

The NESC prescribes a safety factor, K, in pounds per foot, dependent upon loading district, to be added to the resultant ice and wind loading when performing sag and tension calculations. Therefore, the total resultant conductor weight, w, is:

$$w = w_{w+i} + K \tag{4.124}$$

Conductor Tension Limits

The NESC recommends limits on the tension of bare overhead conductors as a percentage of the conductor's rated breaking strength. The tension limits are: 60% under maximum ice and wind load, 33.3% initial unloaded (when installed) at 60°F, and 25% final unloaded (after maximum loading has occurred) at 60°F. It is common, however, for lower unloaded tension limits to be used. Except in areas experiencing severe ice loading, it is not unusual to find tension limits of 60% maximum, 25% unloaded initial, and 15% unloaded final. This set of specifications could easily result in an actual maximum tension on the order of only 35 to 40%, an initial tension of 20% and a final unloaded tension level of 15%. In this case, the 15% tension limit is said to govern.

Transmission-line conductors are normally not covered with ice, and winds on the conductor are usually much lower than those used in maximum load calculations. Under such everyday conditions, tension limits are specified to limit aeolian vibration to safe levels. Even with everyday lower tension levels of 15 to 20%, it is assumed that vibration control devices will be used in those sections of the line that are subject to severe vibration. Aeolian vibration levels, and thus appropriate unloaded tension limits, vary with the type of conductor, the terrain, span length, and the use of dampers. Special conductors, such as ACSS, SDC, and VR, exhibit high self-damping properties and may be installed to the full code limits, if desired.

Approximate Sag-Tension Calculations

Sag-tension calculations, using exacting equations, are usually performed with the aid of a computer; however, with certain simplifications, these calculations can be made with a handheld calculator. The latter approach allows greater insight into the calculation of sags and tensions than is possible with complex computer programs. Equations suitable for such calculations, as presented in the preceding section, can be applied to the following example:

It is desired to calculate the sag and slack for a 600-ft level span of 795 kcmil-26/7 ACSR "Drake" conductor. The bare conductor weight per unit length, w_b, is 1.094 lb/ft. The conductor is installed with a horizontal tension component, H, of 6300 lb, equal to 20% of its rated breaking strength of 31,500 lb.

By use of Eq. (4105), the sag for this level span is:

$$D = \frac{1.094\left(600^2\right)}{\left(8\right)6300} = 7.81 \text{ ft } \left(2.38 \text{ m}\right)$$

The length of the conductor between the support points is determined using Eq. (4.109):

$$L = 600 + \frac{8\left(7.81\right)^2}{3\left(600\right)} = 600.27 \text{ ft } \left(182.96 \text{ m}\right)$$

Note that the conductor length depends solely on span and sag. It is not directly dependent on conductor tension, weight, or temperature. The conductor slack is the conductor length minus the span length; in this example, it is 0.27 ft (0.0826 m).

Sag Change with Thermal Elongation

ACSR and AAC conductors elongate with increasing conductor temperature. The rate of linear thermal expansion for the composite ACSR conductor is less than that of the AAC conductor because the steel strands in the ACSR elongate at approximately half the rate of aluminum. The effective linear thermal expansion coefficient of a non-homogenous conductor, such as Drake ACSR, may be found from the following equations (Fink and Beatty):

$$E_{AS} = E_{AL}\left(\frac{A_{AL}}{A_{TOTAL}}\right) + E_{ST}\left(\frac{A_{ST}}{A_{TOTAL}}\right) \tag{4.125}$$

$$\alpha_{AS} = \alpha_{\text{AL}}\left(\frac{E_{AL}}{E_{AS}}\right)\left(\frac{A_{AL}}{A_{TOTAL}}\right) + \alpha_{ST}\left(\frac{E_{ST}}{E_{AS}}\right)\left(\frac{A_{ST}}{A_{TOTAL}}\right) \tag{4.126}$$

where

E_{AL} = Elastic modulus of aluminum, psi
E_{ST} = Elastic modulus of steel, psi
E_{AS} = Elastic modulus of aluminum-steel composite, psi
A_{AL} = Area of aluminum strands, square units
A_{ST} = Area of steel strands, square units
A_{TOTAL} = Total cross-sectional area, square units
α_{AL} = Aluminum coefficient of linear thermal expansion, per °F
α_{ST} = Steel coefficient of thermal elongation, per °F
α_{AS} = Composite aluminum-steel coefficient of thermal elongation, per °F

The elastic moduli for solid aluminum wire is 10 million psi and for steel wire is 30 million psi. The elastic moduli for stranded wire is reduced. The modulus for stranded aluminum is assumed to be 8.6 million psi for all strandings. The moduli for the steel core of ACSR conductors varies with stranding as follows:

- 27.5×10^6 for single-strand core
- 27.0×10^6 for 7-strand core
- 26.5×10^6 for 19-strand core

Using elastic moduli of 8.6 and 27.0 million psi for aluminum and steel, respectively, the elastic modulus for Drake ACSR is:

$$E_{AS} = \left(8.6 \times 10^6\right)\left(\frac{0.6247}{0.7264}\right) + \left(27.0 \times 10^6\right)\left(\frac{0.1017}{0.7264}\right) = 11.2 \times 10^6 \text{ psi}$$

and the coefficient of linear thermal expansion is:

$$\alpha_{AS} = 12.8 \times 10^{-6}\left(\frac{8.6 \times 10^6}{11.2 \times 10^6}\right)\left(\frac{0.6247}{0.7264}\right) + 6.4 \times 10^{-6}\left(\frac{27.0 \times 10^6}{11.2 \times 10^6}\right)\left(\frac{0.1017}{0.7264}\right)$$
$$= 10.6 \times 10^{-6} \big/ °\text{F}$$

If the conductor temperature changes from a reference temperature, T_{REF}, to another temperature, T, the conductor length, L, changes in proportion to the product of the conductor's effective thermal elongation coefficient, α_{AS}, and the change in temperature, $T - T_{REF}$, as shown below:

$$L_T = L_{T_{REF}}\left(1 + \alpha_{AS}\left(T - T_{REF}\right)\right) \tag{4.127}$$

For example, if the temperature of the Drake conductor in the preceding example increases from 60°F (15°C) to 167°F (75°C), then the length at 60°F increases by 0.68 ft (0.21 m) from 600.27 ft (182.96 m) to 600.95 ft (183.17 m):

$$L_{(167°F)} = 600.27\left(1 + \left(10.6 \times 10^{-6}\right)\left(167 - 60\right)\right) = 600.95 \text{ ft}$$

Ignoring for the moment any change in length due to change in tension, the sag at 167°F (75°C) may be calculated for the conductor length of 600.95 ft (183.17 m) using Eq. (4.111):

$$D = \sqrt{\frac{3\left(600\right)\left(0.95\right)}{8}} = 14.62 \text{ ft}$$

Using a rearrangement of Eq. (4.105), this increased sag is found to correspond to a decreased tension of:

$$H = \frac{w\left(S^2\right)}{8D} = \frac{1.094\left(600^2\right)}{8\left(14.62\right)} = 3367 \text{ lb}$$

If the conductor were inextensible, that is, if it had an infinite modulus of elasticity, then these values of sag and tension for a conductor temperature of 167°F would be correct. For any real conductor, however, the elastic modulus of the conductor is finite and changes in tension do change the conductor length. Use of the preceding calculation, therefore, will overstate the increase in sag.

Sag Change Due to Combined Thermal and Elastic Effects

With moduli of elasticity around the 8.6 million psi level, typical bare aluminum and ACSR conductors elongate about 0.01% for every 1000 psi change in tension. In the preceding example, the increase in temperature caused an increase in length and sag and a decrease in tension, but the effect of tension change on length was ignored.

As discussed later, concentric-lay stranded conductors, particularly non-homogenous conductors such as ACSR, are not inextensible. Rather, they exhibit quite complex elastic and plastic behavior. Initial loading of conductors results in elongation behavior substantially different from that caused by loading many years later. Also, high tension levels caused by heavy ice and wind loads cause a permanent increase in conductor length, affecting subsequent elongation under various conditions.

Accounting for such complex stress-strain behavior usually requires a sophisticated, computer-aided approach. For illustration purposes, however, the effect of permanent elongation of the conductor on sag and tension calculations will be ignored and a simplified elastic conductor assumed. This idealized conductor is assumed to elongate linearly with load and to undergo no permanent increase in length regardless of loading or temperature. For such a conductor, the relationship between tension and length is as follows:

$$L_H = L_{H_{REF}}\left(1 + \frac{H - H_{REF}}{E_C A}\right) \tag{4.128}$$

where

L_H = Length of conductor under horizontal tension H
$L_{H_{REF}}$ = Length of conductor under horizontal reference tension H_{REF}
E_C = Elastic modulus of elasticity of the conductor, psi
A = Cross-sectional area, in.^{2}

In calculating sag and tension for extensible conductors, it is useful to add a step to the preceding calculation of sag and tension for elevated temperature. This added step allows a separation of thermal elongation and elastic elongation effects, and involves the calculation of a zero tension length, ZTL, at the conductor temperature of interest, T_{cdr}.

This ZTL(T_{cdr}) is the conductor length attained if the conductor is taken down from its supports and laid on the ground with no tension. By reducing the initial tension in the conductor to zero, the elastic elongation is also reduced to zero, shortening the conductor. It is possible, then, for the zero tension length to be less than the span length.

Consider the preceding example for Drake ACSR in a 600-ft level span. The initial conductor temperature is 60°F, the conductor length is 600.27 ft, and E_{AS} is calculated to be 11.2 million psi. Using Eq. (4.128), the reduction of the initial tension from 6300 lb to zero yields a ZTL (60°F) of:

$$ZTL_{\left(60^\circ F\right)} = 600.27\left(1 + \frac{0 - 6300}{\left(11.2 \times 10^6\right)0.7264}\right) = 599.81 \text{ ft}$$

Keeping the tension at zero and increasing the conductor temperature to 167°F yields a purely thermal elongation. The zero tension length at 167°F can be calculated using Eq. (4.127):

$$ZTL_{(167°F)} = 599.81\left(1+\left(10.6\times10^{-6}\right)\left(167-60\right)\right) = 600.49 \text{ ft}$$

According to Eqs. (4.105) and (4.111), this length corresponds to a sag of 10.5 ft and a horizontal tension of 4689 lb. However, this length was calculated for zero tension and will elongate elastically under tension. The actual conductor sag-tension determination requires a process of iteration as follows:

1. As described above, the conductor's zero tension length, calculated at 167°F (75°C), is 600.49 ft, sag is 10.5 ft, and the horizontal tension is 4689 lb.
2. Because the conductor is elastic, application of Eq. (4.128) shows the tension of 4689 lb will increase the conductor length from 600.49 ft to:

$$L_{1_{(167°F)}} = 600.49\left(1+\frac{4689-0}{0.7264\left(11.2\times10^{6}\right)}\right) = 600.84 \text{ ft}$$

3. The sag, $D_{1_{(167°F)}}$, corresponding to this length is calculated using Eq. (4.111):

$$D_{1_{(167°F)}} = \sqrt{\frac{3\left(600\right)\left(0.84\right)}{8}} = 13.72 \text{ ft}$$

4. Using Eq. (4.105), this sag yields a new horizontal tension, $H_{1_{(167°F)}}$, of:

$$H_1 = \frac{1.094\left(600^2\right)}{8\left(13.7\right)} = 3588 \text{ lb}$$

A new trial tension is taken as the average of H and H_1, and the process is repeated. The results are described in Table 4.13.

Note that the balance of thermal and elastic elongation of the conductor yields an equilibrium tension of approximately 3700 lbs and a sag of 13.3 ft. The calculations of the previous section, which ignored elastic effects, results in lower tension, 3440 lb, and a greater sag, 14.7 ft.

Slack is equal to the excess of conductor length over span length. The preceding table can be replaced by a plot of the catenary and elastic curves on a graph of slack vs tension. The solution occurs at the intersection of the two curves. Figure 4.67 shows the tension versus slack curves intersecting at a tension of 3700 lb, which agrees with the preceding calculations.

Sag Change Due to Ice Loading

As a final example of sag-tension calculation, calculate the sag and tension for the 600-ft Drake span with the addition of 0.5 inches of radial ice and a drop in conductor temperature to 0°F. Employing Eq. (4.120), the weight of the conductor increases by:

$$w_{ice} = 1.244t\left(D+t\right)$$

$$w_{ice} = 1.244\left(0.5\right)\left(1.108+0.5\right) = 1.000 \text{ lb}/\text{ft}$$

TABLE 4.13 Interative Solution for Increased Conductor Temperature

Iteration #	Length, L_n, ft	Sag, D_n, ft	Tension, H_n, lb	New Trial Tension, lb
ZTL	600.550	11.1	4435	—
1	600.836	13.7	3593	$\frac{4435+3593}{2}=4014$
2	600.809	13.5	3647	$\frac{3647+4014}{2}=3831$
3	600.797	13.4	3674	$\frac{3674+3831}{2}=3753$
4	600.792	13.3	3702	$\frac{3702+3753}{2}=3727$

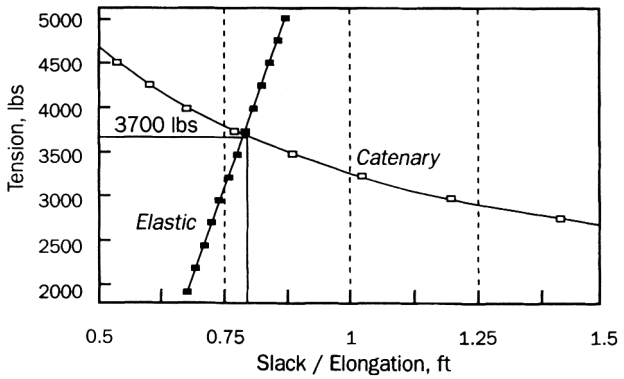

FIGURE 4.67 Sag-tension solution for 600-ft span of Drake at 167°F.

As in the previous example, the calculation uses the conductor's zero tension length at 60°F, which is the same as that found in the previous section, 599.81 ft. The ice loading is specified for a conductor temperature of 0°F, so the ZTL(0°F), using Eq. (4.127), is:

$$ZTL_{(0°F)} = 599.81\left[1+\left(10.6\times10^{-6}\right)\left(0-60\right)\right] = 599.43 \text{ ft}$$

As in the case of sag-tension at elevated temperatures, the conductor tension is a function of slack and elastic elongation. The conductor tension and the conductor length are found at the point of intersection of the catenary and elastic curves (Fig. 4.68). The intersection of the curves occurs at a horizontal tension component of 12,275 lb, not very far from the crude initial estimate of 12,050 lb that ignored elastic effects. The sag corresponding to this tension and the iced conductor weight per unit length is 9.2 ft.

In spite of doubling the conductor weight per unit length by adding 0.5 in. of ice, the sag of the conductor is much less than the sag at 167°F. This condition is generally true for transmission conductors where minimum ground clearance is determined by the high temperature rather than the heavy loading condition. Small distribution conductors, such as the 1/0 AWG ACSR in Table 4.11, experience a much larger ice-to-conductor weight ratio (4.8), and the conductor sag under maximum wind and ice load may exceed the sag at moderately higher temperatures.

The preceding approximate tension calculations could have been more accurate with the use of actual stress-strain curves and graphic sag-tension solutions, as described in detail in *Graphic Method for Sag*

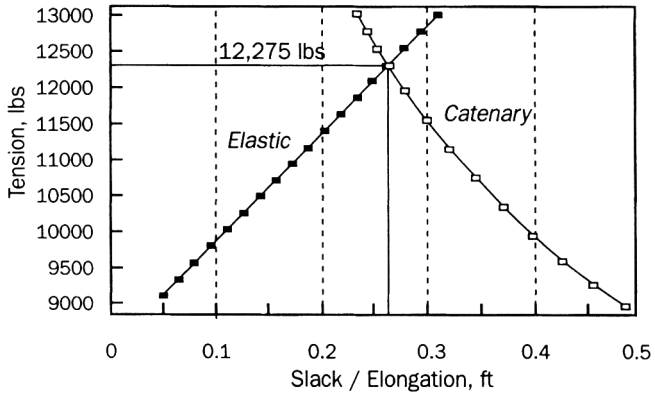

FIGURE 4.68 Sag-tension solution for 600-ft span of Drake at 0°F and 0.5 in. ice.

Tension Calculations for ACSR and Other Conductors (Aluminum Company of America, 1961). This method, although accurate, is very slow and has been replaced completely by computational methods.

Numerical Sag-Tension Calculations

Sag-tension calculations are normally done numerically and allow the user to enter many different loading and conductor temperature conditions. Both initial and final conditions are calculated and multiple tension constraints can be specified. The complex stress-strain behavior of ACSR-type conductors can be modeled numerically, including both temperature, and elastic and plastic effects.

Stress-Strain Curves

Stress-strain curves for bare overhead conductor include a minimum of an initial curve and a final curve over a range of elongations from 0 to 0.45%. For conductors consisting of two materials, an initial and final curve for each is included. Creep curves for various lengths of time are typically included as well.

Overhead conductors are not purely elastic. They stretch with tension, but when the tension is reduced to zero, they do not return to their initial length. That is, conductors are plastic; the change in conductor length cannot be expressed with a simple linear equation, as for the preceding hand calculations. The permanent length increase that occurs in overhead conductors yields the difference in initial and final sag-tension data found in most computer programs.

Figure 4.69 shows a typical stress-strain curve for a 26/7 ACSR conductor (Aluminum Association, 1974); the curve is valid for conductor sizes ranging from 266.8 to 795 kcmil. A 795 kcmil-26/7 ACSR "Drake" conductor has a breaking strength of 31,500 lb (14,000 kg) and an area of 0.7264 in.^{2} (46.9 mm^2) so that it fails at an average stress of 43,000 psi (30 kg/mm^2). The stress-strain curve illustrates that when the percent of elongation at a stress is equal to 50% of the conductor's breaking strength (21,500 psi), the elongation is less than 0.3% or 1.8 ft (0.55 m) in a 600-ft (180 m) span.

Note that the component curves for the steel core and the aluminum stranded outer layers are separated. This separation allows for changes in the relative curve locations as the temperature of the conductor changes.

For the preceding example, with the Drake conductor at a tension of 6300 lb (2860 kg), the length of the conductor in the 600-ft (180 m) span was found to be 0.27 ft longer than the span. This tension corresponds to a stress of 8600 psi (6.05 kg/mm^2). From the stress-strain curve in Fig. 4.69, this corresponds to an initial elongation of 0.105% (0.63 ft). As in the preceding hand calculation, if the conductor is reduced to zero tension, its unstressed length would be less than the span length.

Figure 4.70 is a stress-strain curve (Aluminum Association, 1974) for an all-aluminum 37-strand conductor ranging in size from 250 kcmil to 1033.5 kcmil. Because the conductor is made entirely of aluminum, there is only one initial and final curve.